THE UNIVERSITY OF
SYDNEY

THE ROLE OF CONNEXIN45 IN THE PATHOGENESIS OF VENTRICULAR TACHYARRHYTHMIA

Dr Peter Nabil Awadallah Fahmy, MBChB, FRACP

A thesis submitted for the degree of Doctor of Philosophy at The University of Sydney

Westmead Hospital, Westmead
Millennium Institute, Faculty of Medicine, University of Sydney

November 2015

STATEMENT OF ORIGINALITY

I, Peter Fahmy, hereby declare that this thesis contains work that has not been presented from the award of any other degree at any university. The work presented in this thesis is the result of my own investigation with the assistance from others as acknowledged herein, and contains no material previously published or written by any other person except were due reference is made in the text.

P Fahmy

ACKNOWLEDGMENTS

I am using this opportunity to acknowledge and thank several people who have been involved and mentored me through this period of my life.

I would like to thank Dr Eddy Kizana, not only as an excellent supervisor but also a mentor and a friend. His patience and guidance have helped me through the last few years. He has helped me grow both in research and as a person.

I would also like to say a special thanks to Dr Ajita Kanthan, my colleague and closest friend for all the time spent providing me with advice for my project and life. Thank you for being my friend.

I would like to extend a special thanks to Dr Stuart Thomas for being my co-supervisor and for all his advice during this PhD.

There are a great many from Westmead hospital whom I should thank for their help – Renuka Rao, Jim Poliopoulos, Mehdi Ramezani and Tony Barry. Your support is truly appreciated.

Thank you to the staff of WMI especially Monica, Liz and Virginia. To the staff from CMRI – Ian Alexander, Grant Logan and the rest of the gene therapy group for their advice.

This work was funded by an Australian Postgraduate Award.

PRESENTATIONS, ABSTRACTS AND AWARDS

P Fahmy, A Kanthan, R Rao, I Alexander, E Kizana. (July 2013) "Connexin45 Over-Expression Causes Arrhythmia in Rat Hearts" Heart, Lung and Circulation **22**(7):557-558 (Abstract presented at the World Cardiac Conference)

P Fahmy, A Kanthan R Rao, I Alexander, E Kizana. (2012**).**"Abstract 15082: The Effects of Connexin45 Over-Expression on Cardiac Physiology in the Intact Animal" Circulation 126:A15082. ***Oral*** presentation at AHA 2012.

P Fahmy, A Kanthan, R Rao, E Kizana. (2012)." Efficient Atrial and Ventricular Transduction following Tail Vein Injection of AAV2/9 Viral Vector**"** Heart, Lung and Circulation **21**(s2): s266.

P Fahmy, A Kanthan R Rao, E Kizana. (2012**).**"The Effects of Connexin45 Over-Expression on Cardiac Physiology in the Intact Animal**"** Heart, Lung and Circulation **21**(s2): s108. ***Oral*** presentation at CSANZ 2012

Ross JT, Kanthan A, Rao R, **Fahmy PNA**, Alexander IE, Kizana E. (2011) "Chamber specific cardiac gene delivery using Adeno-associated virus 2/9" Heart, Lung and Circulation **20**(s2): s81.

Awards relating to this thesis

CSANZ travelling scholarship (2012)

Westmead Association Research travelling grant (2011)

Australian Postgraduate Award (2011)

TABLE OF CONTENTS

LIST OF FIGURES

Chapter 1

Chapter 2

Chapter 3

Chapter 4

Chapter 5

LIST OF TABLES

Chapter 1

Chapter 2

Chapter 3

Chapter 4

Chapter 5

LIST OF ABREVIATIONS

$(NH_4)_2SO_4$, ammonium sulphate

µg, microgram (s)

µL, microliter (s)

µm, micrometre(s)

6CF, 6-carboxyfluorescein

AAP, Antiarrhythmic peptide

Ab, Antibody

Ad, Adenovirus

ANP, Atrial Natriuretic Peptide

ATP, Adenosine Triphosphate

AV, Atrioventricular

bFGF, basic fibroblast growth factor

CAD, Coronary artery disease

CBA, Chicken Beta Actin

CBF, carboxyfluorescein

CD31, cluster of differentiation 31

cDNA, Complementary deoxyribonucleic acid

Cfu, colony forming unit

cGMP, Cyclic Guanosine Monophosphate

CMV, cytomegalovirus

CO_2, carbon dioxide

CsCl, Cesium chloride

CV, Conduction velocity

Cx40, Connexin40

Cx43, Connexin43

Cx45, Connexin45

DAPI, 4',6-diamidino-2-phenylindole

DC, direct current

DCF, dichlorofluorescein

DCM, Dilated cardiomyopathy

DEPC, diethyl pyrocarbonate

DMD, Dystrophin Deficient

DMEM, Dulbecco's Modified Eagles Medium

DMSO, dimethyl sulfoxide

DNA, deoxyribonucleic acid

DPBS, Dulbecco's Phosphate Buffered Saline

dsRNA, Double stranded ribonucleic acid

ECG, Electrocardiograph

EDTA, Ethylenediaminetetra-acetic acid

EP, Electrophysiology, electrophysiological

EPS, Electrophysiology studies

FBS, fetal bovine serum

g, gravitational force

GFP, green fluorescent protein

H&E, Haematoxylin and Eosin

HBS, Hepes-buffered saline

HBSS, Hank's Balanced Salt Solution

HCl, hydrogen chloride

HEK, human embryonic kidney

HEPES, 4-[2-hydroxyethyl]-1-piperazineethanesulfonic acid

HRP, horseradish peroxidase

Hz, Hertz

ICD, Implantable cardio-defibrillator

IF, Immunofluorescence

IMDM, Iscove's Modified Dulbecco's Medium

Kg, kilogram

kHz, kiloHz

kV, kilovolt(s)

L, Litre

LAD, left anterior descending artery

LB, Luria-Betani

LV, Left ventricle/ventricular

LVH, Left ventricular hypertrophy

LY, Lucifer Yellow

M, Molar

MCS, Multiple Cloning Site

MEM, minimum essential media

mg, milligram (s)

$MgCl_2$, Magnesium chloride

$MgSO_4$, Magnesium Sulphate

MI, Myocardial Infarction

miRNA, Micro ribonucleic acid

mL, millilitre (s)

Mm, millimetre

mM, milimolar

MQH_20, reagent grade water

MRI, Magnetic resonance imaging

mRNA, messenger ribonucleic acid

MW, molecular weight

Na_2HPO_4, disodium hydrogen phosphate

NaOH, Sodium hydroxide

NBH, N- biotinamide hydrochloride

ng, nanogram (s)

nL, nanoliter (s)

nm, nanometre(s)

NRVM, neonatal rat ventricular myocytes

^oC, degrees Celsius

P = NS, P non-significant

PBS, phosphate buffered saline

PBST - Tween 20 in PBS

PCR, polymerase chain reaction

pH, Potency of Hydrogen ion

PKA, Protein kinase A

PKCα, Protein kinase Cα

PLA probes

PLB, phospholambam

pS, pico-Siemens

PVDF, polyvinylidene fluoride

QPCR, Quantitative Polymerase Chain Reaction

rAAV, Recombinant adeno-associated virus

RE, Restriction endonuclease

RIPA, Radio-Immunoprecipitation Assay

rpm, rotation per minute

rRNA, ribosomal ribonucleic acid

RVM, rat ventricular myocytes

SA, Sinoatrial

SC, subcutaneous

SCD, Sudden cardiac death

SD, Sprague-Dawley

SD, Standard deviation

sh45, silencing Cx45 vector

shNS, non-sense vector

shRNA, short hairpin ribonucleic acid

SURE, Stop Unwanted Rearrangement Events

TAE, Tris-Acetate EDTA

TB, transformation buffer

TBST, Tween 20 in Tris buffered saline

TE, Tris-EDTA

U, units

USB, Universal Serial Bus

UV, ultraviolet

v/v, volume per volume

VEGF, Vascular endothelial growth factor

VF, Ventricular fibrillation

VHD, Valvular heart disease

VT, Ventricular Tachycardia

w/v, weight per volume

WB, Western Blotting

WPRE, Woodchuck hepatitis virus post-transcription

βMHC, beta myosin heavy chain

CHAPTER 1

INTRODUCTION AND LITERATURE REVIEW

1.1 Introduction

Cardiovascular mortality is one of the leading causes of death in the industrialized world. Sudden cardiac death (SCD) occurs mainly following acute myocardial infarction (MI) [1]. Ventricular tachyarrhythmias, namely ventricular tachycardia (VT) and ventricular fibrillation (VF), are the cause of cardiac arrests in the majority of cases. The incidence of spontaneous ventricular tachyarrhythmia and SCD increases with worsening left ventricular ejection fraction. Implantable defibrillators and pharmacotherapy have been the mainstay treatment of such tachyarrhythmia but never the less mortality remains high. Yamada et al. and other authors have reported that intercellular electrical uncoupling mediated by decreased conductance of gap junctions is associated with ventricular tachyarrhythmia in the diseased heart [2-4]. Gap junctions form channels between adjacent cells. The core proteins of these channels are the connexins. Connexins43, 40 and 45 are all found in the mammalian heart. Connexin43 (Cx43) is the most prevalent with alterations in expression associated with both ventricular and atrial arrhythmias.

Connexin40 (Cx40) is predominantly expressed within the atria and has been associated with atrial arrhythmias. Connexin45 (Cx45), the least prevalent and hence the least studied of the three connexins isotypes, has been increasingly associated with fatal ventricular tachyarrhythmias [3].

In this review, I will discuss the mechanism of ventricular tachyarrhythmia and review the data supporting gap junction remodelling, with a focus on Cx45 and Cx43 having an important pathogenic role in such arrhythmias. In addition I will briefly discuss gene therapy vectors and methods of *in vivo* delivery to the heart.

1.2 Sudden Cardiac Death

Cardiovascular disease remains the single most common cause of natural death in developed countries [5]. Sudden cardiac death (defined as “death outside hospital”, “dead on arrival” or “dead in emergency”) from cardiac causes has been estimated to account for approximately 50 percent of all deaths from cardiovascular causes [5, 6]. Acute ventricular tachyarrhythmias account for the majority of SCD [6]. These are often triggered by acute coronary events, occurring in persons with or without

known cardiac disease or in association with structural heart abnormalities [6, 7].

Zipes, Camm et al. have reported an overall incidence of sudden cardiac death of 0.1 to 0.2% per annum in the general population [8]. This number increases dramatically to 10% per annum in Australian patients with reduced left ventricular function following MI and inducible VT at electrophysiological study (EPS) [9]. The cumulative risk of SCD however remains high after MI, accounting for ~ 50% of overall mortality [9].

1.2.1 Mechanism of Sudden Cardiac Death from Arrhythmia

The most common pathophysiological cascade involved in fatal arrhythmias in patients suffering from coronary artery disease or structural cardiac abnormality is VT degenerating into VF then into asystole [10]. The other reported cascade is of bradyarrhythmia or pulseless electrical activity secondary to electromechanical dissociation occurring in patients with advanced heart disease [11]. Patients with various genetic or acquired cardiac repolarisation abnormalities such as ion-channel abnormalities, acquired long-QT syndrome, or left ventricular hypertrophy (LVH); polymorphic VT or torsades de Point are the usual initiating arrhythmias in SCD [7]. Lastly, atrial fibrillation which leads to especially

high ventricular rates could result in SCD in patients suffering from Wolf-Parkinson-White syndrome [7].

Two common patterns have been described in the initiation of fatal arrhythmia in patients with ischemic heart disease [7]. One, where myocardial ischemia is precipitated when the energy demands exceed supply to cardiac muscle. This usually occurs following occlusion of a coronary artery by thrombus and is what leads to life threatening ventricular tachyarrhythmias by alteration of the electrophysiology of the myocardium. Another mechanism by which coronary artery disease may cause sudden death is post infarction, the myocardial scar can provide the substrate for re-entrant ventricular tachyarrhythmias. The latter mechanism occurs independent of the presence of myocardial ischemia. In addition, several other triggering mechanisms have been recognised; including systemic metabolic, neurochemical, neurophysiological factors, and exogenous toxic or pharmacological effects [5, 6, 12]. Table 1.1 summarises the causes of sudden cardiac death in the adult population. Note that coronary artery disease and dilated cardiomyopathy make up the majority cases. Figure 1.1 demonstrates causes and incidence of SCD in adult human.

Table 1.1 Causes of Sudden Cardiac Death in the Adult Population [13]

As seen in the table coronary artery disease and coronary artery disease account for the majority of sudden cardiac death in the adult population.

Causes	Men	Women
CAD	80%	42%
DCM	10%	18%
VHD	5%	18%
Normal	3%	9%
Other	2%	13%

CAD, coronary artery disease; DCM, dilated cardiomyopathy; VHD, valvular heart disease.

1.2.2 Physiology of Ventricular Tachyarrhythmia

Re-entry is the underlying electrophysiological mechanism of VF and VT. Mines et al. in 1914 was the first to define re-entry as a persisting electrical impulse that reactivates an area of previously activated myocardial tissue that is no longer refractory; thereby resulting in a circle movement of activation [14]. The length of such a circle depends on its wavelength. This is defined by the mathematical product of the refractory period and the conduction velocity. The termination of the re-entry by interruption of the circle is proof of this concept. Essentially, a suitable substrate and a trigger are required to initiate an arrhythmia. Myocardial infarction generates arrhythmogenic substrate and triggers through changes in tissue architecture and ion channel expression/function respectively thereby resulting in such a re-entry circuit and ventricular tachyarrhythmias [4]. This has been described with gap junctional uncoupling resulting in conduction slowing and arrhythmia in regions of ischemic myocardium [4]. Similarly, in patients with a remote MI, the scar provides the substrate and ventricular ectopic beats act as the trigger [4].

Figure 1.1: Pathophysiology and Epidemiology of Sudden Cardiac Death [15]

Figure below demonstrates causes and incidence of SCD in adult human.

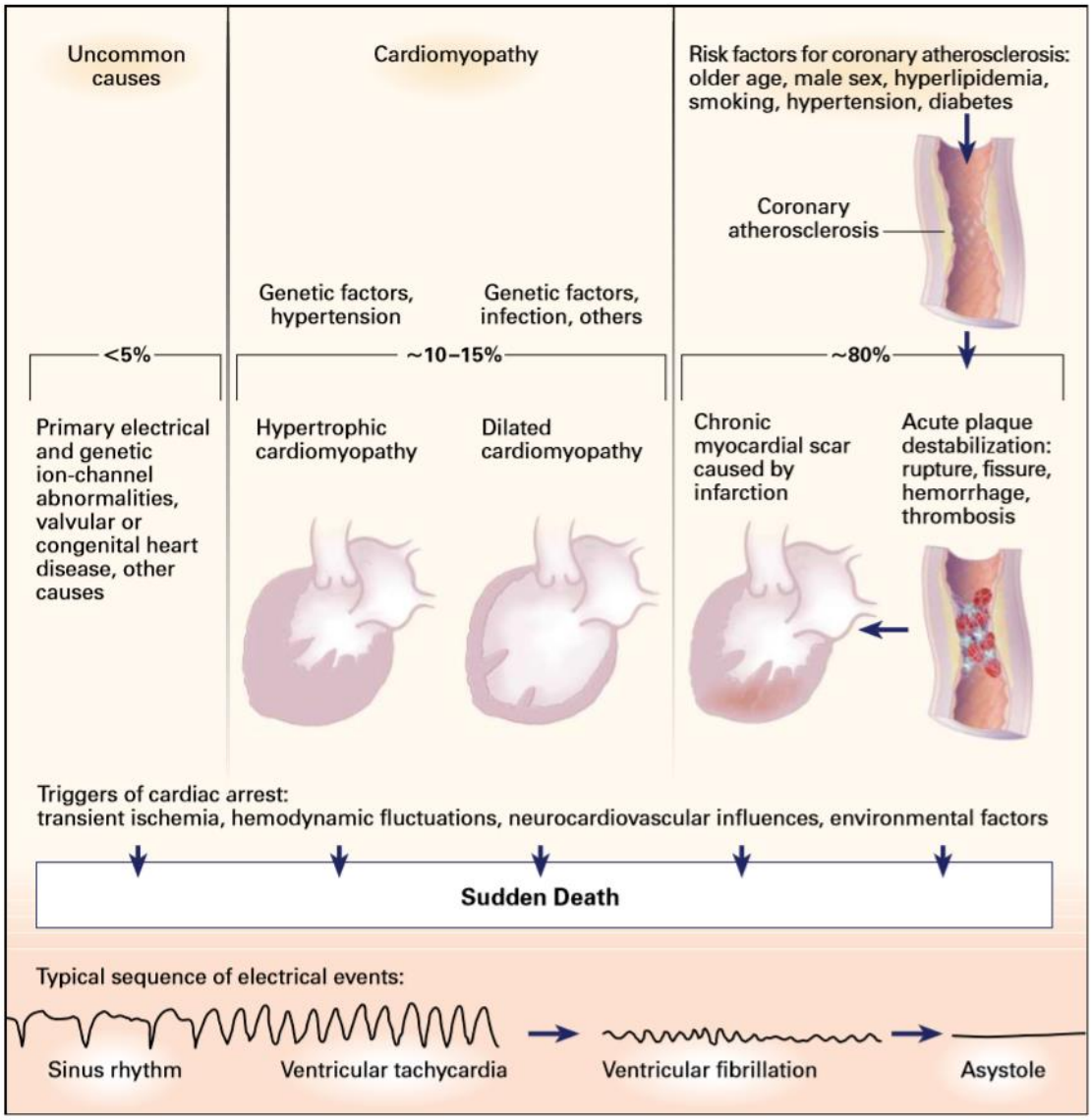

1.2.3 Evaluation of Patients at Risk of Ventricular Tachyarrhythmia

Clinical evaluation of survivors as well as those at risk of SCD is important to identify and initiate preventative management or reduce risk of further SCD. It is therefore necessary to take a detailed history as the initial step. Risk factors for coronary artery disease such as diabetes, hypertension, smoking, family history and hyperlipidaemia are not of much help in predicting patients at risk of tachyarrhythmias or SCD [16]. Those whom however suffer from heart failure; defined as impairment of left ventricular ejection fraction are at higher risk especially with an ejection fraction of less than 35% [8, 13, 17]. Electrocardiography can help diagnose disorders associated with SCD but has a low predictive value. Variables such as width of QRS, voltage length and QT length help in diagnosing QT syndromes and LVH and implicate a higher risk ECG. Electrophysiological (EP) studies can identify patients at risk of SCD; specifically in those in the high risk group (ejection fraction <40%) [18]. The accepted end point is inducible sustained VT, while non-sustained VT, polymorphic VT or VF maybe non-specific findings [18].

1.3 Management of Ventricular Tachyarrhythmia

Contemporary clinical management of VT and VF consists of pharmacological agents and device-based electrical therapy for the prevention and treatment, respectively, of VT/VF and its catastrophic sequelae. Drugs are of moderate efficacy and do not, in most patients, obviate the need for a prophylactic implantable cardio-defibrillator (ICD). In addition to this, many drugs used to prevent VT/VF have serious side-effects including pro-arrhythmia. Implantable cardio-defibrillators are highly effective in detecting and treating VT/VF by either anti-tachycardia pacing or defibrillation. In achieving this ICDs have the capacity to prevent SCD and save lives. The limitations of ICDs are however; the morbidity associated with implantation and maintenance of the hardware, the pain of receiving direct current (DC) shocks while conscious, the anticipatory anxiety of future shocks, the cost in a prohibitive economic environment and the inability of this therapy to directly target the underlying pathophysiology. A subset of patients, who do not achieve satisfactory symptom control with ICD or drug therapy, are eligible for catheter based ablation intervention. These patients typically have an ICD and experience multiple shocks for VT/VF that are not controlled by pharmacotherapy. It can be gleaned that management of patients with VT/VF and at risk of SCD is complex and associated with a significant health and financial

burden [13]. Consequently, an imperative exists to better understand the underlying pathophysiological mechanisms accounting for ischemia induced electrical instability; in the hope of finding specific therapeutic targets.

1.4 Gap Junctions

Most normal myocardial tissue volume is made up of cardiomyocytes; between those cells there are fibroblasts. Fibroblasts are cardiac non-myocytes that are arranged in sheets and strands that run in parallel to the prevailing direction of muscle fibres [19]. Isolated cardiomyocytes and fibroblasts form functional gap junctional channels [20].

Gap junctions mediate the electrical transmission that underlies the hearts coordinated mechanical activity. They play an essential role for normal cardiac function. They are intercellular channels that serve as pathways for the direct cell-to-cell transfer of ions and small molecules in all multicellular systems. In mammalian tissues these channels are ubiquitously expressed and also serve biological functions such as tissue homeostasis, development and differentiation [21, 22].

There has been extensive study in the past of active membrane properties and repolarization; however, cell to cell electrical coupling and its role in conduction slowing in myocardial disease has been the subject of increased scientific attention [23, 24].

Gap Junction Channels

Gap junctions are located at the cell poles in clusters within intercalated discs. A variety of large and small intercalated discs are found parallel to the long axis of the cell, in comparison to the small intercalated discs which are only found in regions at right angles to the long axis [25].

As shown in Figure 1.2 A, gap junctions are formed by the union of two hemi-channels (connexons) each contributed to by two adjacent cells. Biochemically, each hemi-channel contains six connexin proteins surrounding an aqueous pore that can be homomeric (similar connexins in a connexon) or heteromeric (mixed connexins in a connexon) [21, 25-28]. Even within one hemi-channel, different connexins can be integrated which can result in either homotypic (containing the same connexins) or heterotypic (containing different connexins) channel formation as shown in Figure 1.2 B.

Connexins form a multi-gene family of closely related proteins but not identical trans-membrane proteins [29]. Each connexon has its specific biophysical characteristics and forms channels that have unique properties of conductance and permeability. The electrical and biochemical characteristics of each gap junction are dependent on its constituent connexins. Various other mechanisms such as intracellular hydrogen and free calcium concentration, extracellular fatty acid composition and (de)phosphorylation of the individual connexin proteins can modulate the properties of the gap junction [30, 31].

Figure 1.2 Gap Junction Structure

A) A connexon consists of 6 transmembrane connexin. Two cell membranes connected by docked connexons with a central aqueous pore. B) Connexons can vary in the proportion and distribution of their constituent connexin isotypes (green and pink).

A)

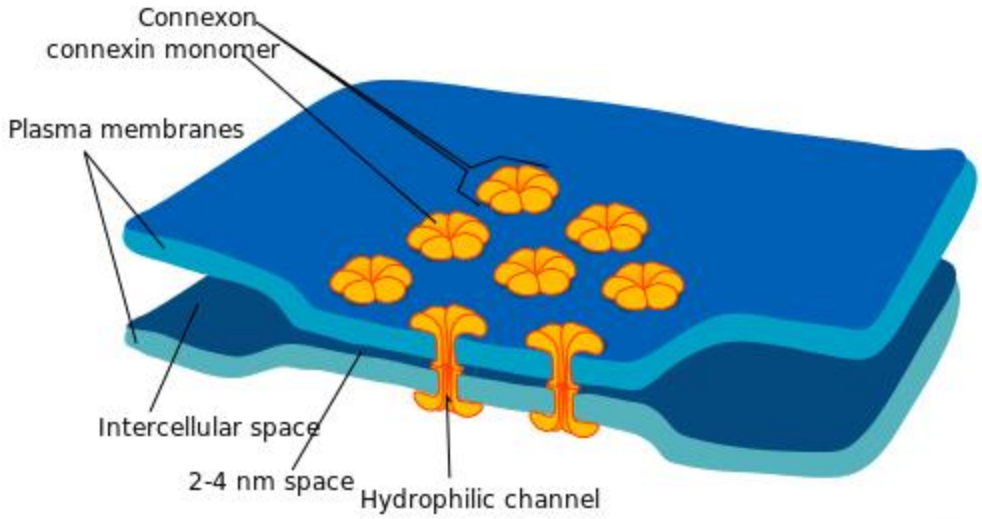

B)

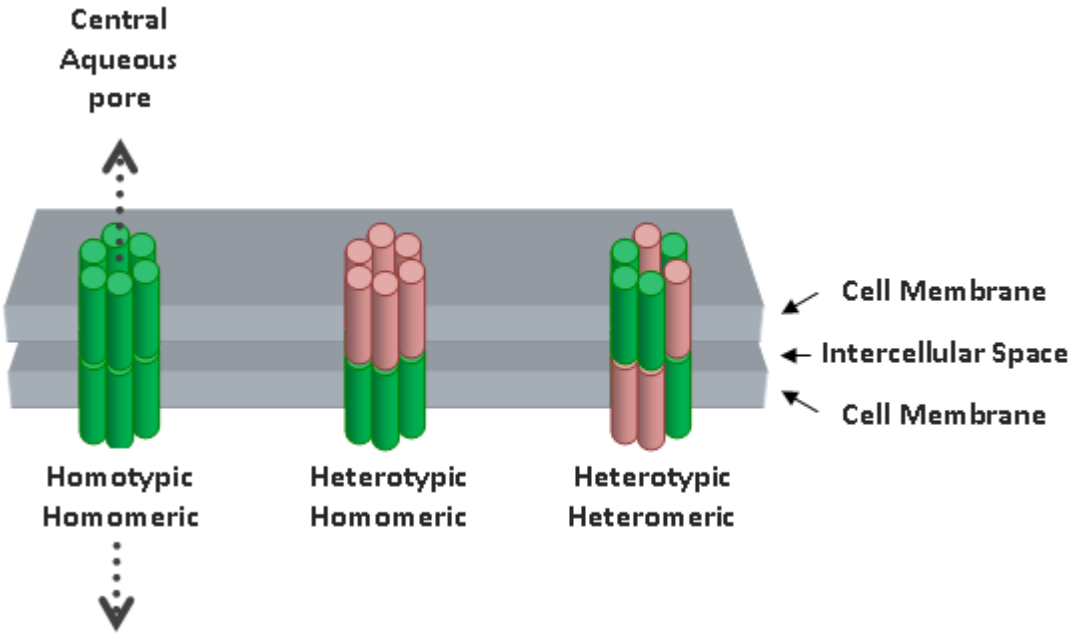
Central
Aqueous
pore
Cell Membrane
Intercellular Space
Cell Membrane
Homotypic
Homomeric
Heterotypic
Homomeric
Heterotypic
Heteromeric

Gap Junction Conductance

Action potential propagation from cell to cell is mediated by current flow through gap junctions. The action potential propagation in cardiomyocytes is dependent on extracellular and intracellular transfer of ions across an action potential wavefront between depolarised and polarised zones as shown in Figure 1.3.

Gap junction conductance is regulated by enhancing factors (such as PKCα or PKA) or reducing factors (such as hydrogen, calcium, sodium, loss of ATP) [32]. The number of gap junctions can be regulated in the long term by factors affecting the expression or degradation of connexins [33]. The propagation of action potential is determined by sodium channel availability, tissue architecture (including cell morphology and interstitial collagen strands) and gap junctions [32].

Figure 1.3 Action Potential Propagation

Figure below demonstrates depolarisation of wavefront across coupled myocytes from depolarised (blue) to polarised (red). Gap junction in green

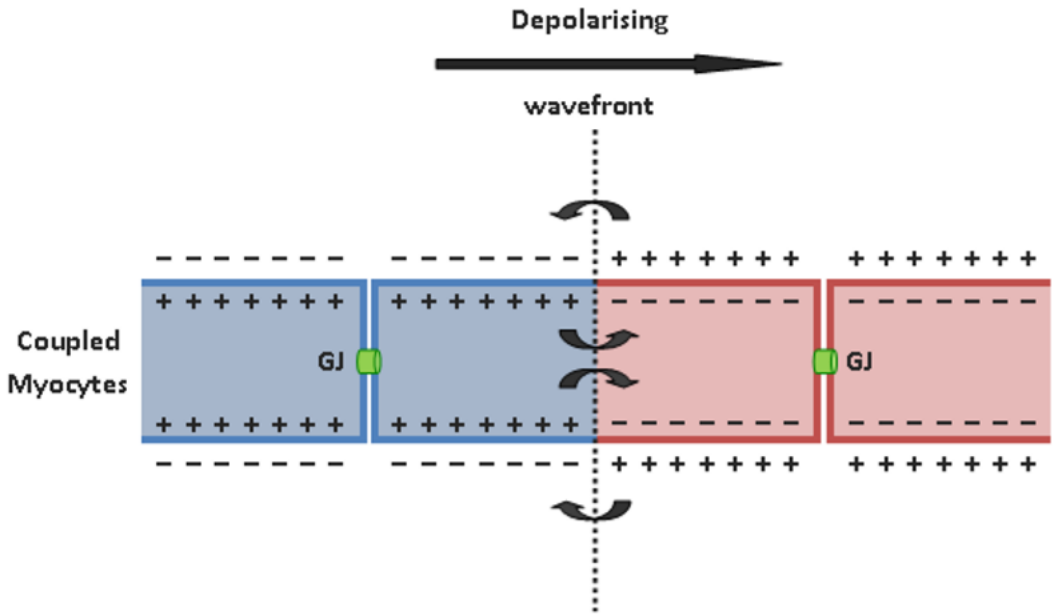

Role of Gap Junctions in Arrhythmia

Within the heart, gap junctions are responsible for the coordinated propagation of electrical activity that triggers the sequential contraction of the cardiac chambers. The current flow through the gap junctions is primarily through the intercalated discs at the end-to-end intercellular connections. Gap junctions affect the cell to cell electrical coupling in the heart. The magnitude of cell to cell electrical coupling is modulated by the type of connexon expressed; their distribution and density as well as by their rates of expression and degradation [34].

Propagation in cardiac muscle has been noted to be faster in the longitudinal than in the transverse axis of the cells [35]. Experiments using the gap junction uncouplers such as heptanol or palmitoleic acid have been carried out and revealed that transverse propagation is more sensitive to electrical uncoupling, block occurred more promptly for transverse than for longitudinal propagation. The decrease in conduction velocity following the uncoupling supports an increased risk of arrhythmogenesis following uncoupling [35, 36].

Arguments against a role of gap junctions in electrical coupling were also implicated as experiments by Jongsma and Wilders et al. reported that a 90% decrease in the number of gap junctions was required to reduce conduction velocity by only 25% [37]. This was under normal/standard conditions. In addition, in simulated ischemia in cell pairs, gap junction coupling remained large enough to balance action potential duration between the coupled cells until in-excitability occurred [38].

Studies that support the role of gap junction in arrhythmia included experiments with heterozygous Cx43 knockout mice revealing 25% reduction in conduction – a modest effect never the less [39-41]. On the other hand, Lerner et al. reported increased pacing induced ventricular tachycardia in Cx43+/− mice than in Cx43+/+ [40]. Moreover, numerous studies had shown an antiarrhythmic effect of peptides like AAP10, AAPnat or rotigaptide enhancing gap junction conductance [42-46].

Ventricular Tachyarrhythmia and Gap Junctions

There are two main patterns in the initiation of fatal arrhythmia post myocardial infarction. In the event of acute ischemia, gap junctions can be rendered non-functional by pH-dependent post-translational

modifications resulting in a substrate for functional re-entry. Gap junction uncoupling occurs after 20–30 minutes of ischemia. Ischemia results in the depletion of ATP and the accumulation of H^+ and Ca^{2+} in the cytoplasm of ischaemic cells, which has shown to decrease gap junction conductance in isolated paired cardiomyocytes [47, 48]. Intracellular rise of long chain acylcarnitines has also been reported to cause gap junction uncoupling [42].

Of note, it has also been reported that structural uncoupling by interstitial collagen deposition can contribute to VF [32].

In the chronic post-infarction heart, the role of gap junctions is less clear. Explanted hearts of patients undergoing cardiac transplantation for advanced ischemic heart disease were studied by Smith et al [24]. In normal myocardium (free from histologically detectable structural damage), there was no difference in the size of distribution of labelled gap junctions, or in their number per intercalated disk, between left ventricular tissue (in which functional impairment was severe) and right ventricular tissue (in which functional impairment was minimal). Gap junctions in cardiac myocytes that were however at the border of

healed infarct zones showed widespread generalised derangement. Instead of being aggregated into discrete intercalated disks, gap junctions were spread extensively over myocyte surfaces. This disorderly organisation may contribute to alterations in conduction that are capable of precipitating re-entry arrhythmias. They also reported that some infarct areas were bridged by continuous strands of myocytes, coupled to one another by gap junctions, hence linking healthy myocardium on either side. These bridges were reported in some instances to be no wider than a single attenuated myocyte. They hypothesized that avoidance of arrhythmia may therefore depend on the continued survival of this single cell.

As described in the previous section ventricular tachyarrhythmia occur as a result of focal conduction slowing at the infarct border-zone. This has been studied by and is understood to be contributed to by down-regulation of Cx43 and inhomogeneity in the peri-infarction area [49]. This region of slow conduction forms an essential part of the fixed re-entry substrate [23, 50]. Moreover, there might be structural uncoupling by interstitial collagen deposition. This in addition to either down-regulation of Cx43 or the up regulation of Cx45. The latter has been purported to be associated with ventricular tachyarrhythmia.

Atrial Fibrillation and Gap Junctions

Similarly in the atrium, gap junctional remodelling is also believed to provide a pro-arrhythmic substrate by altering action potential conduction. Slowing action potential propagation can promote arrhythmia according to the classical re-entry model or due to fibrillatory conduction. In atrial fibrillation, inhomogenic expression of connexins has been found with areas of almost normal expression and areas with nearly no expression [51]. Other authors observed a lateralisation of gap junctions [52, 53].

1.5 Connexins

Connexins are a family of proteins that constitute the building blocks of gap junctions (Figure 1.4). Each connexin has its own capacity to influence the biophysiological properties such as: voltage dependence, channel conductance and permeability of the resulting gap junction. Connexin proteins are made up of four transmembrane alpha helices and two extracellular loops [54]. Each connexin has three highly conserved cysteine residues, which make disulphide bonds between the loops and are essential for the formation of a functional gap junction channel. There have been 21 connexins protein isoforms found to date in the human proteome with different physiological and regulation processes [34, 55].

Figure 1.4 Connexin Structure

A connexin (pink) consists of 4 trans-membrane α helices (M1, M2, M3, M4) linked together by 2 extracellular loops (EL1, EL2) and 1 cytoplasmic loop (CL). Both the N-terminus and C-terminus have an intracellular location.

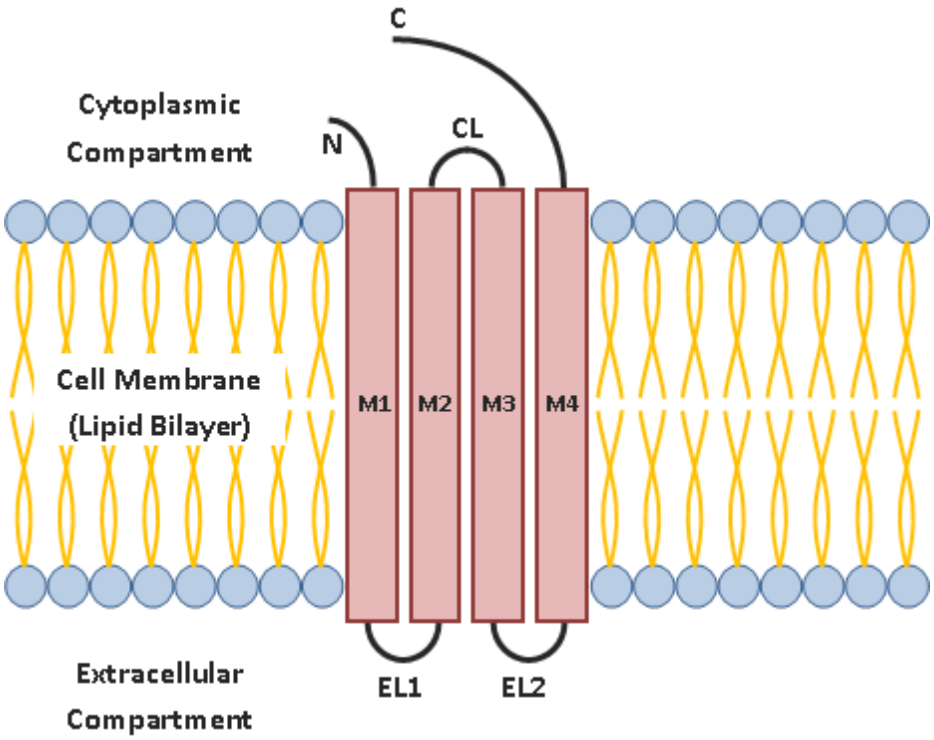

1.5.1 Connexin Distribution in the Myocardium

In the heart, the most prominent connexins associated with electrically active tissue are Cx43, Cx40, and Cx45. Connexin isotype expression varies between different chambers and structures of the heart. The dominant ventricular connexin is Cx43 [22, 56, 57]. This connexin is expressed in nearly all myocytes of the working atrial and ventricular mammalian myocardium regardless of the stage of development. However, it is not found in the nodal cells of the sino-atrial (SA) and in small amounts in the atrio-ventricular (AV) node [58-60]. Davis et al. demonstrated in human cells that bundle branch cells (the fastest conducting cells in the heart) contained the largest gap junctions with extensive levels of Cx43, 40 and 45. Nodal cells, on the other hand, have slower conduction and thereby had the smallest gap junctions with small levels of Cx45 and Cx40 expressed. Atrial myocytes express moderate amounts of Cx40, 43 and 45, while ventricular myocytes expressed only Cx43 and 45 [60].

Expression of connexins may differ between mammalian species. In rodents, Cx43 is not found in the His-Bundle and the proximal parts of both bundle branches but is present in the distal parts [61]. In large animals, it is found in all parts of the ventricular conduction system.

Connexin45, in rodents, is present in the AV node and the ventricular conduction system and only in very low levels of the surrounding atrial and ventricular myocardium [62]. It is not found in the SA node of rodents but has been noted in the SA node of rabbits. Connexin40 is found in low levels of the SA node of rabbits, dogs and cows [61]. It is found mainly in the ventricular conduction system where it co-localizes with Cx45 [31]. It is known to be strongly co-expressed with Cx43 in the atrial myocardium except in rat atrial myocardium. Of note, Cx40 is also present in ventricular myocardium during foetal and neonatal development but this does decline substantially until it is virtually absent in the adult stages [31].

1.5.2 Connexin43

Connexin43 gap junctions are permeable to organic ions and molecules of less than 1K Da [63]. Three different conductance's have been described, 20-30pS, 40-60pS and 70-100 pS depending on phosphorylation as well as open or closed state of the hemi-channels [63]. The molecular weight of Cx43 is between 41 to 46 kDa depending on its phosphorylated state. The conductance and permeability of gap junctions composed of Cx43 can be modulated by

intracellular pH, intracellular calcium or ATP concentration. In summary, cGMP-dependent protein kinases, protein kinase C, protein tyrosine kinase, casein kinase reduce the cell to cell conductance and permeability; while mitogen activated protein kinases (in cardiomyocytes) and PKA do the opposite by increasing the cell to cell permeability and conductance[63].

1.5.3 Connexin43 and Ventricular Arrhythmia

Connexin43 has been implicated in several studies as one of the main connexins associated with ventricular tachyarrhythmia [24, 64-66].

Connexin43 and Acute Myocardial Infarction

Connexin43 is found in its phosphorylated state in normal perfused hearts. With ischemia Cx43 becomes dephosphorylated due to an activation of mitochondrial K_{ATP} and reduced energy available for protein kinases [67]. This then leads to cellular uncoupling and as a result of the hemichannels remaining open, cell death and eventual irreversible tissue injury.

Connexin43 Distribution in Chronic Myocardial Infarction Model

Following myocardial infarction, Ursel et al. have reported in their longitudinal study (canine model) that as the infarcts healed, resting potential, action potential amplitude, and upstroke velocity returned to normal by 2 weeks, while action potential duration took two months to return to normal [68]. Never-the-less because of diminished connections between cells and slow conduction persisted in healed infarcts contributing to the occurrence of chronic arrhythmias [68].

Peters et al. studied Cx43 content in gap junctions in ischemic hearts and in hypertrophied human hearts [69]. They carried out quantitative immunohistochemistry studies on surgically obtained myocardial samples. They reported a significant reduction in gap junction surface area in those with ischemic myocardium (0.0027 $\mu m^2/\mu m^3$), in hypertrophied hearts (0.0031 $\mu m^2/\mu m^3$) when compared to normal myocardium (0.0051 $\mu m^2/\mu m^3$) [69]. They also noted a reduction in content of Cx43 in the diseased myocardial gap junctions as compared to the normal myocardium. This study showed that the reduction in surface area of gap junction may lead to reduction in conduction velocity and thereby increased ventricular tachyarrhythmia.

Transgenic studies

Several studies of transgenic mice with either knockout or heterozygous knockout Cx43 have been studied [39, 70-72]. Those with Cx43 deletion (-/-) died shortly after birth and therefore investigators were unable to record any electrical activity. On the other hand, in one study, heterozygous (Cx43 +/-) neonatal mice had a 30% slower conduction in paced hearts compared to wild type (Cx43 +/+) [70]. In this same study, conduction velocity worsened in adult mice with a 44% reduction in heterozygous compared to wild type mice. These studies in Cx43 gene altered mice were, however, not always consistent as Morley and his associates had noted no change in conduction velocity between heterozygous Cx43 deficient and wild type mice [72]. Morley used optical voltage mapping, a different and more accurate method to measure conduction velocity in these mice. A further study by Stephan et al. used a murine model genetically engineered to express decreasing levels of Cx43 [73]. They reported that a heterogeneous reduction of Cx43 of 18% leads to conduction slowing compared to wild type mice and more importantly leads to an 80% increase in lethal tachyarrhythmias.

Somatic studies:

Xun Ai and associates have studied the effects of Cx43 in rabbit myocardium [74]. They had initially noted that rabbits with heart failure had a reduction in expression of Cx43 as well de-phosphorylation of Cx43. This likely contributed to reduced cell coupling and therefore an increase in SCD from arrhythmia. This led to them to both knockdown and over-express Cx43 using adenovirus vector transmission in rabbit myocardium. Knockdown of Cx43 led to decreased intercellular coupling (assessed by Lucifer Yellow (LY) dye transfer); while overexpression of Cx43 in their heart failure rabbit model improved dye coupling compared to controls. They noted that the overexpressed Cx43 protein was located throughout the myocytes membrane (similar pattern to their control group) and the phosphorylation status was also comparable to those of the heart failure controls.

Roell et al. undertook an interesting study where they were able to show that that transplantation of embryonic cardiomyocytes in mice with myocardial infarcts protects against the induction of ventricular tachycardia [75]. Engraftment of skeletal myoblasts, bone marrow cells or cardiac myofibroblasts, did not offer the same protection against VT

induced by pacing. They reported that engraftment of embryonic cardiomyocytes resulted in improved electrical coupling between the surrounding myocardium and the infarct region as well as increased conduction velocity, and decreased the incidence of conduction block within the infarct. They then genetically engineered skeletal myoblasts to express Cx43 and engrafted them into infarcted hearts revealing a similar protection against VT to that achieved by engrafting embryonic cardiomyocytes. Hence they deduced that engraftment of Cx43-expressing myocytes has the potential to reduce ventricular arrhythmias in the post-infarct model through the augmentation of intercellular coupling [75].

Greener et al. also studied the effects of Cx43 over expression in a post-infarct VT pig model [64]. Following infarction by transient left anterior descending (LAD) coronary artery occlusion, pigs with inducible VT were treated with adenoviral Cx43, or βgal, or no gene transfer. They reported a 60% reduction in VT inducibility following Cx43 gene therapy compared to controls. The Cx43 protein levels were two fold higher in the infarct border of those treated with Cx43 compared to controls suggesting a mechanistic effect of Cx43 in slowing conduction and inducing arrhythmia in the healed scar border.

Human Studies of Connexin43

There have been several human studies showing an association between expression levels of Cx43 and heart diseases with increased susceptibility to ventricular tachyarrhythmias [69, 76, 77].

Peters et al. studied Cx43 content in gap junctions in ischemic hearts and in hypertrophied human hearts reporting reduced expression of Cx43 [69]. Other studies have also confirmed that there was a reduction in Cx43 expression in other forms of heart disease, including ischemic cardiomyopathy, dilated cardiomyopathy and inflammatory cardiomyopathies [76, 77]. These conditions are all associated with an increased risk of SCD due to ventricular tachyarrhythmias. This supports the hypothesis that altered expression of Cx43 leads to abnormal coupling between cardiomyocytes which in turn leads to conduction slowing and thereby the propensity to SCD through ventricular tachyarrhythmias [23].

1.5.4 Connexin45

Channel Properties:

Most investigations into the function of gap junctions composed of Cx45 have been done on immortalised, gap-junction deficient cells such as SkHep1 or Hela cells[31, 78-80]. It has been cloned in mouse, human and rat DNA. Its coding region consists of 396 amino acids in the human and rat genome, and 395 amino acids in the mouse genome [81]. Gap junctions composed of Cx45 are selective for cations [61, 81]. Veen et al. have reported them to be voltage dependant with half maximal activation at +/- 20mV. Connexin45 has also been noted to be more sensitive to intracellular pH than Cx43, with complete block occurring at a pH of 6.3 [82]. Multiple studies have assessed its permeability properties and noted that it was moderately permeable to fluorescent dyes LY, dichlorofluorescein (DCF) but not 6-carboxyfluorescein (6CF) [31, 79]. There are 15 possible phosphorylation sites for PKC in human Cx45 and 17 in rodents and mice, mainly on the serine but also on the tyrosine residues [31]. With regards to its size as its name suggest its size is 45kD – 48kD (depending on phosphorylated state). Valiunas et al. reported that Cx45 gap junctions have relatively small unitary

conductance for (~26pS) but were still able to pass some fluorescent dyes [83].

Connexin45 and Myocardial Development

Connexin45 is the first connexin to be expressed in the heart and is therefore essential for foetal myocardial development [84, 85]. Sebastien et al. have shown that Cx45 protein expression can be detected in the mouse heart at day 8.5 to 9.5 post conception but the beyond day 10.5 post conception the protein could no longer be detected with immunofluorescence microscopy [59]. Immunoblotting technique, however; continued to detect the protein in the neonatal heart implying it was still being synthesized. In the major part of the adult mouse heart Cx45 was undetectable except in the anterior regions of the interventricular septum and in trace amounts in the ventricular free wall; supporting its presence in the myocardial conduction system.

Connexin45 and Arrhythmia

In the adult heart under pathological conditions, such as heart failure, increased expression of Cx45 can occur [86]. Pathological conditions can also affect other connexins, for example, Cx43 has been shown to be

reduced in failing hearts [77, 87]. Reduced Cx43 expression may result in diminished coupling and thereby contribute to re-entrant tachyarrhythmia. However there has been data from Cx43 knockout mice showing that there needs to be a 70-90% reduced expression to manifest into a significant conduction delay or arrhythmia [88, 89]. It seems that the more modest reductions observed in heart disease are unlikely to be the cause of abnormal rhythm generation. Therefore it is conceivable that the up-regulation of Cx45 may have an effect of electrical conduction. One possible mechanism for this is that ventricular gap junctions in diseased hearts are made up of Cx43, Cx45 or oligomerize with each other to form mixed Cx43/Cx45 channels. From a biophysical perspective Cx45 gap junctions display a much lower unitary conductance than Cx43 channels, a property that underpins their prevalence in the AV and atrial nodes. These sites physiologically demand slow but safe electrical conduction. The functional effects of heteromeric Cx43/Cx45 channel formation on gap junctional intercellular coupling have been assessed in heterologous expression systems and in primary myocytes [80, 81, 90]. The resulting heteromeric gap junctions yielded disparate functions to their homomeric counterparts raising the possibility that heteromeric channel formation may be one mechanism by which intercellular communication can be altered.

Transgenic Models

In a transgenic, cardiac-restricted, Cx45 over-expressing mouse model there was an increased incidence of spontaneous and inducible ventricular tachyarrhythmia [90]. Moreover there have been studies using a knockout mouse model, which died from heart failure in utero at embryonic day 10. The embryonic hearts were found to be dilated due to defective vascular development. However even with the absence of Cx45, heart contractions were initiated but there was conduction block though the atrioventricular canal and the contractions in the outflow tract were not co-ordinated with those in the ventricle. This does support the previously mentioned studies of Cx45 being present in the ventricular conduction system. Cecilia lo et al. also reported that knockout embryos exhibited an endocardial cushion defect due to failure of cells in the myocardium to requisite epithelial-mesenchymal transformation [62]. This suggested that Cx45 has a role to play in the development of the endocardial cushion.

This is in contrast to a recent study by Yamada el al. where they created lines of mice that were either Cx45 deficient or Cx45 overexpressed hearts [91]. The Cx45 deficient hearts that survived did not have any electrophysiological differences to those of the wild type mice. More-over, in contrast to their previous study, this study of Cx45 overexpressed mice

did not show any *in vitro* differences in electrophysiological properties [3]. Of note the overexpressed mice had a two-fold increase in Cx45 and the studies were *in vitro* whole heart preparations. This may be the reason for the difference in observed results.

While some of the studies in genetically altered mice support our hypothesis that up-regulation of Cx45 contributes to conduction slowing and arrhythmia formation the strength of the findings is limited by the models employed. The use of transgenic mice to study connexin biology and arrhythmia is limited by changes in the expression of unintended molecules and the high-level of structural abnormalities encountered [62]. The latter could explain the genesis of any arrhythmia independent of the molecular alteration. While it is agreed that use of conditional transgenics may overcome these limitations, the somatic gene transfer approach would be superior in this context for the following the reasons. Firstly, acute genetic changes will be induced in the adult heart essentially mimicking those likely to occur in the context of acute myocardial disease. Secondly, heterogeneity of gene transfer also mimics the heterogeneous pattern of connexin expression in the diseased heart and is likely to result in higher levels of arrhythmia burden than the low levels seen by Betsuyaku et al. [90]. Employing systemic transfer method of gene it is likely that transmural heterogeneity will also be achieved.

1.6 Viral Vectors

The predominant use of viral vector systems in the preclinical models of gene therapy is a reflection of the increased gene transfer efficiencies achievable with these systems. For gene therapy to be successful, an appropriate amount of the therapeutic gene must be delivered into the target tissue without substantial toxicity.

Gene delivery systems can be broadly classified into either non-viral physico-chemical systems and recombinant viral systems [92, 93]. I will concentrate on the latter in this section of the review. The three most commonly used viral vector systems are shown in Table 1.2.

Adenoviral and Lentiviral Vector Systems

Historically, recombinant human adenoviral vectors have been the most commonly used vectors in pre-clinical gene therapy models and in clinical cardiovascular gene therapy [94]. This vector system has been widely used given the high functional vector titres achievable, ease of production and broad target cell tropism, particularly within the cardiovascular system [95]. All major cardiac cell types can be efficiently transduced by adenoviral vectors both *in vivo* and *in vitro*. The pattern of *in vivo* transduction in mammalian species is dependent on the method of delivery. Guzman et al. showed a direct myocardial injection results in

intense transduction at the site of injection, while Barr and his associates used an intra-coronary delivery system resulting in a more widespread transduction in the distribution of injected coronary vessel [96, 97]. Disadvantages of using the adenoviral vector system include its capacity for evoking an intense immune and inflammatory reaction, the pre-existence of neutralising antibodies to commonly used vectors, the *de novo* development of these antibodies (therefore inability to re-administer same vector serotype), and the lack of vector integration [95].

Lentiviral vectors transduce target cells by genomic integration [95]. The first developed lentiviral vector system was based on the human immunodeficiency virus (HIV) type 1 [98]. The advantages of this system is the ability to confer long-term stable gene expression, the capability of transducing mitotically quiescent cells, relative ease of production and an increased packaging capacity when compared to recombinant adeno-associated viral (rAAV) vectors [95]. The major disadvantages are the pathogenicity of the parental virus and development of an immune response following cardiac delivery [95].

Recombinant Adeno-Associated Virus Gene Transfer Vectors

Recombinant adeno-associated virus vectors are derived from the dependant parvovirus rAAV type 2 [99]. This vector system has a number

of advantageous attributes such as a lack of parental agent pathogenicity and vector-related cytotoxicity, minimal immunogenecity, and the capacity for stable long-term transgene expression through genomic integration [100]. These vectors also possess natural tropism for striated muscle and can confer stable long-term transgene expression in cardiac muscle in immunocompetent hosts [101]. They are therefore a favourable vector system in clinical studies.

The major limitations of rAAV vector systems include the difficulty in production of high-titre vector stocks of consistent purity and bioactivity, a limited packaging capacity of 4.8 kb and the possibility for the formation of pre-existent neutralising antibodies in human population.

A number of additional rAAV serotypes have been described. Pseudo typing rAAV-2 genomes modifies vector tropism and has been found to markedly enhance cardiac muscle transduction when capsid serotypes six, eight and nine are used [102].

Recombinant Adeno-Associated Virus Vector 2-9

Recombinant adeno-associated virus vector 2 serotype 9 has been extensively studied in recent years. It is a human isolate and the terminal galactose is the primary cell surface receptor for the rAAV9 [103]. Co-

receptors however remain unknown [104]. Studies in rodent and mice hearts have revealed higher transduction with rAAV9 than rAAV1, rAAV5, rAAV7, or rAAV8 following direct intramyocardial administration [105, 106]. However, other studies have reported less efficient transfer of rAAV9 compared to rAAV6 or rAAV8 when transendocardial administration was used [107, 108]. Despite this, Fish et al. as well as Pleger et al. have successfully used rAAV9 vectors via intracoronary administration in gene therapy trials involving porcine heart failure models [109, 110]. Importantly, rAAV9 is more effective in cardiac gene transfer via the intravenous route when compared to rAAV1 or rAAV6 [104]. A further point to comment on is that rAAV9 has been observed to display broad bio-distribution in off-target organs after administration than rAAV6 [104]. Never-the-less pre-existing humoral immunity to rAAV9 is lower than rAAV1 or rAAV6 in humans [111].

Table 1.2 Comparisons of Major Viral Vector Systems

Vectors	Adenovirus	rAAV	Lentivirus
Functional Titre (per mL)	Up to 10^{12}	Up to 10^{10}	Up to 10^{9}
Genome	dsDNA	ssDNA	ssRNA
Insert Capacity	7 to 30 kb	4.8 kb	10 kb
Integration	No	Yes (random[a])	Yes (random)
Pattern of transgene expression	Transient	Long-term	Long-term
Cell-cycle dependent transduction	No	No[b]	No
Host/Vector interactions	Cytotoxic and immunogenic	Minimally immunogenic	Minimally immunogenic

a *rep* positive vectors are capable of site-specific integration

b Transduction efficiency may be influenced by target cell mitotic activity

1.7 Myocardial Vector Delivery Methods

Catheter-based Myocardial Delivery

Several methods could be used to allow catheter delivery of genes to the myocardium including, intracoronary route, endocardial delivery or by retro-infusion of the coronary veins.

Intracoronary delivery has been reported to result in variable transduction efficiencies. This may be due to biocompatibility of catheters and vectors, differences between animal species or vector related variability such as titre. Gene transfer efficiency has also been reported to be limited with only 50% transduction efficiency [112].

Percutaneous endocardial delivery is limited to focal gene transfer to the myocardium thereby it is best applied to therapeutic angiogenesis or to focal arrhythmia therapy [113, 114]. Steerable needle-tip catheters through which vector can be injected into specified regions of endocardium have been developed and evaluated in both animal models and in human trials [115-117].

Retro-infusion of the coronary veins is the most recent described method out of the three. It involves infusion of a vector retrograde via the coronary veins and has been reported to result in gene transfer

efficiencies comparable to intracoronary injection with its use been validated in animal models [118-120].

Direct Myocardial Delivery

Some investigators believe that there is an advantage of direct myocardial injection of angiogenic growth factors or genes over the intracoronary delivery method. This may be achieved via the transthoracic or sub-ziphisternal approach. The direct approach is the desired method for regional myocardial ischemia and focal arrhythmia therapy. Use of this model in the literature has been mainly in animal models. It has been used both in small and large animal models. It has been described in a rat MI model where injection of human vascular endothelial growth factor (VEGF) 165 cDNA in the MI border zone induced angiogenesis [121]. Similarly in an ovine study, sheep which received intramyocardial injections of a plasmid encoding VEGF165 in the border zone had shown fractional shortening and wall thickening improvement in this area as compared with controls [122]. Other animal studies have successfully used this method of gene transfer and validated its efficiency in gene transfer [123, 124]. This direct-injection method offers a readily applicable delivery route to produce a highly localized expression of transgenes; however, transduction is restricted to the area surrounding the site of

injection. Another significant limitation is that acute inflammatory responses due to injury tend to develop at the injection sites and hence may limit the therapy and enable an adaptive immune response against the vector.

Pericardial Delivery

Myocardial gene delivery has been described via the pericardial space. The rationale for utilizing this approach is its anatomical proximity to the myocardium and the accessibility of the pericardial sac for percutaneous vector delivery. This method has been utilized in animal models including a rabbit model of chronic myocardial ischemia where basic fibroblast growth factor (bFGF) delivered via the pericardial space demonstrated enhanced new epicardial small vessel growth [125]. However in a dog MI model, administration of Ad/VEGF165 did not demonstrate increase in serum VEGF levels or improved collateral perfusion [126]. On the other hand, pericardial expression of the gene was noted 2 weeks following delivery of the gene. The benefit of this mode of delivery is prolonged exposure of the administered gene across a wider area of targeted surface. Animal models have supported the feasibility and safety of this

delivery mode but the suitability in patients with pericardial adhesions following multiple procedures is not feasible [127, 128].

Surgical Delivery

Surgical gene delivery is the most invasive approach and would be associated with significant morbidity associated with accessing the myocardium. This said it can potentially be performed while the patient is undergoing coronary artery bypass grafting or thorascopically.

Gene delivery via multiple direct injections into the myocardium in open-chested small animal models is well established [129]. This however results in only limited transgene expression to the targeted area. Hajjar et al. have described an improved method of delivery into the aortic root via a catheter introduced into the left ventricular cavity while the ascending aorta and pulmonary artery are transiently occluded [130]. Modifications to this method have also been described [131, 132]. The major limitation to this method is its invasive nature and this would limit its use in human trials; except in the setting of cardiac surgery.

Systemic Delivery with Myocardial Transduction

Systemic delivery has been getting wider interest especially with the development of vectors that specifically target the myocardium such as the rAAV6 and rAAV9. The benefit being its ease of use and widespread exposure of the gene throughout the myocardium. The major disadvantage is first-pass uptake by low-affinity receptors in the lungs or metabolism in the liver resulting in decreased bioavailability for myocardial uptake as a result of the intravenous infusion [133]. A study by Bostick et al. demonstrated efficient transduction with facial vein injection in mice throughout the entire heart with rAAV9 microdystrophin gene therapy. This further translated into phenotypic changes with amelioration of electrocardiographic abnormalities in dystrophin-deficient mouse (DMD) model [134]. It is expected that utilising other peripheral veins and the same vector would result in similar results. On the other hand, intravenous bolus injection of bFGF has been ineffective in inducing an angiogenic response in a canine model of myocardial ischemia felt to be as a result of uptake by low affinity receptors in lung system [128]. Thereby the correct vector system needs to be chosen carefully to prevent first pass metabolism or uptake by low affinity receptors. I proposed the use of rAAV9 vector via the peripheral rat vein for transduction of myocardium in our experiments.

1.8 Summary

In summary, cardiovascular mortality remains the leading cause of death in the industrialised world. Ventricular tachyarrhythmias are the major cause of cardiac arrest in the majority of cases. Anti-arrhythmic drugs have failed to reduce incidence of cardiac death. While ICDs are effective against ventricular tachyarrhythmia, their use is associated with a significant morbidity. Therefore our understanding of post-MI induced arrhythmia is important and appears to be incomplete.

Re-entry arrhythmias are a prominent feature of ischemic heart disease. In experimentally induced MI, EP studies have identified the border zone of myocardial infarcts as sites in which slow conduction, responsible for sustained re-entry, arises. Slow conduction, attributable to intercellular uncoupling, and areas of complete conduction block, persist at the sites of experimentally induced infarction after healing, thereby contributing to chronic arrhythmogenesis. In human ischemic cardiac disease, a reduction in the size and density of gap junctions in these cells has been reported [24].

It is well understood that the low resistance pathways that allow the electrical impulse to flow rapidly and repeatedly between cardiac muscle

cells, ensuring that their mechanical responses are orderly and synchronous in the healthy heart, are formed by gap junctions. It is thereby clear that gap junctions have a significant role in modulating tissue conduction velocity, and through aberrant expression lowers the threshold for arrhythmia.

Gap junctions are formed of various connexins. Pathophysiological changes are reflected by the chamber specific expression and function of connexin isoforms. Connexin expression itself is clearly dynamic in expression and affected by many intracellular and extracellular factors. Influential factors that affect conductance include the degree of connexin phosphorylation, connexin location, and total junctional connexin content. To add to the complexity, changes such as transgenic alterations, somatic gene transfer, or arrhythmia induction may alter connexin physiology.

Abnormal Cx43 and Cx45 in the ventricle are associated with ventricular arrhythmias, while abnormal Cx40 in the atria is associated with atrial fibrillation. Connexin43 has been well studied in the MI model. In the acute MI, Cx43 has been described to be reduced and lateralised in the infarct zone, and this has also been extended to the chronic MI model [64-66, 135]. These alterations correlated with heterogenous conduction by *in vivo* measures and slowed conduction velocity during *ex vivo* testing [64].

Greener et al. have showed that gene transfer–mediated overexpression of Cx43 increased the absolute amount of phosphorylated and intercalated disk-localized Cx43, improved conduction velocity, and reduced VT inducibility [64]. Hence it may be extrapolated that Cx43 expression and function is important for ventricular conduction velocity and arrhythmia mechanism.

Connexin45 on the other hand remains not well investigated. There are studies supporting its overexpression in human heart failure and it association with increased arrhythmogenesis. Moreover transgenic mice models have been created that do support the hypothesis of Cx45's involvement with conduction slowing and increased arrhythmogenesis [90]. This area remains under evaluated and hence the aim of this PhD.

The success in gene therapy in the clinical era is dependent on several key factors: appropriate vector platforms, efficient delivery methods, documentation of clinical feasibility and consistent safety and efficacy. Choosing the appropriate vector and method of delivery is therefore paramount.

The most difficult issue with human and animal studies is to use models

that mimic disease state controls. Clearly patients with myocardial ischemia are not adequate controls for valvular, dilated or inflammatory cardiomyopathies. Transgenic models while widely used have several disadvantages and do not mimic the human diseased heart. Somatic gene transfer presents itself as the most appropriate technique to assess true functional significance of relative connexin isotype expression. With the appropriate control vector and delivery method, the confounding factors identified may be avoided.

Based on the above literature review, Cx45 pathophysiology will be studied using a rAAV9 vector system and somatic gene transfer. Once establishing that Cx45 expression may contribute to ventricular arrhythmia, it is important to study it in a disease model. The rat infarct model is used given its ease of production and both Cx43 and Cx45 expression will be modulated to further understand arrhythmia in the MI model.

CHAPTER 2

MATERIALS AND GENERAL METHODS

In this chapter methods are described. These have been employed across most of the research project. Specialized methods or variations of these general methods are described in their respective results chapters

2.1 Molecular Biology

2.1.1 Chemicals, Reagents, and Plastic/Glassware

Analytical grade chemicals and reagents were used and the suppliers of these are indicated throughout the text. Also, only reagent grade water (MQH_20) was used when solution production required water.

All plastic and glassware were washed, rinsed with MQH_20, and autoclave sterilized prior to use.

2.1.2 Bacterial Strains and Plasmids

Sure 2 super-competent cells were used (genotype: e14-(McrA-) Δ(mcrCB-hsdSMR-mrr)171 endA1 gyrA96 thi-1 supE44 relA1 lac recB recJ sbcC umuC::Tn5 (Kanr) uvrC [F´ proAB lacIqZΔM15 Tn10 (Tetr) Amy Camr source: Stratagene]. Tables 2.1 and 2.3 below described the plasmids used in this research project. All plasmids used had an ampicillin resistance gene.

Table 2.1: DNA Plasmids used within this Research Project

Plasmid	Description	Source
Adeno-associated viral vector 9	Viral vector rAAV subtype 2/9 known to be specific for cardiomyocytes	Dr Jim Wilson, The University of Pennsylvania, USA
pXX6 plasmid	Helper plasmid	Children Medical Research Institute, Sydney, Australia
rAAV9 Capsid plasmid	rAAV Capsid plasmid	
pPPT.CX45	LV plasmid encoding cDNA for rat Cx45	Vector plasmids produced by Eddy Kizana prior to research program based on pRRLsin18.cPPT.CMV.eGFP.WPRE Sydney, Australia
pPPT.Cx43	LV plasmid encoding cDNA for rat Cx43	
pPPT.NS11	Plasmid encoding a non-silencing gene	
pPPT.shRNA	LV plasmid encoding a shRNA to silence Cx45	
pPPT.GFP	LV plasmid encoding enhanced Green fluorescence protein	
pPPT.CX43	LV plasmid encoding cDNA for rat connexin43	

pUC18	Transformation control plasmid	Thermo Scientific, United States

2.1.3 Bacterial Growth Media

Escherichia coli were grown in Luria-Betani (LB) broth, NZY+ broth or on solid LB-agar. Fresh broth was prepared when required using 0.5% (w/v) yeast extract (Sigma-Aldrich), 1% (w/v) tryptone (Sigma-Aldrich), and 1% (w/v) sodium chloride (Sigma-Aldrich) dissolved in MQH_20. Bacteriological agar 1.5% (w/v) was added to fresh broth when LB-agar was required. Media was autoclave sterilized at 121°C for 20 minutes. Ampicillin at a concentration of 100µg/mL was added after the media was cooled to approximately 55°C, and poured into 10cm petri dishes and then left in a reverse cycle hood to cool down and solidify.

Fresh NZY+ broth was prepared using 1% (w/v) NZ amine (Sigma-Aldrich), 0.5% (w/v) yeast extract, and 0.5% (w/v) sodium chloride dissolved in MQH_2O. The pH was adjusted to 7.5 by using sodium hydroxide (Sigma-Aldrich) then autoclave sterilized. Prior to use 12.5mL of 1M $MgCl_2$, 12.5mL of 1M $MgSO_4$, 20mL of 20% (w/v) and ampicillin 100µg/mL was added per litre of media.

2.1.4 Propagation of Plasmids

2.1.4.1 Cloning DNA using SURE 2 Super Competent Cells

SURE2 (Stop Unwanted Rearrangement Events) cells obtained from STRATAGENE were thawed on ice, and 100µL of cells were aliquoted into pre-chilled 14-mL BD Falcon polypropylene round–bottom tubes on ice. Two µL of the Beta-ME provided by STRATAGENE was added to the cells and incubated on ice for 10 minutes with gentle swirling every 2 minutes. Fifty ng of the DNA was added to the cells and incubated on ice for 30 minutes. After the tubes were heat-pulsed in a 42^{o}C water bath for 30 seconds, they were further incubated on ice for 2 minutes. Nine hundred µL of preheated (42^{o}C) NZY broth was added and incubated at 37^{o}C for 1 hour with shaking at 250rpm. A hundred µL of the mixture was then plated on LB agar plates. Plates were incubated at 37^{o}C overnight. Approximately 50 colonies are expected. The efficiency of those cells ≥1.0 10^{X9} cfu/µg of required DNA.

2.1.4.2 Making a Glycerol Stock

A starter culture was produced by inoculating 5mL LB broth with a single fresh colony of transformed cells in a 14mL polypropylene tube and then incubated for 6-8 hours on an orbital shaker at 37**º**C. The starter culture

was added to 200mL of LB broth and incubated on an orbital shaker at 240rpm at 37ºC overnight. Spectrophotometry would be used to assess that cultures reached mid-log phase growth (absorbance of 0.4 at 600nm). The next morning, a glycerol stock was made by mixing 850µL of the bacterial suspension with 150µL of glycerol stock (Sigma-Aldrich) and subsequently stored in a -80ºC freezer. For long term storage after 24hours the stock was then transferred to liquid nitrogen storage until further use.

2.1.4.3 Small Scale Production of Plasmid DNA

Small scale preparation were firstly carried out to confirm the plasmid DNA according to the alkaline lysis method using commercially available buffers provided by Qiagen mini prep kit. Five mL LB medium was inoculated with a single colony from a freshly streaked selective plate or from our glycerol stock. This was incubated for 16 hours at 37^{o}C on an orbital shaker and pelleted at 6000 x g for 3 minutes at room temperature. The bacterial pellet was then resuspended in 250µL of Buffer P1 containing RNASE A. The mixture was transferred to a micro-centrifuge tube. Cells were lysed with a 250µL of buffer P2 and mixed thoroughly by inverting the tube 4-6 times; then incubated for 5 minutes at room temperature. Genomic DNA, protein, and cell debris were precipitated

with the addition of 350µL of buffer N3 and mixed thoroughly at room temperature. This was then centrifuged for 10 minutes at 13,000 rpm (Sorvall RC 6+ centrifuge). The supernatant was applied to a QIAprep spin column by pipetting and centrifuged for 60 seconds at 13,000 rpm. The flow-through was discarded and the spin column was washed by adding 0.5mL Buffer PB and centrifuged at 13,0000rpm for 1 minute. The flow-through once again then centrifuged for a further minute. The QIAprep column was placed in a clean 1.5mL microcentrifuge tube. To elute the DNA, 50 µL buffer EB (10mM tris-HCl, pH 8.5) was applied to the centre of the QIAprep spin column, let it stand for 1 minute then centrifuged for 1 minute at 13,000rpm. Spectrophotometry was then used to assess DNA concentration and purity. A Nanodrop was then used to assess DNA concentration and purity. DNA was also subjected to restriction endonuclease digestion followed by agarose gel electrophoresis and UV imaging to confirm the DNA characteristics.

2.1.4.4 Maxiprep Plasmid DNA Extraction

A starter culture was made by inoculating 5mL of LB broth from a glycerol stock of the required plasmid DNA in a 14mL polypropylene tube and incubated for 6 hours on an orbital shaker at 37ºC. One mL of the starter culture was then added to a 200mL of LB broth in a 1L conical flask on an

orbital shaker at 240rpm at 37ºC overnight. The following morning, the culture was pelleted at 6,000g for 15 minutes at 4ºC. The supernatant was discarded and the bacterial pellet was processed by the alkaline lysis method using a commercially available Qiagen HiSpeed Plasmid Maxi kit according to the manufacturer's protocol. The cell pellet was resuspended in 10mL of buffer P1 containing RNase A. Followed by lysis with the addition of 10mL of buffer P2 and incubated for 5 minutes at room temperature. Genomic DNA, protein, and cell debris were precipitated with the addition of 10mL of chilled buffer P3 and incubated for 10 minutes at room temperature. A HiSpeed Maxi Tip was equilibrated with 10mL buffer QBT during the incubation period. The lysate was then filtered with a QIAfilter cartridge onto the HiSpeed Maxi Tip and allowed to pass through the resin by gravity flow. Following 60mL of buffer QC was used to wash the HiSpeed Maxi Tip and the DNA eluted using 15mL of buffer QF into a 50mL polypropylene tube. DNA was precipitated with 10.5mL of 100% (v/v) isopropanol (Sigma-Aldrich) for 5 minutes. The elute/isopropanol mixture was filtered through a QIAprecipitator. Five mL of 70% (v/v) ethanol (Fronine) was then used to wash the QIA precipitator and air dried. DNA was subsequently eluted with 1mL of Tris buffer. Nanodrop was then used to assess DNA concentration and purity prior to storage in a -80°C freezer. The yield of plasmid DNA achieved varied between 0.2mg to 1.5mg.

2.1.4.5 Gigaprep (Large scale) Production of Plasmid DNA

To extract large amounts of plasmid specifically plasmid pXX6, the Qiagen High Speed Maxi Prep was used according to the manufacturer's protocol. The cell pellet was resuspended in 125mL of buffer P1 containing RNase A. Lysis was enacted with the addition of 125mL of buffer P2 and subsequent incubation for 5 minutes at room temperature. Genomic DNA, protein, and cell debris were precipitated with the addition of 10mL of chilled buffer P3 and subsequent incubation for 125 minutes at room temperature. During the incubation period, a HiSpeed Giga Tip was equilibrated with 75mL buffer QBT. The lysate was filtered with a QIAfilter cartridge onto the HiSpeed Giga Tip and allowed to pass through the resin by gravity flow. The HiSpeed Maxi Tip was washed with 600mL of buffer QC and the DNA eluted using 100mL of buffer QF into two 50mL polypropylene tube. DNA was precipitated by mixing with 70mL of 100% (v/v) isopropanol (Sigma-Aldrich) and centrifuged at 15000g for 30mins at 4°C and the supernatant removed. The pellet was washed with 10mL of 70% (v/v) ethanol (Fronine) and centrifuged at 15000g for 10mins at 4°C. The supernatant was then removed carefully and the pellet air dried. The pellet was dissolved in 1mL of Tris buffer. DNA concentration and purity of the new plasmid stock was assessed with Nanodrop prior to storage in a -80°C freezer. The yield of plasmid DNA varied between 1mg to 4mg.

2.1.4.6 Estimation of Plasmid DNA Concentration and Purity

The concentration and purity of DNA was determined by spectrophotometry measuring absorbance at wavelengths of 260nm and 280nm. This method assumes that 50µg of DNA to have an absorbance of 1.0 at 260nm and pure DNA has a 260/280 absorbance ratio of 1.8 (Sambrook et al.) [136].

DNA samples were routinely subjected to spectrophotometry and measurements were made at one or two dilutions.

2.1.4.7 Agarose-gel Electrophoresis

Horizontal agarose-gel electrophoresis was used to analyse plasmid DNA following restriction enzyme digest. Preparation of the agarose gel was at 0.8% (w/v) agarose (Amresco) in TAE (40 mM Tris-acetate and 1 mM EDTA) heated at low power microwave oven until the agarose was molten. Following ethidium bromide (Sigma-Aldrich) was added at 1 µg/mL once the agarose was cooled to about 55^{o}C. When it had set, 1 to 3 µL of 6 x 6 gel loading buffer (30% (v/v) glycerol, 0.25% (w/v) bromophenol and 0.25% (w/v xylene-cyanol FF in MQH_2O) was added to

5 to 15 µL of DNA sample and loaded onto the gel. Molecular weight marker I (Bioline - Roche Colecular Products), was used to estimate the size of DNA fragments. The gel was run in 1 X TAE buffer at a constant voltage of 100 Volts until the dye front had moved a suitable distance. A UV trans-illuminator was used to examine the gels and then photographed using a Gel Doc 100 (Bio-Rad) Camera.

2.1.4.8 Restriction Endonuclease Digestion of Plasmid DNA

Restriction endonuclease digestion of DNA was performed according to the manufacturer's specifications. Diagnostic restriction endonucleases were performed on 500-1000 ng of plasmid DNA using 5 – 10 units of enzyme. The digests were performed in 1.5mL polypropylene microcentrifuge tubes in the presence of the appropriate buffer in a total volume of 20 µL of MQH_2O. The digests were incubated at the requisite temperature for 1 hour then were analysed by agarose-gel electrophoresis for DNA characterisation.

2.2 Cell Culture

2.2.1 Cell Lines, Reagents, and Plastic/Glassware

Table 2.2 lists the cell lines and respective culture conditions used during this project.

Cell culture media was freshly supplemented with the cell culture grade reagents specified in Table 2.2 prior to the commencement of individual experimental protocols.

For subculture and other manipulations, human embryonic kidney (HEK293) cells were washed with Dulbecco's Phosphate Buffered Saline (DPBS) (lacking calcium and magnesium) (Lonza) and detached and aggregated using 0.05% Trypsin/0.5mM EDTA solution (Sigma-Aldrich).

Sterile filtered foetal bovine serum (FBS; SAFC Biosciences), was stored at -20ºC. When required it was heat inactivated by warming to 37ºC for 30 minutes. Ten mL of Dulbecco's Modified Eagles Medium (DMEM) with FBS was added to the detached aggregate to inactivate the trypsin.

Cell culture plastic ware including culture flasks and serological pipettes were obtained from Falcon and Corning and were only used once. All glassware was washed, rinsed with MQH_2O and autoclave sterilized prior to use.

Table 2.2: Cell Types used in Cell Culture Experiments

Cell Type	Description	Source	Medium
HEK293	Human embryonic kidney cells	Children's Medical research Institute, Westmead Children's hospital	1,2
NRVM	Primary Day 2-3, neonatal rat ventricular myocytes	Adult Sprague Dawley rats, Animal Resourced Centre, Western Australia	3,4,5,6

1. Dulbecco's Modified Eagles Medium (DMEM; Invitrogen) supplemented with 10% (v/v) FBS (SAFC Biosciences)
2. Iscove's Modified Dulbecco's Medium (IMDM; Invitrogen) supplemented with 10% (v/v) FBS (SAFC Biosciences).
3. Hank's Balanced Salt Solution (HBSS; Invitrogen)
4. HBSS with 1mg/mL Ultrapure Trypsin (Trypsin 4.066 USP u/mg, Chymotrypsin 12.13 USP u/mg; USB Corporation)
5. HBSS with 1mg/mL Collagenase Type 2 (245u/mg; Worthington)
6. Medium 199 (Invitrogen) supplemented with 1% HEPES Buffer Solution (Invitrogen), 1% MEM Non-Essential Amino Acids (Invitrogen), 1.75g Glucose (Sigma-Aldrich), 2mM L-Glutamine (Invitrogen), 1.5μm/L Vitamin B12, 20U/mL Penicillin solution (Sigma), and 2% or 10% (v/v) FBS (SAFC Biosciences).

2.2.2 General Cell Culture Methods

Cell culture methods employed in this research project are detailed by Sambrook et al. [136]. Cells were grown in disposable polystyrene flasks/dishes (Falcon, Greiner and Corning) or sterile glassware containing their respective media as detailed in the above Section 2.2.1. All cultures were incubated in a 5% CO_2 environment at 37ºC.

2.2.2.1 Cell Counting using a Haemocytometer

Adherent cells were counted following trypsinisation into a single cell suspension at a concentration of 10^5 to 10^6 cells per mL. A 10uL aliquot was applied beneath each side of a cover slipped haemocytometer (Neubauer). A 10X objective of an inverted microscope (Olympus CK2) was used to count live cells. The number of cells in the 4 major outer corners of each of the 2 chambers (8 squares in total) was averaged, corrected for dilution, and multiplied by 10^4 to give the number of cells per mL.

2.2.2.2 Subculture of Adherent HEK293 Cells

When cultures became approximately 70% confluent or were required for experimentation, cells were subcultured by enzymatic detachment and

replating. Culture media was firstly aspirated from the flask and the cells were washed once with 5mL PBS. Two mL of 0.05% Trypsin/EDTA solution was added to the culture and placed at 37ºC humidified chamber for 2 minutes to further cell detachment. Trypsin was then subsequently inactivated by the addition of 10mL of culture media. To further dis-aggregate the cells the media was pipetted up and down approximately 5 times. An aliquot of the cell suspension was seeded into a new culture flask with fresh culture media according to the dilution required. Cells were split one to three times per week depending on their growth kinetics.

2.2.2.3 Short and Long term Storage of HEK293 cells

To allow short term and long term storage, cells required were detached by trypsinisation during exponential growth and pelleted by centrifugation (1500rpm, 5 minutes). Media was aspirated and the cells resuspended at 2 X 10^6 per mL in storage media consisting of culture media with 20-50% FBS and 10% (v/v) DMSO (Sigma-Aldrich). Cell suspension aliquots of 1mL were placed in sterile cryovials (Nunc) and stored at -80ºC for short term storage. Twenty four hours later, those needed for long term storage were then moved to liquid nitrogen.

To recover cells from short and long term storage, cells were rapidly thawed in a 37ºC water bath. The contents of the cryovial was mixed with 9mL of warmed (37ºC) culture media to remove the DMSO, pelleted at 1500 rpm for 5 minutes, and resuspended in fresh culture media following aspiration of the supernatant.

2.2.3 Primary Cell Culture

2.2.3.1 Plating Surface Preparation

Surfaces of 8 well plates intended for cardiomyocytes culturing were sterilized with ultraviolet light for 1 hour on the day of ventricular harvesting from rat pups. Surfaces were then coated at room temperature using a fresh 25mg/mL solution of fibronectin powder (BD Biosciences) dissolved in MQH_20 that had been previously filter sterilized with a 0.45µm PVDF syringe driven filter.

2.2.3.2 Isolation of Neonatal Rat Ventricular Cardiomyocytes

These cultures were established by Dr Ajita Kanthan in Westmead Millennium Institute. Neonatal RVMs suspended in culture media were

supplied for experimental use in this project. The experiments for procuring NRVMs were approved by the Westmead Hospital Animal Ethics Committee.

Two litters of rat pups (1 -3 days old Sprague-Dawley) were used for each dissection. Pups were sprayed with 70% ethanol, decapitated with a large pair of straight surgical scissors (Roboz Surgical Instrument Co), and their chests opened with angled delicate scissors (Roboz Surgical Instrument Co). Ventricles were excised and minced in ice cold Hank's balanced salt solution (HBSS) without calcium and magnesium (Sigma-Aldrich). Following 2 rinses with ice cold HBSS, ventricular tissue was transferred to a glass jar containing 40mL of trypsin/HBSS solution, and agitated on an orbital shaker at 75rpm at 4ºC for 16 hours. The media was then aspirated and discarded. Warm 10% serum culture media was added and gently agitated in a 37ºC water bath for 4 minutes. The media once again was aspirated and discarded. Fresh collagenase/HBSS (8mL) was added to the tissue and gently agitated in a 37ºC water bath for 1 minute. The collagenase/HBSS solution was aspirated and discarded. Eight mL of fresh collagenase/HBBS solution was added to the tissue and gently agitated in a 37ºC water bath for 1 minute. To assist with myocytes dissociation, the tissue and media was pipetted up and down once with a

10mL serological pipette. The media was aspirated and added to ice cold HBSS and kept on ice. Again 8mL of collagenase/HBSS was added to the tissue and the process repeated 3 times. The 4 aliquots of HBSS solution containing dissociated cells were pelleted at 50 x g at 4ºC for 8 minutes. The supernatant was aspirated and the pellets resuspended in 8mL of ice cold HBSS. The cell suspension was then filtered with a 40µm cell strainer (BD Biosciences). The filtrate was centrifuged at 50 x g at 4ºC for 6 minutes and the supernatant was aspirated and discarded. The pellet was resuspended in warm 10% serum culture media, pre-plated into a 150cm^2 tissue culture flask, and incubated at 37ºC at 5% CO_2 for 2 hours. This pre-plating step allowed for the removal of fibroblasts.

Media containing non-attached cardiomyocytes was then aspirated and placed into a 50mL polypropylene tube. The tissue culture flask was rinsed carefully with 10% serum culture media and the rinse also added to the 50mL polypropylene tube. The media was gently mixed by pipetting up and down once. Cells were then counted as described in Section 2.2.2.1. A further 10% serum culture media was added to the cell suspension to achieve a final density of 7x10^5 cardiomyocytes/mL. A confluent monolayer was achieved at 24 hours post plating at this density.

2.2.3.3 Post Plating Care of Cardiomyocyte Cultures

Twenty four hours after plating cardiomyocytes, media was aspirated and the myocytes washed once with pre-warmed 37°C PBS. Pre-warmed to 37°C fresh 10% serum culture media was added to the myocytes and the cells returned to the humidified incubator. To prevent the growth of fibroblasts, media was replaced with fresh pre-warmed to 37°C 2% serum culture media at 48 hours and 90 hours post plating.

2.3 Production and Application of Recombinant Adeno-Associated Viral Vectors 2/9

2.3.1 Recombinant Adeno-associated Viral Vector Plasmids

Recombinant adeno-associated virus serotype 2/9 vector was used throughout this research project. The plasmids used for vector production were cloned by Dr Renuka Rao in the lab and sequencing was carried out to determine a forward orientation relative to Chicken Beta Actin (CBA) promoter. The vectors also contained the Woodchuck hepatitis virus post-transcription (WPRE) regulatory element. The Cx45, Cx43 and GFP were sub-cloned from the respective Lentivirus vectors (Table 2.4) (from Dr Eddy Kizana) into the Multiple Cloning Site (MCS) of the rAAV vector back-bone (Figure 2.1). For the silencing vector, RNA polymerase III

promoter (H1) together with a short hairpin RNA (shRNA) for Cx45 or a scrambled Non-Silencing sequence was sub-cloned upstream to the CBA promoter into the KpnI site. For controls GFP reporter in the rAAV vector and the empty vector were used. For a list of plasmids generated for this project see Table 2.3

Figure 2.1 Vector Map

Vector map for rAAV-9. Transgenes GFP, Cx43 or Cx45 were inserted in the same site downstream of the CBA (chicken beta actin) promoter. WPRE = woodchuck hepatitis virus post-transcriptional regulatory element ****

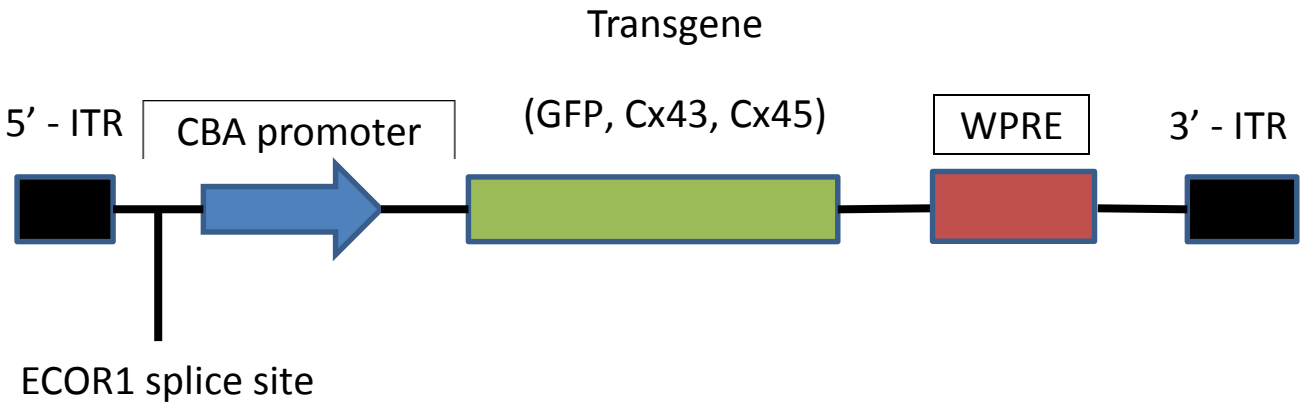

Table 2.3 Plasmids

Plasmid	Description	Source
pXX6 plasmid	Helper plasmid	Children Medical Research Institute, Sydney, Australia
rAAV9 Caspid plasmid	AAV Caspid plasmid	
rAAV.Cx45	Vector AAV.Cx45.WPRE	Dr Renuka Rao Westmead Millennium Institute, Sydney, Australia
rAAV.GFP	Vector AAV.GFP.WPRE	
rAAV.Cx43	Vector AAV.Cx43.WPRE	
rAAV.sh45	Silencing vector H1868 AAV.Sh.Cx45.WPRE	
rAAV.shNS	Non-Silencing vector H1NS AAV.NS.WPRE	

Table 2.4 Lentiviral Vectors

Vector	Description	Source
pRRLsin18.cPPT.CMV.GFP.WPRE	Lentiviral GFP	Dr Eddy Kizana Westmead Millennium Institute, Sydney, Australia
pRRLsin18.cPPT.CMV.Cx43.WPRE	Lentiviral Cx43	
pRRLsin18.cPPT.CMV.Cx45.WPRE	Lentiviral Cx45	

2.3.2 Vector Production

Recombinant AAV vectors were produced using a helper-virus free system by calcium-phosphate co-precipitation transfection of the three vector plasmids into HEK293 cells. The method well described by Xinping Huang and Steven Gray was used and runs over several days [137-139]. All Solutions used are listed in Table 2.5.

The cells were cultured as mentioned previously and then using trypsin were split with a 1/5 or 1/10 ratio depending on need.

Table 2.5 Reagents used for Vector Production

Reagent	Description
TE(10%)	Tris 0.061g 1mM final EDTA 0.019g 0.1mM final Made to 500mL with MQH_20 after adjusting to pH 8 and autoclaved
2M $CaCl_2$ (147.02 MW)	29.404g of $CaCl_2.2H_2O$ in 100mL MQH_20. Autoclaved
2XHepes-buffered saline (HBS)	NaCl 8.182g 280mM final HEPES 5.959 50mM final Make up to 500mL with MQH_20 after adjusting to pH 7.0 and autoclaved
0.15M Na_2HPO_4	10.647g in 500mL MQH_20. Adjusted to pH 7.1 and autoclaved
Resuspension Buffer	NaCl (58.44 MW) 2.922g 100mM final $MgCl_2.6H_2O$ (203.3MW) 0.2033g 2mM final

	1M tris (121.14MW) 5mL 10mM final Made up to 500mL MQH_20. Adjusted to pH 8.0 and autoclaved
Citric Saline 10X	KCl (74.5513 MW) 50.3g 1.35M final Sodium Citrate (294.1 MW) 22.05g 0.15M final Dissolved in MQH_20 and adjusted to 500mL. Autoclaved. Diluted 1:10 with sterile $MQH_20$to prepare a 1X solution (50mL of 10X citric saline plus 450mL water)
Growth Medium	DMEM 10% FBS
Transfection Medium	IMDM 10% FBS
Maintenance Medium	DMEM 2% FBS

2.3.2.1 Preparing HEK293 cells for Transfection

HEK293 cells were seeded onto one hundred and twenty 10cm tissue culture dishes at $3.5x10^{x6}$ cells/dish with 8mL of growth medium. The cells were 50-70% confluent at time of transfection. The following morning the growth medium was replaced with Transfection Medium three hours before transfection. The dishes were changed 4 at a time carefully while leaving 2mL of old medium on the cells so they do not dry out. Removing and replacing 6mL of medium gently with a 25mL disposable pipette.

2.3.2.2 Transfection Solution

The triple plasmid transfection was done with the following plasmids using the Calcium Phosphate method

15µg DNA/Dish:

3µg Vector DNA

3µg Packaging/Capsid Plasmid

9µg Helper plasmid

Solution A

	Volume 120 dishes (mL)	
3 x Plasmid DNA	X	2mg
100% TE	Y	
2M CaCl2	7.5	0.5M
Total	**60**	

Solution B

	Volume 120 dishes (mL)
2 x HBS	59.4
0.15M Na_2HPO_4	0.6
Total	**60**

Four mL of Solution A was aliquoted into 15 polypropylene (opaque) 15mL round-bottom tubes. Four mL of Solution B was aliquoted to 15 polystyrene (clear) 15mL round–bottom tubes. Solution A was slowly added drop wise using a P200 pipette, while mixing to Solution B to precipitate the DNA. Solution mix was then incubated for 20 minutes at room temperature before adding precipitate to cells, 1mL per dish. Cells were incubated overnight at 37^{o}C. Sixteen hours Later the medium was changed to Maintenance Medium. Sixty hours after transfection, the cells were harvested from the transfected dishes by scraping cells into the medium. They were pipetted 5 times using a 10mL pipette to help take off as much of the cells from the dishes and collected into 50mL tubes. The cells were pelleted by centrifugation at 1500rpm for 5 minutes. The supernatant was discarded. The pellets were then resuspended by using 15mL of Resuspension Buffer starting from tube one and then transferred to tube two and so on. This step was repeated a further five times to a cumulative total of 90mL of Resuspension Buffer from the 120 dishes.

2.3.2.4 Vector Purification and Concentration

The reagents are listed in Table 2.6

The cell suspension was frozen and thawed 3 times in a dry ice/100% ethanol bath (approximately 20 minutes for each freeze and thaw cycle), then centrifuged at 4000rpm for 15 minutes. The supernatant was collected and the pellet discarded. Benzonase (Sigma) was added to the supernatant at 50units/mL and incubated at 37^{o}C for 30 minutes. The mixture was centrifuged at 4000rpm for 10 minutes and the supernatant collected. Ice cold saturated $(NH_4)_2SO_4$ was added to the supernatant at 1/3 of the original volume and incubated on ice for 10 minutes. After centrifugation at 4000rpm for 15 minutes, the supernatant was collected and this time 2/3 of original volume ice cold saturated $(NH_2)_2SO_4$ was added to the supernatant and incubated on ice for 20 minutes. Following centrifugation at 12,000g for 15 minutes the supernatant was discarded. The pellet was then resuspended in at total of 60mL of 1.37g/mL CsCl solution and transferred into 6X10mL SW41 Centrifugation tubes (Beckman, UltraClear, 14x89mm). One mL of 1.5g/mL CsCl was added to the bottom of each tube using a Pasteur pipette as a cushion. The tubes were balanced and then ultra-centrifuged in a SW41 rotor (Sorvall RC 6+) at 16^{o}C for 40 hours at 36000rpm. After 40 hours the tubes were taken out of the rotor; 2mL was removed from the top of each tube. Using a 21

gauge needle the bottom of the tubes was pierced and solution collected in 1mL fractions into 14mL polypropylene round-bottom tubes. The fractions were analysed by qPCR to determine which fractions had the highest concentration of virus. The fractions with the highest yield (usually 2-3 fractions) were pooled together and dialysed twice with PBS (with calcium and magnesium) using a Slide-A-Lyzer Dialysis Cassette (10,000 MWCO, 3mL - 9mL Pierce Cat 66810). The second dialysis was kept on overnight in the cold room (4^{o}C) while being stirred slowly. Next morning the dialysis fluid was replaced with fresh PBS, this time with 5% Glycerol added and dialysed for an additional 4 hours. The virus was then concentrated with Vivaspin 20 (100,000 MWCO) at 3000g at 4^{o}C to get a total of 1mL final concentration. This was then divided equally into 10 tubes each containing 100µL of concentrated virus. Two µL was frozen separately for PCR the next morning following a single freeze and thaw as would be the case with virus used for animal experiments. The sample left for qPCR was then thawed on ice and diluted into 1:10^{3}, 1:10^{4}, 1:10^{5} and 1:10^{6} and was used to ascertain the amount of viral vector by qPCR. The yield was usually 1.0 – 1.5x10^{13}/mL.

Table 2.6 Reagents for Vector Purification and Concentration

Reagent	Description
Saturated ammonium sulphate solution	530g of $(NH_4)_2SO_4$ dissolved in 1L of water and pH adjusted to 7.0 while warming to help it dissolve. Solution was filter sterilized using a 0.45mcm cellulose filter (Nalgene) pre-wet with a few drops of water. Stored at 4^oC.
Cesium chloride solution 1.5g/mL in PBS	33.75g of CsCl was dissolved in PBS (with Calcium and Magnesium) adjusted to a final volume of 50mL. 1mL of the solution was weighed to check the density of the solution to get 1.5g/mL -> if it weighed less, then more CsCl was added to the solution. Solution was then filter sterilized through a 0.2µm filter pre-wet with a few drops of water. Then stored at room temperature
Cesium Chloride solution 1.37g/mL in PBS	50g of CsCl was dissolved in PBS (with Calcium and Magnesium) adjusted to a final volume of 100mL. 1mL of the solution was weighed to check the density of the solution to get 1.5g/mL -

	> if it weighed less, then more CsCl was added to the solution. Solution was then filter sterilized through a 0.2µm filter pre-wet with a few drops of water. Then stored at room temperature
Dialysis Solution 4L made	PBS (with Calcium and Magnesium) $CaCl_2$ anhydrous 0.1g/L $MgCl_2.6H_2O$ 0.1g/L

2.3.4 Assigning Titre to Vectors

Recombinant AAV2/9 titre was assigned by qPCR as described by Huang et al.[137]

2.3.4.3 Real Time Quantitative PCR of Genomic DNA

Sequences for the rAAV forward primer AAV1277F (5'-CCGTTGTCAGGCAACGTG), reverse primer AAV1361R (AGCTGACAGGTGGTGGCAAT), and probe (5' –[6FAM]TGCTGACGCAACCCCCACTGGT[TAM]) were used as described by Huang el al. and manufactured by Sigma Aldrich [137, 140]. A master mix was made up with 1µL of probe, 0.8µL of each forward and reverse primers, 4.9µL of DNASEfree RNA (Sigmal Aldrich) and a master mix 12.5µL (Bioline), and 5µL of DNA per PCR reaction. As a negative template control, 5µL of H_20 was used.

All reactions were carried out in triplicate and amplifications were performed with 1 cycle of 95°C for 10 minute, 35 cycles of 95°C for 15 seconds, and 60°C for 2 minutes using a Rotor-Gene 6000 PCR cycler (Corbett) or Rotor-Gene 3000 PCR cycler (Corbett). Concurrent standard curves were generated using 7 serial 10 fold dilutions from

10^8molecules/µL of the plasmid AAV-CBA-WPRE digested iECOR1. The number of vector DNA molecules in each sample reaction was calculated by comparing threshold cycle values of samples to the standard curve. To determine the final viral vector titre, the number of vector DNA molecules of each sample reaction was corrected for dilution and then averaged.

2.4 Immunohistochemistry – Staining for Connexins

2.4.1 Antibodies for Immunohistochemistry

Primary and secondary antibodies used during experiments are listed in Table 2.7. Antibodies that required storage at -20°C were divided into 10µL aliquots using microcentrifuge tubes to minimise freeze-thaw cycles.

Antibody Validation

Specificity of antibodies to Cx43, Cx45 and GFP were validated using non-transduced HEK293 cells that are known to be devoid of connexins and GFP. Specific antibody reactivity was established in cells transfected plasmids expressing each of these transgenes.

Table 2.7: Immunohistochemistry Antibodies

Primary Ab Specificity		Host Species	Source	Dilution
Connexin45		Mouse, monoclonal	Millipore	1 in 200
Connexin43		Rabbit, monoclonal	Millipore	1 in 800
Connexin43		Mouse, Monoclonal	Millipore	1 in 250
Connexin43		Rabbit, Polyclonal	Chemicon	1 in 250
Connexin45		Rabbit Polyclonal	Gift from Dr M. Koval, Department of Medicine, Washington University School of Medicine, St. Louis, Missouri USA	1 in 200
Secondary Ab Specificity	**Fluorophore**			

Mouse Fc	Alexa Fluor 488	Goat, $F(ab')_2$ fragment	Invitrogen	1 in 1000
Rabbit Fc	Alexa Fluor 594	Goat, $F(ab')_2$ fragment	Invitrogen	1 in 2000
Mouse Fc	Alexa Fluor 594	Goat, $F(ab')_2$ fragment	Invitrogen	1 in 2000

2.4.2 Ventricular Tissue Sectioning

All Cryo-sectioning was performed with a Microm HM 505E microtome cryostat. The temperature of the cooling chamber was set at -20°C prior to the commencement of tissue handling and cutting. Frozen ventricular tissue embedded in OCT compound were mounted on a cryostat chuck pre-cooled with dry ice, and placed on the cryostat arm. A microtome knife was used to initially trim the specimen, and then cut 5µm-7µm sections of ventricle that were transferred to glass slides (Superfrost Ultra Plus; Thermo Scientific) and kept on in the chamber until transfer to -20^{o}C freezer until required for use.

2.4.3 Fixation, Permeabilisation and Immunostaining

Ventricular tissue sections and cell cultures were fixed, permeabilised and immunostained using the same method. Samples were fixed with 4% (w/v) paraformaldehyde for 15 minutes at room temperature. Paraformaldehyde was freshly prepared by dissolving 3.2g in 80mL of PBS containing calcium and magnesium at 56^{o}C. The pH was adjusted to 7.4 with 5M NaOH. Slides were then washed 3 times with PBS for 5 minutes each time. As the primary antibody epitopes are intracellular antigens, samples were subject to permeabilisation with 0.1% (v/v) Triton

X-100 (Sigma-Aldrich) in PBS for 15 minutes. This was followed by 3 gentle washes with 0.05% (v/v) Tween 20 (Sigma-Aldrich) in PBS (PBST) for 5 minutes each on an orbital shaker. Following the wash and permeabilisation non-specific sites were blocked with a blocking solution from Dako (Protein Block, serum-Free) for 1 hour. The blocking solution was then removed and samples were then incubated with primary antibody diluted in blocking solution overnight at 4°C.

The following morning, samples were washed 3 times with PBST for 5 minutes each on an orbital shaker. Secondary antibody, diluted with 0.1% (v/v) cold fish skin gelatine in PBST, was added to samples for 1 hour at room temperature in the dark. This was followed by 3 gentle washes with PBST for 5 minutes each on an orbital shaker in the dark. Samples were then dried for half an hour before being cover slipped (Deckgläser; Menzel-Gläser) mounted with Prolong Gold anti-fade reagent with DAPI (Life Technologies). This was then allowed to set in the dark, overnight and 4°C.

2.4.4 Co-immunostaining

Co-immunostaining was carried out using a protocol similar to the above method with some modification. Ventricular tissue sections and cell cultures were fixed, permeabilised and immunostained using the same method. Samples were fixed with 4% (w/v) Paraformaldehyde for 15 minutes at room temperature. Paraformaldehyde was freshly prepared by dissolving 3.2g in 80mL of PBS containing calcium and magnesium at 56^{o}C. The pH was adjusted to 7.4 with 5M NaOH. Slides were washed 3 times with PBS for 5 minutes each time. Samples were subject to permeabilisation with 0.1% (v/v) Triton X-100 (Sigma-Aldrich) in PBS for 15 minutes. This was followed by 3 gentle washes with 0.05% (v/v) Tween 20 (Sigma-Aldrich) in PBS (PBST) for 5 minutes each on an orbital shaker. Following the wash and permeabilisation non-specific sites were blocked with a blocking solution from Dako (Protein Block, serum-Free) for 1 hour. The blocking solution was then removed and samples were then incubated with primary antibody diluted in blocking solution overnight at 4°C. Given this was for co-immunostaining, two primary antibodies were mixed and used (both had different host species to allow different secondaries to be used).

The following morning, samples were washed 3 times with PBST for 5 minutes each on an orbital shaker. Secondary antibody, diluted with 0.1% (v/v) cold fish skin gelatine in PBST, was added to samples for 1 hour at room temperature in the dark. Again given this was for co-localisation studies, 2 different secondaries corresponding to the primary antibody species were mixed together as per the above Table 2.7 (2 different fluorescent markers were used for detection). This was followed by 3 gentle washes with PBST for 5 minutes each on an orbital shaker in the dark. Samples were then dried for half an hour before being cover slipped (Deckgläser; Menzel-Gläser) mounted with Prolong Gold anti-fade reagent with DAPI (Life Technologies). This was then allowed to set in the dark, overnight and 4°C.

2.4.5 Fluorescent Image Acquisition and Processing

Imaging was performed under oil immersion using either an inverted wide field fluorescent microscope (Leica DMIL and Nuance FX system Camera (420-720nm, 20-40nm bandwidth, Cooled Sony ICX285) with a 40X – 100X objective (Leica 40X/0.50 Ph2 /1.1 506273 HI plan 1) or a confocal laser scanning microscope (Olympus FV 1000) using a 40X – 60X objective (Olympus 40X/1.30/0.20 (WD) Oil UPLFLN). Digital images from the Leica microscope were acquired into PC based software (Nuance

imaging software version 3.1) using a digital camera (Nuance FX) fitted to the microscope. Digital images from the confocal microscope were directly acquired into PC based software (Olympus FV10-ASW Version 1.7).

Table 2.8: Filter Sets for Leica DMIL Microscope

Filter Sets	Exciter (nm)	Emitter (nm)
DAPI	315 – 420	385 - 515
GFP	430 – 510	475 - 575
DsRed	480 – 570	565 ALP

Table 2.9: Excitation Wavelengths and Emission Filter Sets for the Olympus Confocal Microscope

Filter Sets	Excitation (nm)	Emission (nm)
WU2	BP 330 - 385	BA 420
NIBA3	BP 470 - 495	BA 510 - 550
WIG3	BP 530 - 550	BA 575 IF

2.5 Histology – Inflammation and Fibrosis

2.5.1 Inflammation - Haematoxylin and Eosin (H&E) Staining

Ventricular tissue sections were produced as described in section 2.4.2. The technique of H&E staining as described by LG Luna was performed with a Shandon Linear Stainer provided by Westmead Millennium Institute [141].

Ventricular sections were initially immersed in Haematoxylin for a total of 4 minutes, Scott's Bluing solution for 1 minute, and 0.1% Eosin for 1 minute. A 1 minute wash with tap room temperature water was performed following each step. Samples were then dehydrated with absolute ethanol for 30 seconds and placed in xylene clearing solution Following, the slides were coverslip mounted with a hydrophobic mounting agent, Ultramount No4 with colourfast (Fronine). Slides were allowed to set overnight.

Following image acquisition as described in Section 2.5.3, images were assessed manually for inflammation by two independent observers. The technique described by Igarashi et al was used to grade inflammation on a scale of 1 to 5 Table 2.10 [142].

2.5.2 Fibrosis - Pico-Sirius Red staining

Ventricular tissue sections produced as described in Section 2.4.2. Sections were fixed with 4% paraformaldehyde for 15 minutes and then washed 3 X in PBS for 5 minutes each. Following, sections were placed in Pico-Sirius red solution (0.1% Direct Red 80 (Sigma), 0.1% Fast Green FCF (Sigma), Saturated Picric Acid (Sigma)) for 1 hour in the dark on an orbital shaker. Sections were then washed twice carefully with MQH_20 followed by 3 washes in 100% ethanol for 1 minute each to assist in dehydration of the sections. They were then air dried for 1 hour and then immersed in xylene clearing solution for 5 seconds before cover slip mounting with a hydrophobic mounting agent, Ultramount No4 with colourfast (Fronine). Slides were left overnight to set. Sections were then analysed with custom made software designed (By Tony Barry from the Centre of Heart Research, Sydney, Australia) to objectively calculate the relative areas of red (collagen) and green stains (myocytes).

Table 2.10 Inflammation Scores

Scores	Inflammation
1	No inflammation
2	Occasional inflammation present
3	Diffuse affecting <50% of the image
4	Diffusely present and more than 50% of image
5	Near complete presence of inflammation present

2.5.3 Image Acquisition and Processing

An upright microscope (Leica DMBL) was used to visualise the samples then a 40X objective (Leica 40X/0.65 N plan /0.17/D 506099 Ph2) was used for acquisition of images from 4 random areas of each section under oil immersion. Sections from the apex, mid and base of each heart analysed were acquired to get an average amount of fibrosis. The PC based software, Spot Advanced version 4.1, was used to directly acquire digital images from a Spot RT KE camera fitted to the microscope.

2.6 Immunoblotting

2.6.1 Antibodies for Immunoblotting

Primary antibodies and secondary used during experiments are listed in table 2.7. Secondary antibodies used during experiments are listed in table 2.11. Antibodies that required storage at -20°C were divided into 10-15µL aliquots using microcentrifuge tubes to minimise freeze-thaw cycles.

Table 2.11: Secondary antibodies for immunoblotting

Secondary Ab Specificity	Label	Host Species	Source	Dilution
Mouse Fc	HRP	Goat	Sigma	1 in 10000
Rabbit Fc	HRP	Goat	Sigma	1 in 10000

2.6.2 Protein Extraction

Ventricular tissue

Frozen collected ventricular tissue was placed into an ice cold round bottom microcentrifuge tube. Tissue used for protein extraction was flash frozen in nitrogen when collected. Tissue was divided into 50mg sections using a scalpel on metal plate over a surface of dry ice then placed in a new microcentrifuge tube and kept on dry ice. An ice cold steel ball (Qiagen) was inserted into the tube along with 500µL of ice cold lysis solution (RIPA buffer (Sigma-Aldrich), 1% (v/v) phosphatase inhibitor cocktail 2 (Sigma-Aldrich), and 4% (v/v) protease inhibitor cocktail (Sigma-Aldrich). The tissue was subjected to disruption with bead milling for 3 minutes using a TissueLyser (Qiagen) set to 30Hz. This was done twice to ensure the tissue was well homogenised. Suspensions were then centrifuged at 10,000rpm for 5 minutes at 4°C. The supernatant was decanted into a second microcentrifuge tube and kept on ice ready for protein estimation.

2.6.3 Protein Estimation

Protein estimation was performed using the Bradford method [143]. Standards and samples were assayed in triplicates. Bovine serum

albumin (1mg/mL) was added, in 1µL increments from 1µL to 8µL, to different wells of a 96 well plate, and used to generate a standard curve. Extracted protein samples were diluted 5 fold with MQH_20 and 1µL added to wells. Protein assay dye reagent concentrate (Bio-Rad) was diluted 4 fold and 200µL was added to each well. The absorbance used to measure was 595nm using a Victor^2 Multilabel Counter (PerkinElmer life Sciences). The amount of protein was calculated by comparing its absorbance to the standard curve. This was then corrected for the dilution and averaged to determine the original protein concentration of an individual lysis supernatant.

2.6.4 Immunoblotting

Precast polyacrylamide 4-12% gradient Bis-Tris gels (NuPAGE; Invitrogen) were used. These were placed in a gel electrophoresis chamber (XCell SureLock Min-Cell; Invitrogen) containing running buffer (MOPS, NuPAGE; Invitrogen). For each sample, 20mg of protein was diluted in a microcentrifuge tube to a final volume of 20µL with 2µL of reducing agent (NuPAGE; Invitrogen), 5µL of LDS sample buffer (NuPAGE; Invitrogen), and MQH_20. Samples were then subjected to 95°C heat for 10 minutes to denature proteins and then loaded into separate gel wells. A pre-stained protein ladder (PageRuler Plus; Thermo

Scientific) was used to assess protein separation and approximate protein sizes and was placed on wells adjacent to the study samples. A 200V constant current gradient was applied to the gel for 1 hour. Protein was transferred from the gels to a membrane using the IBLOT gel transfer system (Invitrogen), following electrophoretic separation. Gels were placed in a gel transfer stack (Invitrogen) and the IBLOT's default 7 minute transfer protocol was used. Membranes were then blocked with a solution of 5% skim milk in TBST (0.05% Tween 20, Tris-Buffered Saline) for 2 hours and subsequently incubated with primary antibody diluted in blocking solution. They were placed on an orbital shaker for gentle shaking overnight at 4°C.

The following morning, 3 washes with TBST were carried out for 5 minutes each, and incubated with secondary antibody diluted in blocking solution for 1 hour. Again this was placed on an orbital shaker for gentle shaking. The membranes once again were washed with TBST 3 times for 5 minutes each. SuperSignal Pico Chemiluminescent substrate (Thermo Fisher Scientific) blotting detection reagents was then added on to the membrane for 5 minutes, which had been mixed in a 1:1 ratio according to the manufacturer's instructions. To enable detection of weak signals, SuperSignal west Femto (Thermo Scientific) was mixed with a ratio of

1:10 with the Pico substrate, and then added to the membrane for 5 minutes. Membranes were transferred to an autoradiography cassette (Hypercassette; Amersham Biosciences). In a dark room, an X-ray film (Hyperfilm ECL; Amersham) was exposed to the Nitrocellulose membranes in the autoradiography cassette. The time required of exposure was dependant on the demands of the experiment. Films were then processed with an AGFA film processor according to the manufacturer's protocol.

2.7 Quantification of Tissue mRNA

2.7.1 Messenger RNA Extraction and Purification

Extraction and purification of mRNA was performed using an RNAeasy Mini Kit (Qiagen) according to the manufacturer's protocol. Ventricular tissue was firstly cut into 50mg pieces and then transferred frozen to a round bottom microcentrifuge tube placed in dry ice. Following, 350µL of buffer RTL (Qiagen) along with a stainless steel bead (Qiagen), were placed within the microcentrifuge tube. The tissue was then subjected to homogenisation with bead milling for 3 minutes using a TissueLyser (Qiagen) set to 30Hz. This was then repeated again.

The lysate was centrifuged at 20,000 x g for 3 minutes at 21°C. All subsequent centrifugation steps were performed at 8,000 x g at 21°C as per the manufacturer's instructions. The supernatant was carefully aspirated and placed in a fresh microcentrifuge tube. A 350µL volume of 70% ethanol was added to the supernatant and mixed with pipetting. The resulting solution was transferred to an RNAeasy spin column in 2 successive 350µL aliquots which were centrifuged for 15 seconds each. The column was washed using 700µL of buffer RW1 with centrifugation for 15 seconds. The column was then washed using 500µL of buffer RPE, with centrifugation for 15 seconds. This step was repeated but this time centrifugation was for 2 minutes for the second wash. After placing a new collection tube, the RNAeasy spin column was then centrifuged for 1 minute to eliminate any possible carryover of buffer RPE. A new collection tube was again placed and 30µL volume of RNase-free water was added to the column and used to elute the RNA with centrifugation for 1 minute. RNA samples were placed on ice. Nanodrop was used to assess RNA concentration and purity as described in Section 2.1.4.6, however with the assumption that 40µg of mRNA had an absorbance of 1.0 at 260nm and pure mRNA had a 260/280 absorbance ratio of 1.8.

2.7.2 Complementary DNA Synthesis from mRNA

Messenger RNA was converted to cDNA with reverse transcription using the Superscript First Strand Synthesis system (Invitrogen) according to the manufacturer's instructions.

A volume of mRNA containing 1µg of mRNA was diluted to 15µL using 0.5µL of 10mM dNTP mix, 0.5µL of oligo(dT) primer, and DEPC-treated water. The mixture was incubated at 70°C for 5 minutes and then placed on ice for 1 minute. A reaction mix, consisting of 5µL of 5X RT buffer, 2µL of DEPC-treated water, 2µL of 0.1M DTT, 1µL of RNaseOUT, and 1µL of Superscript was made up. The reaction mix was added to the RNA/primer mixture and the resultant mixture was incubated at 37°C for 5 minutes, then 45°C for 60 minutes. The sample was then placed on ice ready and cDNA concentration assessed as described in section 2.1.5.

2.7.3 Real Time Quantitative PCR for cDNA

Real time PCR for cDNA was carried out using Corbett Rotorgene 3000 with Platinum SYBER Green qPCR Master Mix (Invitrogen). SYBER Green is a cyanine dye that fluoresces when bound to double-standard

DNA and thereby allows the accumulation of a PCR product to be monitored over time.

Oligonucleotides were designed and bought from GeneWorks. The forward and reverse primer sequences for all genes used are in Table 2.12. The components of PlatinumR SYBER Green qPCR SuperMix-UDG include PlatinumR *Taq* DNA Polymerase and SYBER Green I dye. The PlatinumR SYBER Green qPCR Super-Mix-UDG combines the automatic "hot-start" technology of PlatinumR Taq DNA Polymerase with integrated uracil-DNA glycosylase (UDG) carryover prevention technology and SYBER Green I fluorescent dye to deliver excellent sensitivity in the quantitation of target sequences. Standards were made by pooling 3µL/sample into a micro-centrifuge Eppendorf tube to get a total of 33µL diluted to a total of 110µL of MQH_2O. The standards S1-S7 were made by diluting 1:5 up to 7 times. The cDNA to be measured were diluted by diluting this further 1:5 up to 7 times. The cDNA to be measured were also diluted 1:5 with MQH_2O.

Average melting temperature for all primers was 60^{o}C. A melt curve analysis was performed at the end of each run to confirm that specific

products were generated and that the fluorescence was not as a result of primer-dimer formation. The Rotor Gene 3000 qPCR software version 4.0.1 (Corbett research) was used to analyse the results. Average of the cycle threshold values for all genes were normalised to the housekeeping gene (18s). The Delta-Delta cycle threshold data analysis method was used to calculate the fold change for each gene.

Table 2.12 Forward and Reverse Primer Sequences

Oligo name	Sequence (5'-3')
Rat ANP	Forward CAA CAC AGA TCT GAT GGA TTT CA Reverse CCT CAT CTT CTA CCG GCA TC
Rat βMHC	Forward ATC CCT GGA TCA GGA CAA GA Reverse AGC TTC AGG TCA CCC TCC A
Rat Connexin43	Forward AGC CTG AAC TCT CAT TTT TCC TT Reverse CCA TGT CTG GGC ACC TCT
Rat Connexin45	Forward GGG AAA GCA ACA AAC AAA GT Reverse AAA GGC ATC ATA GCA GAC ATT
Eucaryotic 18s rRNA probe	Catalogue No. 4319413 E (Invitrogen)

Table 2.13 Real time PCR reaction contents

Real-time PCR cocktail	Volume per reaction (µL)
PlatinumR SYBER Green Master Mix	5
Forward primer (10µM)	0.4
Reverse primer (10µM)	0.4
dH_2O	0.2
Diluted cDNA template	4
Total volume	**10**

2.8 Duo-link

The Duo-link In-Situ Kit (O-link – sigma Aldrich) was used with the primary antibodies previously described (Table 2.7) to show protein to protein interaction (Duo-Link Starter Kit Mouse/Rabbit). The method was performed according to the manufacturer's instructions and as previously described by Soderberg et al. [144]. Ventricular tissue was cut and the sections were fixed, permeabilised and stained with primary antibody overnight at 4^{o}C as previously described in Section 2.4.3. All washes were carried out on an orbital shaker with gentle agitation. The following day, the slides were washed twice with 1x Wash Buffer A for 5 minutes each. In the meantime, the two PLA probes were diluted 1:5 in Antibody Diluent (Anti-mouse and anti-rabbit). The PLA probe solution was applied to the slides and incubated in a pre-heated humidity chamber for 1 hour at 37^{o}C. Slides were then again washed twice with 1x wash Buffer A. For the ligation step, Ligation stock was diluted 1:5 with high purity water, Ligase added to the ligation solution at 1:40 dilution and then placed onto slides for incubation in a pre-heated humidity chamber for 30 minutes at 37^{o}C. Slides were then washed twice with 1x Wash Buffer for 2 minutes each. For the amplification step the amplification stock was diluted 1:5 in high purity water to make the amplification solution. Polymerase was then added to the solution at 1:80 dilution and applied to the slides and

incubated in a pre-heated humidity chamber for 100 minutes at 37^{o}C. Slides were transferred to a dark room and samples were washed twice with 1x Wash Buffer B for 10 minutes each followed by a single wash of 0.01x Wash Buffer B for 1 minute. Slides were dried over half an hour and cover-slipped with a minimal volume of Duolink In Situ Mounting Medium with DAPI. Slides were stored at -20^{o}C overnight before microscopy was performed.

2.9 Co-immunoprecipitation

This experiment was performed with the assistance of Dr Renuka Rao. Ventricular heart tissue from Cx45 overexpressed rat was flash frozen in liquid Nitrogen and stored at -80^{o}C. The tissue was the pulverized, homogenized and lysed in a buffer solution containing 1.5% NP-40, 1% Triton X-100, 0.1% SDS, 0.1% BSA and protease inhibitors. For the pull-down, either monoclonal anti-Cx43 or monoclonal anti-Cx45 was incubated with protein G sepharose for 1 hour on a shaker at 4^{o}C. Beads were washed with lysis buffer 3 X at 4^{o}C. The lysate containing an equivalent of 1mg protein each was then incubated with the antibody bound beads in the presence of the Protease inhibitor cocktail (Sigma cat. #P8340) for 1 hour at 4^{o}C to immunoprecipitate Cx43 and Cx45 associated proteins, respectively. Mouse IgG1 (Sigma cat. # 1538) was

used as a negative control. The immunoprecipitates were spun down in a microcentrifuge at 16,000 x g for 15 min at 4^{o}C, washed 3 x in lysis buffer with BSA, and suspended in sample loading buffer with β-mercaptoethanol, heat inactivated at 95^{o}C for 10 minutes and subjected to immunoblot analysis as described above. Rabbit Polyclonal anti-Cx45 (kind gift from Dr M. Koval) and Rabbit Polyclonal anti-Cx43 (Chemicon) were used for immunoblotting.

2.10 *In Vivo* Studies

All animal experiments were approved by the Western Sydney Area Health Service Animals Ethics Committee. Female Sprague Dawley rats weighing approximately 200gm were used for all experiments and were sourced from the Australian Resources Centre (ARC, Canning Vale, West Australia). Rats were housed under conditions of constant ambient temperature (22^{o}C), humidity and a 12hour light/dark cycle. Rats were fed a commercial pellet (Allied Foods, Sydney, Australia) and had access to food and water. They were housed in cages (550 x 370 x 170mm), with open wire tops and wood shavings for bedding. There was a maximum of three rats per cage. When protocol was complete, all animals were sacrificed by using CO_2 chamber.

2.10.1 Anaesthesia, Intubation, Ventilation, and Positioning

Anaesthesia was initiated in a custom made Perspex chamber with a mix of oxygen and 5% isoflurane (Aerrane; Baxter Healthcare) supplied via flexible PVC tubing from a small animal anaesthetic machine (The Stinger; Advanced Anaesthesia Specialists). The flow rate into the box was set at 4mL tidal volumes. Once unconscious, rats were positioned, dorsal surface downwards, on a custom made intubation board that facilitated neck extension. Under direct laryngoscopy the tongue was pulled out with straight serrated forceps (Fine Science Tools) and passing a rigid hippocampal tool (Fine Science Tools) into the pharynx to support the anterior neck tissues. Once the vocal cords were visualised, the tubing of an 18 gauge intravenous cannula (Becton, Dickinson and Company) was passed under direct vision using a Seldinger technique. Following, rats were transferred to a bread board (Ikea) with their dorsal surface downwards. The cannula was attached with flexible PVC tubing to a small animal ventilator (Harvard Apparatus) set to deliver 2.5 mL tidal volumes at a rate of 70 breaths per minute. The ventilator received a mix of oxygen and 2% isoflurane from the small animal anaesthetic machine. Prior to carrying out EP studies or thoracic surgery; the upper and lower limbs were held fixed, extended at the shoulders and hips, by rubber bands looped around hooks screwed into the bread board. For tail vein injections the rat was placed on the ventral surface on the bread board or turned to

the ventral surface following the thoracic surgery to facilitate the visualisation of the tail vein easily.

If however, only tail vein injections were to be carried out the rat would not need to be intubated but instead following induction of anaesthesia in the Perspex chamber the rat was transferred ventral surface onto the bread board and the nose was placed in a nose cone. This was attached with flexible PVC tubing to the small animal anaesthetic machine and a mix of 4% isofluorane and oxygen was delivered.

2.10.2 Surface Electrocardiography

Four Unipolar needle electrodes (AD Instruments) were placed subcutaneously at the infra-clavicular and iliac fossa regions bilaterally. One ground lead was also placed subcutaneously in the abdominal region. Two lead electrocardiograms were generated combining potentials from left / right lower and right / left upper electrodes pairs. Bio-potentials, sampled at 2 kHz, were amplified with an Octal Bio Amp (AD Instruments) and digitised using a Powerlab 16/30 (AD Instruments) data acquisition system. Using the Windows based version of Labchart Pro 7

(AD Instruments) running on a Dell laptop, data was recorded via a USB. No software filtering was used. All data were analysed offline in detail.

2.10.3 Trans-oesophageal Cardiac Stimulation

A 5 French octapolar catheter (Biosense Webster) connected to the Octal Bio Amp was passed via the oral cavity into the oesophagus and positioned at the point where recordings from the middle 2 electrodes had the largest ventricular electrograms amplitudes. Recordings were made from the middle 2 electrodes only and stimulation was delivered through the distal 2 electrodes only. The ventricle was captured using a constant 60 volt stimulus of 1 millisecond duration via an isolated pulse stimulator (Model 2100; A-M Systems). To drive the stimulator via its trigger input, custom designed software installed on a second windows based laptop (Hewlitt-Packard) was used.

The EP protocol involved an attempt to induce ventricular tachycardia or ventricular Fibrillation through programmed stimulation. The latter was achieved by pacing with a drive train of 8 stimuli at a coupling interval of 180 milliseconds followed by extra-stimuli. The coupling interval between the drive train and the extra-stimulus started at 150 milliseconds and was

progressively reduced in 10 milliseconds step downs to ventricular refractoriness. A total of 4 extra-stimuli were applied, with shortening of the coupling interval for every extra stimuli. Further if no ventricular tachycardia was induced then burst ventricular pacing with a 90 milliseconds cycle length for 30 seconds was carried out, after a 3 minute rest period a further burst of pacing at cycle length 60 milliseconds was also carried out to induce VT/VF.

Ventricular tachyarrhythmia was defined as ventricular tachycardia when monomorphic/polymorphic wide complex tachycardia and lasted greater than 3 seconds and ventricular fibrillation was defined rapid irregular wide complex beats that last greater than 3 seconds.

2.10.4 Tail Vein Injection of Vector

Following anaesthesia, the rat was placed on the bread board with the ventral surface facing downwards. A tourniquet was applied at the proximal end of the rat tail using a rubber band. The tail was warmed in water at 37^{o}C for 30 seconds. This dilated the veins and made them easier to visualise and cannulate. A 25 gauge needle was used to cannulate the vein at its most distal end, once blood flow was demonstrated through the

syringe, the tourniquet is removed and the viral vector (1 x 10^{12} vector genomes diluted to 500 µL of 0.9% Saline) was injected slowly. Following vector injection a 500µL of 0.9% Saline was flushed through. The rat was then removed from the nose cone and left to recover in its box.

2.10.5 Thoracic Surgery

A total of 10µg of Buprenorphine hydrochloride (Temgesic; Schering-Plough) and 1mg enrofloxacin (Baytril 50; Bayer Healthcare AG) were separately diluted in 1mL of PBS each and administered subcutaneously by injection. The hair of the anterior chest was moistened with 70% (v/v) ethanol (Fronine), shaved with electric clippers (Remington; Spectrum Brands), and removed. Skin disinfection was performed with 10% w/v Povidine-Iodine solution (Betadine; Sanofi-Aventis) or Cholhexidine applied for a minimum of 5 minutes prior to skin incision. Two hundred nL of Lignocaine 0.1% was administered subcutaneously prior to incision to allow it time to work prior to ligation of the coronary artery.

A horizontal incision of the skin from the ventral midline to the left anterior axillary line was made at the level of the 4^{th} intercostal space using a scalpel. To mobilise the surrounding skin, blunt dissection with straight

haemostats (Fine Science Tools) of the underlying superficial fascia for up to approximately 1cm on both sides of the incision was performed. The muscles of the left chest wall superficial to the ribs were also separated by blunt dissection with straight haemostats (Fine Science Tools). The thoracic cavity was punctured via the 4th intercostal space using curved haemostats (Fine Science Tools). The punctured intercostal muscles were blunt dissected with the same curved haemostats and a Castroviejo retractor (Roboz) was inserted to hold open the dissected intercostal space. The left atrium was visualized and just below it, a hole was made in the pericardial sac with curved forceps (Fine Science Tools). This was then carefully dissected off all the way to the distal ventricular apex. The LAD coronary artery was identified at the level of the left atrial appendage and a 6-0 75cm suture was placed around the artery approximately 1-2mm below the appendage. The suture ends were passed through a polyethylene tube to form a “snare” like loop with the free ends. The snare loop was then pulled for 10 seconds to assess for area of cyanosis and then released with return to normal colour thereby demonstrating adequate occlusion of the LAD. When approximately 40-50% of the anterior visualised wall was seen to be cyanosed, the occlusion was then re-applied permanently. If adjustments were required, the suture was removed and the last step was repeated to get an equal amount of cyanosis for all rats. Following the LAD occlusion, the retractor was

removed and the rib space closed with a two stitches of 3.0 coated vicryl suture (Ethicon). The skin incision was then closed with a horizontal mattress technique using a 3.0 coated vicryl suture (Ethicon). The rat was then placed in the cage to recover. Drinking water for rats was supplemented with 0.01% enrofloxacin (Baytril 25; Bayer Healthcare AG).

2.10.6 Telemetry Implantation

Two weeks following transduction, a subset of animals were anaesthetised, intubated and ventilated as described above. Telemetric devices (ADI instruments MLE 1010) were implanted into 5 rats injected with rAAV.GFP and 5 rats injected with rAAV.Cx45 as previously described by Brockway et al [145]. A midline abdominal incision was made from the xiphisternum 3cm in size, the fascia was carefully dissected and the abdominal cavity exposed. The body of the telemetric device was inserted into the abdomen above the bladder of the rat and sutured to the abdominal musculature. One electrode was then sutured to the xiphisternum. The other electrode was then passed underneath the skin layer (with blunt dissection) and sutured to the second right intercostal space. The abdominal musculature and skin were then sutured and the rat recovered. Analgesia was achieved by administering buprenorphine (0.5mg/Kg SC) prior to the rat recovering from anaesthesia and at later

time intervals as needed. Rats were placed in cages with two battery chargers connected to the wireless receivers (ADI instruments TR101). Rats were regularly observed every 12 hours for the first 48 hours and if any sign of distress further buprenorphine was administered.

Telemetry was recorded continuously for 2 weeks prior to the final study endpoint.

2.10.7 Ventricular Tissue Extraction, Preparation, and Storage

Adult rats were euthanized with CO_2 in a custom made Perspex chamber box for 10 minutes and then weighed. Rat were then laid dorsal surface down and the chest wall cut open with scissors to the right of the midline. The heart was detached from the mediastinum just above the base and rinsed with PBS and weighed. The heart was dissected transversely leaving the atria behind. For histology and immunohistochemistry studies, the hearts were placed in a vinyl specimen mould (Cryomold; Sakura) filled with Tissue-Tek OCT compound (Sakura). The mould was then frozen with liquid nitrogen and transferred to a -80°C freezer for storage. For protein and mRNA studies, hearts were placed in microcentrifuge

tubes, frozen in liquid nitrogen and transferred to a -80°C freezer for storage.

2.11 Data Analysis and Statistics

NQuery Advisor (Statistical Solutions) was used to estimate the required sample sizes.

Quantitative data were expressed as mean ± standard deviation (SD) (or standard error of the mean (SEM) which will noted in the text – otherwise it would SD). Continuous variables (such as QRS width, PR interval) were analysed using Student T tests or Mann-Whitney U test. Statistical analysis for 2x2 tables (such as in ventricular tachyarrhythmia inducibility) were performed using Fischer's exact test (if samples in a cell were ≤ 5) or using two sample Pearson's Chi-square (X^2) test (2 x 2 table) on the SPSS (Version 17). Significance was set at $P \leq 0.05$. Statistics were carried out with the assistance of Ms Karen Byth (Westmead hospital statistician).

CHAPTER 3

THE EFFECTS OF CONNEXIN45 OVEREXPRESSION ON CARDIAC PHYSIOLOGY

3.1 Introduction

Cardiovascular mortality is the leading cause of death in the industrialized world. Sudden cardiac death occurs most often after acute MI and ventricular tachyarrhythmias are responsible for the majority of cases. Implantable defibrillators and pharmacotherapy have been the mainstay treatment for such tachyarrhythmias but mortality remains high. Yamada, Rogers et al. and other authors have reported that intercellular electrical uncoupling mediated by decreased conductance of gap junctions is associated with ventricular tachyarrhythmias in the diseased heart [2, 4].

Gap junctions facilitate the inter-cellular flow of ions necessary for the propagation of electrical impulses within the myocardium. This in turn allows for coordinated mechanical activity throughout the heart. Gap junctions are formed by the union of two hemi-channels (connexins) each contributed by two adjacent cells. Each hemi-channel contains six

connexin proteins surrounding an aqueous pore and can be formed from a single connexin isotype (homomeric channels) or a mixture of isotypes (heteromeric channels) [21, 25-28]. The biophysical properties (conductance and permeability) of a gap junction are determined by the mix of connexin isotypes that constitute it.

The connexin isotypes 43, 40 and 45 have been identified within the mammalian heart. Connexin43 is the most prevalent, being expressed throughout the heart [146], while the less abundant Cx40 is predominantly located within the atrium. Connexin45, the least prevalent and least studied, is mainly found in the ventricular conduction system and AV node.

Peters et al. studied myocardial infarcts in a canine model and noted that myocardial gap junctions have a significant role to play in arrhythmogenesis, being one of the principal determinants of cardiac conduction velocity [23, 147, 148]. In particular, healed infarcts had smaller and fewer gap junctions in the fibrotic myocardium adjacent to infarcts, and was associated with a reduction in the proportion of side-to-side vs. end-to-end intercellular connections. Immunohistochemistry studies revealed that the lateral part of the central common pathway consisted of myocytes with reduced intercalated disc content of Cx43. An

increase in lateralised membranous Cx43 expression in myocytes was noted but its functionality was not investigated [23]. With early infarction, on the other hand (before fibrotic healing); the Cx43 gap junctions in myocytes abutting the infarct showed disorganization similar to that described in healed human infarcts, suggesting that this disturbance is an early pathophysiological cellular response, and not simply due to later fibrotic distortion. It is understood that this disorganisation is what facilitates re-entry circuits and the propensity to ventricular arrhythmia.

In the setting of heart failure, a condition associated with SCD, an increase in ventricular Cx45 expression and reduction in Cx43 expression has been identified [77, 87, 149]. The present study was performed to explore the role of Cx45 in cardiac physiology and arrhythmogenesis. Using acute somatic gene transfer, Cx45 was overexpressed in normal adult rat hearts. We found that widespread expression of Cx45 was associated with conduction slowing and an increased propensity for inducible ventricular tachyarrhythmia.

3.2 Materials and Methods

Study Protocol (Fig 3.1)

Two hundred gram adult Sprague Dawley female rats were used in this study protocol. Three study groups were used; all rats received $1x10^{12}$ vector genomes (diluted in 0.9% Saline to a quantity of 500 µL) of either rAAV.GFP (n=15), rAAV.Cx43 (n=15) or rAAV.Cx45 (n=22) injected via the tail vein. Electrophysiology studies were performed immediately prior to vector injection and 28 days later.

This study was approved by the Animal Research Ethics Committee of Westmead Hospital. The study protocol conformed to the guidelines set for animal research by the National Health and Medical Research Council, Australia

Figure 3.1 Study Protocol Diagram

A total of 3 groups were studied. The rAAV.GFP acted as the control group. The other 2 groups were rAAV.Cx45 and rAAV.Cx43. All rats underwent baseline EPS followed by transduction. EPS was then repeated at day 28 followed by removal of ventricular tissue. The ventricles were then probed for Cx45, Cx43 protein and mRNA levels, and inflammation and fibrosis with histological analysis.

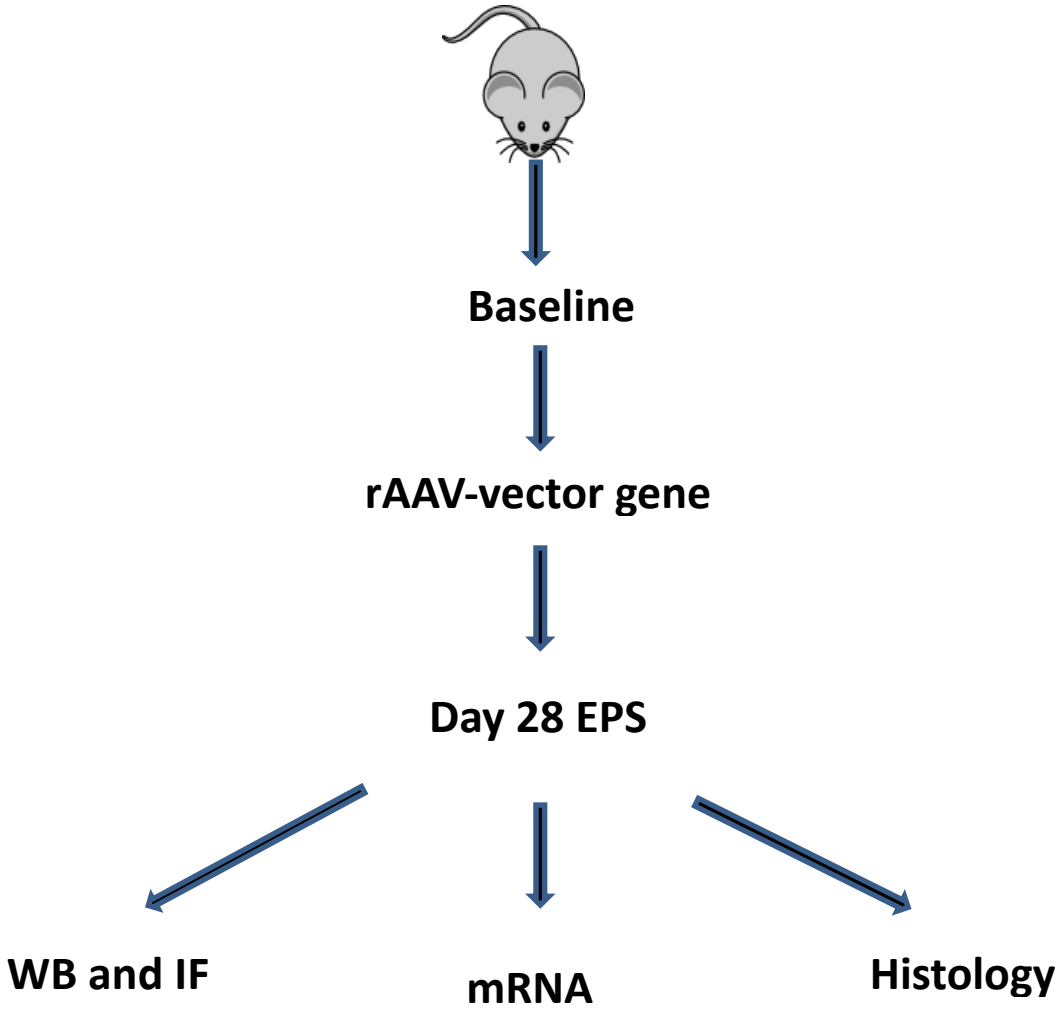

WB: Western Blot, IF: Immunofluorescence, EPS: Electrophysiology studies

3.2.1 Recombinant Adeno-associated Viral Vector Production

Vector stocks encoding GFP, Cx43, and Cx45 were produced using the calcium precipitation method as described in Section 2.3. In summary, the cDNA for rat Cx45 and Cx43 was PCR amplified from a rat cardiac cDNA library, subjected to automated sequencing and sub-cloned into the recombinant adeno-associated virus vector 2 (rAAV2) backbone. As a control vector for the overexpression studies, the cDNA encoding GFP was also sub-cloned into the same vector backbone. Recombinant AAV vectors pseudo typed with capsid serotype 9 were produced using a helper-virus free system by calcium-phosphate co-precipitation transfection of the three vector plasmids into HEK293 cells as per Xiao et al [150-152]. Following plating of 120 petri dishes (10cm diameter) with HEK293 cells, 3 plasmids (vector plasmid, helper plasmid, and adenovirus helper plasmid) were transfected into HEK293 cells using the calcium phosphate precipitation method. Vector-containing cells was collected 48 hours after transfection, pelleted and subjected to three freeze/thaw cycles to release the vector. Cellular debris was pelleted and the supernatant treated with Benzonase and precipitated with saturated ammonium sulphate. Vector was purified through a CsCl gradient and dialysed against PBS. Vector titre was determined by qPCR on vector

stocks as described by Huang et al and using primers manufactured by Sigma Aldrich [140, 153]. Sequences for the rAAV forward primer AAV1277F (5'-CCGTTGTCAGGCAACGTG), reverse primer AAV1361R (AGCTGACAGGTGGTGGCAAT), and probe (5' – [6FAM]TGCTGACGCAACCCCCACTGGT[TAM]) .

3.2.2 Neonatal Rat Ventricular Myocyte Studies

Neonatal rat ventricular myocytes were prepared as described in Section 2.2.3.2. In summary NRVMs were isolated from 2-3 day old rat Sprague Dawley rat pups by enzymatic digestion as previously described [154]. Cells were cultured on 24 well plates. Neonatal RVMs were transduced with rAAV.Cx45 in the order of $1X10^{11}$ vector genomes per well. Forty eight hours later they were fixed and immuno-stained.

3.2.3 *In Vivo* Studies

In vivo studies were carried out as described in section 2.10. All rats were anesthetised, intubated and ventilated with a mixture of oxygen and 2% isoflurane for EPS and telemetry device implantation.

3.2.3.1 Surface Electrocardiography

Electrophysiological studies were performed as described in Section 2.10.3. In brief, four unipolar needle electrodes (AD Instruments) were placed subcutaneously at the infra-clavicular and iliac fossa regions bilaterally. One ground lead was also placed subcutaneously in the abdominal region. Two lead electrocardiograms were generated combining potentials from left / right lower and right / left upper electrodes pairs. Bio-potentials, sampled at 2 kHz, were amplified with an Octal Bio Amp (AD Instruments) and digitised using a Powerlab 16/30 (AD Instruments) data acquisition system. Data was recorded, via USB, using the Windows based version of Labchart Pro 7 (AD Instruments) running on a Dell laptop. No software filtering was used. All data was analysed offline. The PR and QRS intervals were calculated using the Lab chart software and by randomly sampling 10 continuous beats.

3.2.3.2 Trans-oesophageal Cardiac Stimulation

As described in Section 2.10.3, a 5 French octapolar catheter (Biosense Webster) connected to the Octal Bio Amp was passed via the oral cavity into the oesophagus and positioned at the point where recordings from the middle 2 electrodes had the largest ventricular electrogram amplitudes. Recordings were made from the middle 2 electrodes only,

while stimulation was delivered through the distal 2 electrodes only. The ventricle was captured using a constant 60 volt square shaped stimulus of 1 millisecond duration via an isolated pulse stimulator (Model 2100; A-M Systems). Custom designed software installed on a second windows based laptop (Hewlitt-Packard) was used to drive the stimulator via its trigger input.

Programmed ventricular stimulation was used to induce ventricular tachycardia. Hearts were paced with a drive train of 8 stimuli at a coupling interval of 180 millisecond followed by up to four extra-stimuli starting at 150 millisecond and progressively reduced in 10 millisecond decrements to ventricular refractoriness. If programed ventricular stimulation failed to induce VT, then ventricular burst pacing was performed once at a cycle length of 90 milliseconds for 30 seconds and repeated once, if required, 3 minutes later at a cycle length of 60 milliseconds.

3.2.3.3 Implantable Telemetry

As described in Section 2.10.6, two weeks following transduction, a subset of animals were anaesthetised, intubated and ventilated as described above. Telemetric devices (ADI instruments MLE 1010) were

implanted into 5 rats injected with rAAV.GFP and 5 rats injected with rAAV.Cx45 as previously described [145]. Briefly, a midline abdominal incision was made from the xiphisternum 3cm in size and the abdominal cavity exposed. The body of the telemetric device was inserted into the abdomen above the bladder of the rat and sutured to the abdominal musculature. One electrode was then sutured to the xiphisternum and the other to the second right intercostal space. The abdominal musculature and skin were then sutured and the rat recovered. Analgesia was achieved by administering buprenorphine (0.5mg/Kg SC) prior to the rat recovering from anaesthesia and at later time intervals as needed. Rats were placed in cages with two battery chargers connected to the wireless receivers (ADI instruments TR101). Telemetry was recorded continuously for 2 weeks prior to the final study end point.

3.2.3.4 Tail Vein Vector Injection

Tail vein vector injections were performed immediately after baseline EPS as described in Section 2.10.4. In summary, a 25 gauge needle was used to cannulate the tail vein at its most distal end and viral vector injected over 30 seconds. The tail vein was flushed with 500μL normal saline.

3.2.3.5 Tissue Preparation

As described in Section 2.10.7, at the end of the study period, rats were euthanized with CO_2 and weighed. Hearts were removed, rinsed with PBS and subsequently weighed. For histology and immunohistochemistry studies, hearts transduced with rAAV.Cx43 or rAAV.Cx45 were immediately embedded in Tissue-Tek OCT compound (Sakura). For rats transduced with rAAV.GFP, hearts were fixed in 4% PFA overnight at 4^{o}C prior to embedding in Tissue-Tek OCT. All embedded tissue was frozen in liquid nitrogen and transferred to -80°C storage. For protein and mRNA studies, hearts were placed into microcentrifuge tubes, frozen in liquid nitrogen and transferred to -80°C storage. Heart tissue was subsequently sectioned into 6µm slices and mounted onto glass slides for immunostaining, inflammation and fibrosis studies.

3.2.4 Morphometric Studies

All rats and their hearts were weighed at the end of the protocol.

3.2.5 Immunostaining

As previously described in Section 2.4, the ventricle was excised and stored at day 28 and after the EP studies were performed. Ventricular

sections were fixed with 4% (w/v) paraformaldehyde, subject to permeabilisation with 0.1% (v/v) Triton X-100 (Sigma-Aldrich) in PBS for 15 minutes and blocked with Dako Protein Block, serum-Free. Samples were then incubated with primary antibody (mouse monoclonal anti-Cx45 1:200 Millipore and rabbit monoclonal anti-Cx43 1:800 Millipore) diluted in blocking solution overnight at 4°C. Secondary antibody (Alexa488-conjugated anti-mouse, 1:1000, Invitrogen; or Alexa594-conjugated anti-mouse, 1:2000, Invitrogen; or Alexa594-conjugated anti-rabbit, 1:2000, Invitrogen), diluted with 0.1% (v/v) cold fish skin gelatine in PBST, was applied to the slides for 1 hour at room temperature in the dark. Samples were cover slipped (Deckgläser; Menzel-Gläser) mounted with Prolong Gold anti-fade reagent with DAPI (Life Technologies) and allowed to set in the dark, overnight and 4°C. Imaging was performed using either an inverted wide field fluorescent microscope (Leica DMIL) with a 40X – 100X objective (Leica 40X/0.50 Ph2 /1.1 506273 HI plan 1) or a confocal laser scanning microscope (Olympus FV 1000) using a 40X – 60X objective (Olympus 40X/1.30/0.20 (WD) Oil UPLFLN).

For co-localisation studies described in detail in Section 2.4.4, we combined primary antibodies as well secondary antibodies following the same process as above but secondary antibodies used were Alexa488-

conjugated anti-mouse, 1:1000 and Alexa594-conjugated anti-rabbit, 1:2000, Invitrogen. This allowed different fluorescence to be able to note the different antibodies at the same time. Of note under fluorescence when the two antibodies were combined and seen at the same time, the fluorescence was yellow.

3.2.6 Inflammation - Haematoxylin and Eosin Staining

The technique of H&E staining was performed with a Shandon Linear Stainer described in Section 2.5.1. Heart sections were immersed in Haematoxylin for four minutes, Scott's Bluing solution for one minute, and 0.1% Eosin for one minute. Samples were dehydrated with absolute ethanol for 30 seconds and placed in xylene clearing solution. Images were then assessed manually for the extent of inflammation and graded based on a scale by Igarashi et al. [142] (1 - absent, 2 - occasionally present, 3 - ≤ 50% affected, 4 – 50% to 90% affected, 5 - ≥ 90% presence).

3.2.7 Pico-Sirius Red Staining for Fibrosis

As described in Section 2.5.2, heart tissue sections were fixed with 4% paraformaldehyde followed by 3 washes in PBS for 5 minutes. Sections were placed in Pico-Sirius red solution (0.1% Direct Red 80 (Sigma), 0.1%

Fast Green FCF (Sigma), Saturated Picric Acid (Sigma)) for 1 hour then washed in 100% ethanol for 1 minute each to dehydrate the sections. Samples were air dried then immersed in xylene clearing solution before cover slip mounting. Sections were processed with custom made software designed to objectively calculate the relative areas of red (collagen) to the area of the tissue section as described in Section 2.5.3 (Fig 3.2).

Figure 3.2: Image Processing of Pico-Sirius Red Tissue Staining

Representative images from a GFP ventricle section showing Pico-Sirius Red staining on the left (collagen coloured red, remaining tissue coloured green) and a software processed image on the right (collagen identified as red, remaining tissue as blue). The formula (red pixels x 100) / (red pixels + blue pixels) was used to calculate the percentage fibrosis within processed images

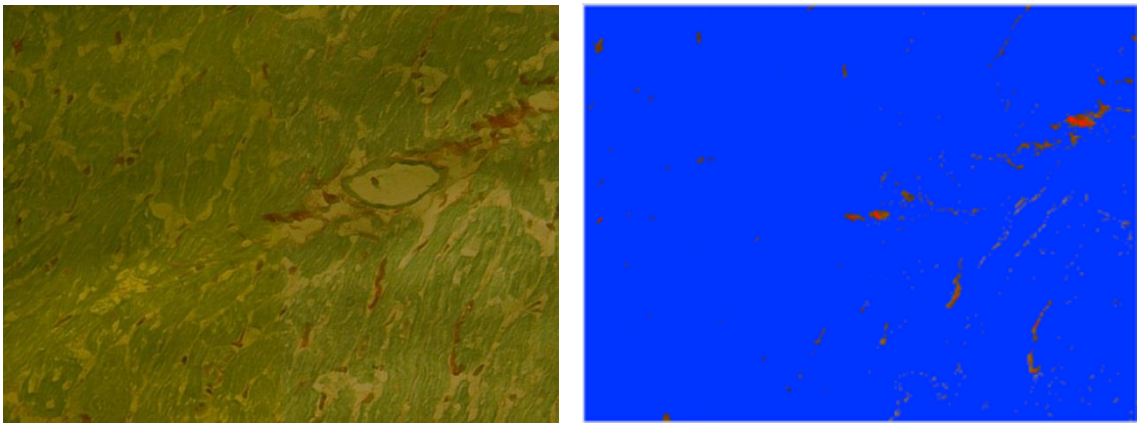

3,956 red pixels
94,990 blue pixels
4.00% fibrosis

3.2.8 Immunoblotting

Primary antibodies used during experiments were described above and in Section 2.6.4. Tissue used for protein extraction was flash frozen in nitrogen when collected. Fifty mg tissue along with 500µl of ice cold lysis solution (RIPA buffer (Sigma-Aldrich), 1% (v/v) phosphatase inhibitor cocktail 2 (Sigma-Aldrich), and 4% (v/v) protease inhibitor cocktail (Sigma-Aldrich) was subjected to disruption with bead milling using a TissueLyser (Qiagen) set to 30Hz. Samples were pelleted and supernatant recovered. Protein estimation was performed using the Bradford method using a Bio-Rad protein assay kit. The absorbance used to measure was 595nm using a Victor^2 Multilabel Counter (PerkinElmer life Sciences). Protein was loaded into precast polyacrylamide 4-12% gradient Bis-Tris gels (NuPAGE; Invitrogen) and SDS-PAGE electrophoresis was performed in 1X NuPAGE MOPS (Invitrogen) buffer in reducing conditions as per the manufacturer's instructions. Protein membrane was transferred from the gels to a membrane using the IBLOT gel transfer system (Invitrogen), following electrophoretic separation. Gels were placed in a gel transfer stack (Invitrogen) and the IBLOT's default 7 minute transfer protocol was used. Membranes were then blocked with a solution of 5% skim milk in TBST (0.05% Tween 20, Tris-Buffered Saline) for 2 hour and subsequently incubated with primary antibody diluted in blocking solution overnight at 4°C.

The following morning following washes, samples were incubated with secondary antibody (HRP-linked rabbit anti-mouse, 1:10000, Sigma; or HRP-linked goat anti-rabbit, 1:10000, Sigma) diluted in blocking solution for 1 hour. SuperSignal Pico Chemiluminescent substrate (Thermo Fisher Scientific) blotting detection reagents was then added on to the according to the manufacturer's instructions. At times when extra luminescence was required then in addition to the Pico substrate, SuperSignal west Femto (Thermo Scientific) was mixed with a ratio of 1:10 dilution and added to the membrane for 5 minutes. Membranes were transferred to an autoradiography cassette (Hypercassette; Amersham Biosciences). In a dark room, chemiluminescence film (Hyperfilm ECL; Amersham) was exposed to the protein membranes in the autoradiography cassette. Films were then processed with an AGFA film processor according to the manufacturer's protocol.

3.2.9 Duo-Link

The Duo-link In-Situ Kit (O-link – Sigma Aldrich) was to detect protein to protein interaction as described in Section 2.8. The method was performed according to the manufacturer's instructions and as previously described by Soderberg et al [144]. Primary antibody was incubated overnight at 4^{o}C. The slides were washed twice with 1x Wash Buffer A

for 5 minutes. The two PLA probes were diluted 1:5 in Antibody Diluent, applied to the slides and incubated in a pre-heated humidity chamber for 1hour at 37^{o}C. Slides were then again washed twice with 1x wash Buffer A. For the ligation step, Ligation stock was diluted 1:5 with high purity water, Ligase added to the ligation solution at 1:40 dilution and then placed onto slides for incubation in a pre-heated humidity chamber for 30 minutes at 37^{o}c. Slides were then washed twice with 1x Wash Buffer for 2 minutes each. For the amplification step the amplification stock was diluted 1:5 in water to make the amplification solution. Polymerase was then added to the solution at 1:80 dilution and applied to the slides and incubated in a pre-heated humidity chamber for 100 minutes at 37^{o}c. Slides were transferred to a dark room and samples were washed twice with 1x Wash Buffer B for 10minutes each followed by a single wash of 0.01x Wash Buffer B for 1 minute. Slides were dried and cover-slipped with a minimal volume of Duolink *in Situ* Mounting Medium with DAPI. Slides were stored at -20^{o}C overnight before confocal microscopy was performed.

3.2.10 Co-immunoprecipitation

As previously described in Section 2.9 ventricular tissue was initially flash frozen and stored at -80^{o}C. The tissue was pulverized, homogenized and

lysed in a buffer solution containing 1.5% NP-40, 1% Triton X-100, 0.1% BSA and protease inhibitors. Either monoclonal anti-Cx43 or monoclonal anti-Cx45 antibody was incubated with protein G sepharose for 1 hour on a shaker. The lysate was incubated with antibody bound beads plus protease inhibitor cocktail for 1 hour at 4^{o}C to immunoprecipitate Cx45 and Cx43 associated proteins respectively. A non-specific IgG was used as a negative control. Following that the immunoprecipitate was spun down in a micro centrifuge at 16,000 x g for 15 min at 4^{o}C. The precipitate was then washed 3 x in lysis buffer with BSA, and suspended in lysis buffer without BSA plus sample buffer with β-mercaptoethanol for immunoblot analysis. Rabbit Polyclonal (anti)-Cx45 and Rabbit Polyclonal (anti)-Cx43 were used for immunoblotting.

3.2.11 Statistics

Continuous variables were analysed using student T tests or Mann-Whitney U test. Ventricular tachyarrhythmia inducibility was assessed using the fisher exact or X^2 tests. All statistics were conducted at the ≤ 0.05 significance level. Data are presented as mean +/- SD.

3.3 Results

3.3.1 NRVM Studies

To assess the functionality of the rAAV.Cx45 vector, *in vitro* studies were performed. Neonatal RVMs treated with rAAV.Cx45 demonstrated widespread transduction with the expected localisation at junctional membranes (Figure 3.3). Controls with no vector transduction were carried out alongside and did not reveal any signal. Figure 3.4 demonstrates western blot images of Cx45 in NRVMs.

Figure 3.3: Immunostaining of NRVM

Fluorescence microscopy was performed on Cx45 labelled rat ventricular myocytes following transduction with a rAAV.Cx45. These cells are devoid of endogenous Cx45. The immunoreactive signal is clearly seen localizing at the junctional membrane between adjacent cells confirming the expression of Cx45 from this vector construct. No signal was seen in control cells (right panel).

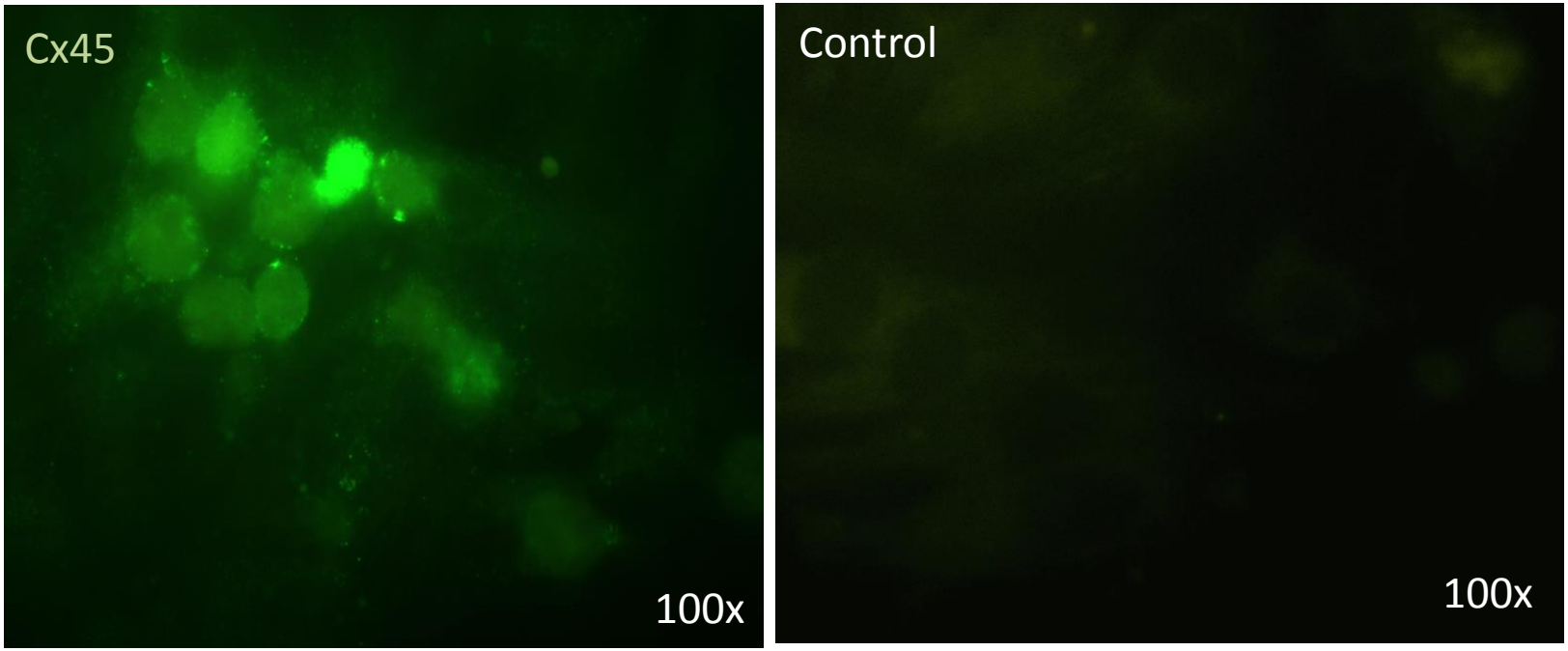

Figure 3.4 Western Blot image of Connexin45 in NRVMs

Western blot image of Cx45 protein expression in NRVM's. This revealed increased signal in rAAV.Cx45 transduced NRVM's and no signal in the control (n=3 in each group).

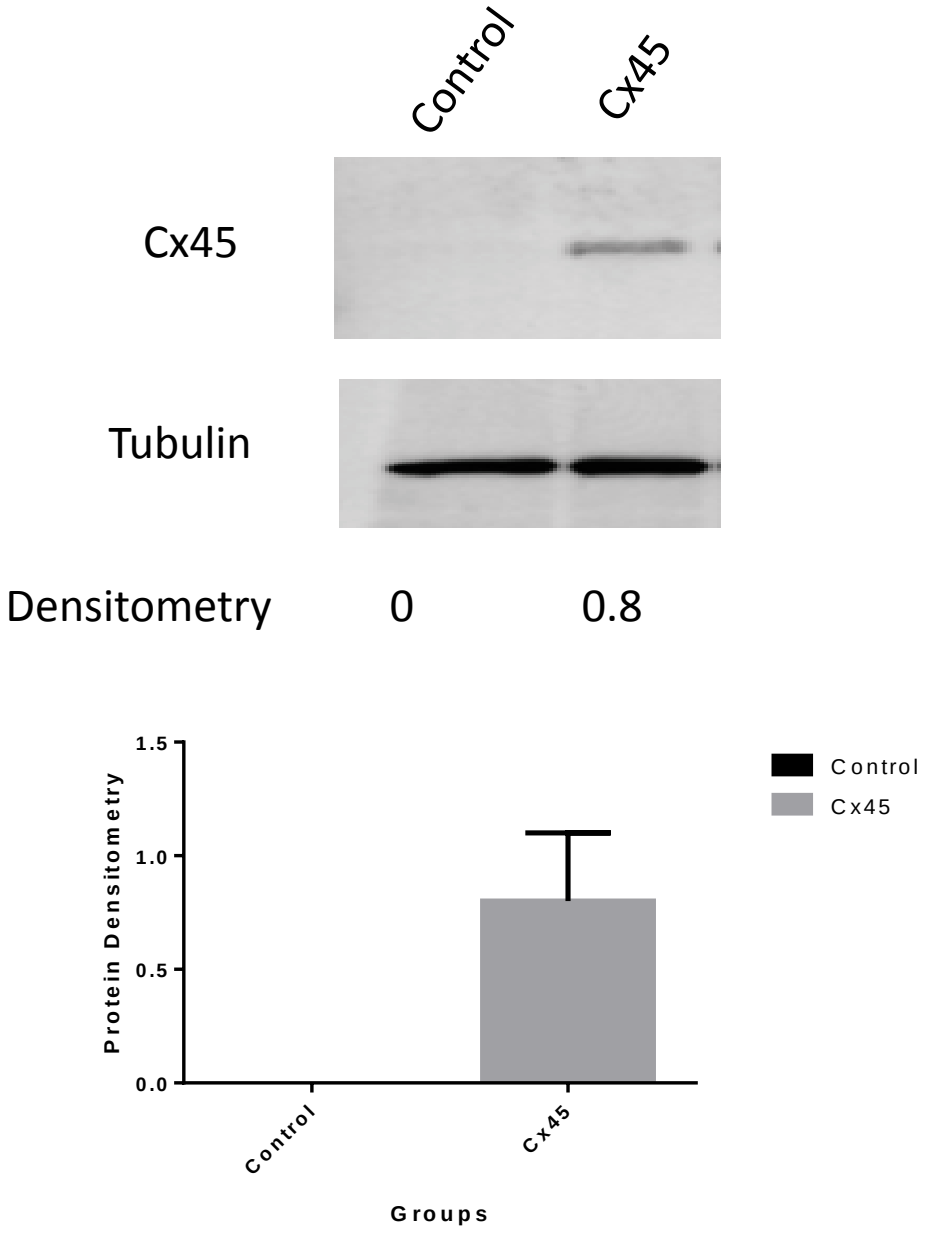

3.3.2 Protein/mRNA Expression Studies

Tail vein injection of rAAV.GFP resulted in widespread transduction of cardiac myocardium as shown in Figure 3.5. Both rAAV.Cx43 and rAAV.Cx45 gene transfer also resulted in a widely transduced myocardium (Figure 3.5). Overexpression of Cx45 protein and mRNA was confirmed with Western blotting and qPCR, respectively (Figure 3.6, Table 3.1).

Figure 3.5: Fluorescent Microscopy Images Showing Expression of GFP, Cx43 and Cx45 in Transduced Rat Myocardium.

Spontaneous fluorescence of GPF and fluorescent immunostaining of ventricular myocardium with Cx43 (red) and Cx45 (green). Images reveal a widespread transduction and localisation of connexins in the intercalated discs.

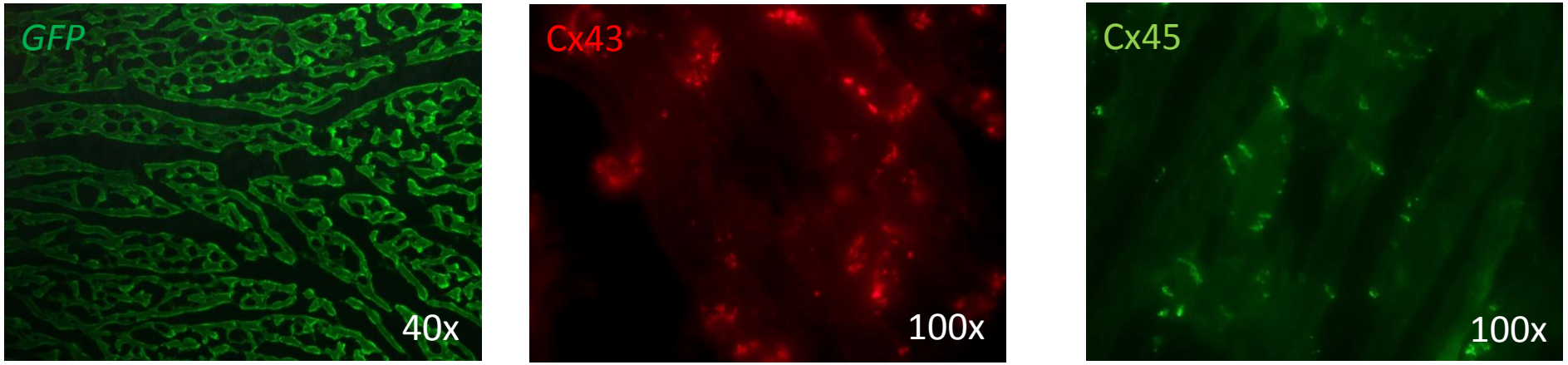

Figure 3.6 Western Blot images Showing Cx45 and Cx43 Expression in Transduced Rat Myocardium.

Top image “A)” reveals significant Cx45 protein detected in Cx45 overexpressed myocardium. Bottom image “B)” reveals as expected Cx43 is detected in all groups but overexpressed in the Cx43 group.

A) Cx45 Protein levels (n=3 in each group)

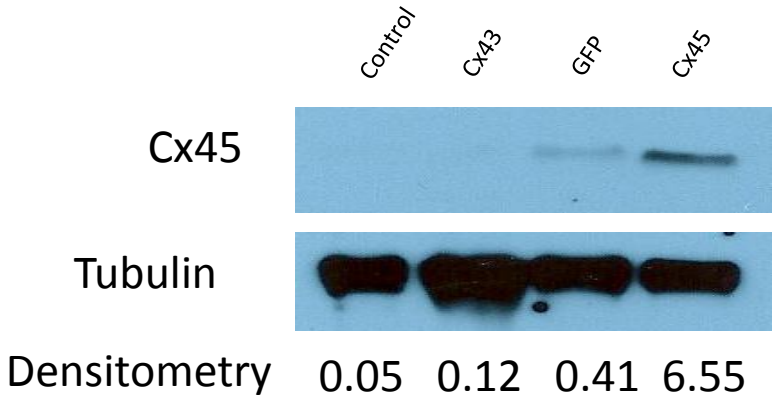

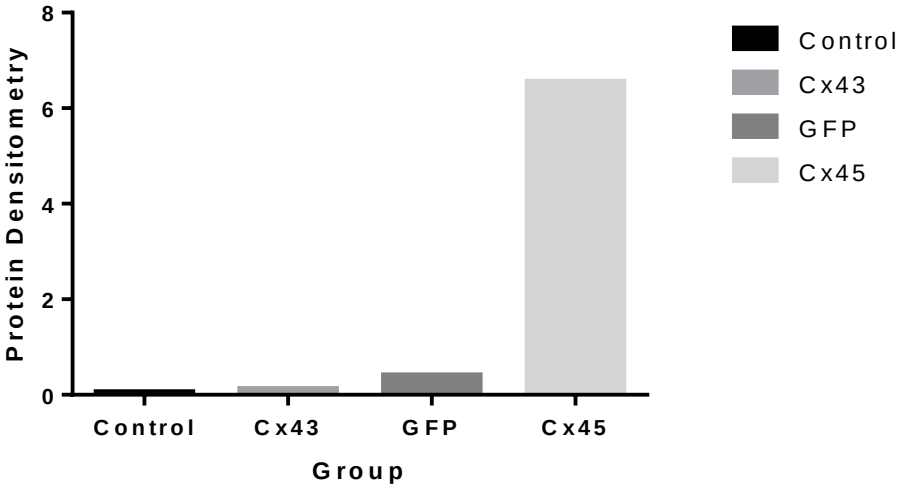

B) Cx43 Protein levels 9 (n=3 in each group)

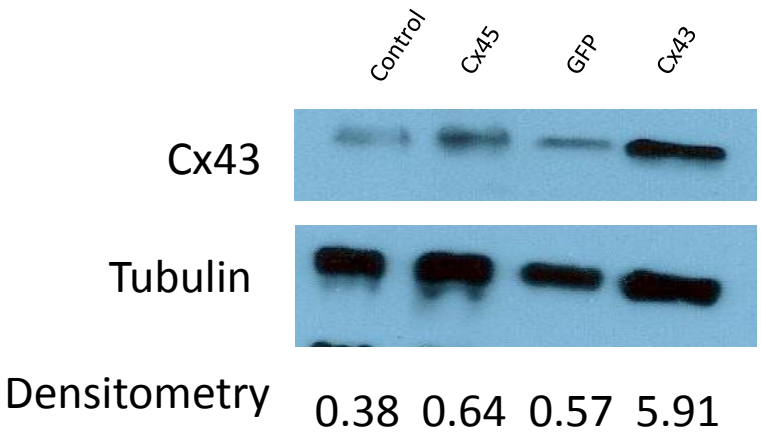

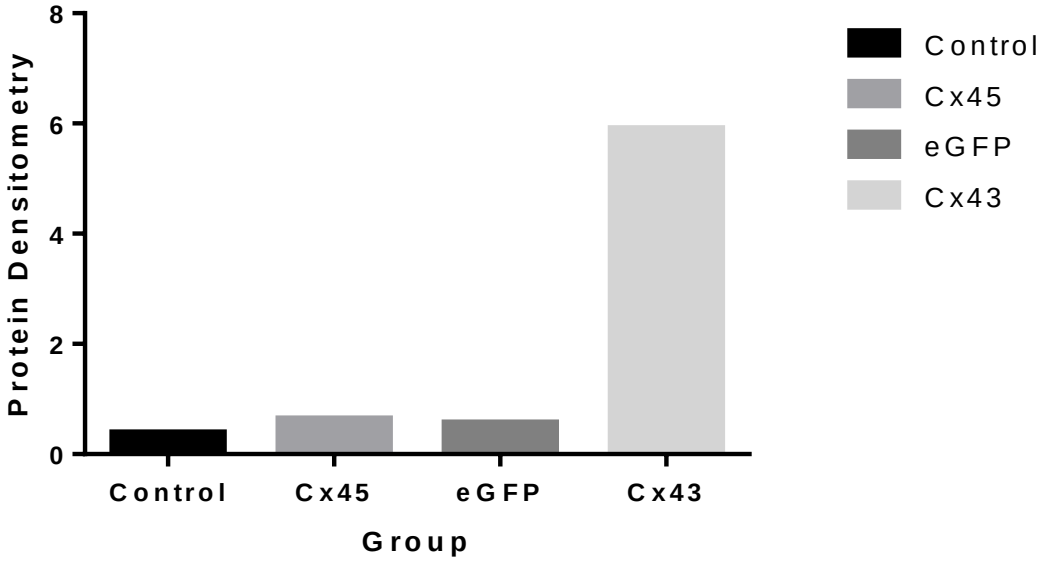

Table 3.1: Mean Cx45 and Cx43 mRNA expression results in transduced rat myocardium.

A) Compares GFP to Cx43-overexpressed group and reveals a significant increase in Cx43 mRNA expression in the Cx43-overexpressed group.

B) Compares GFP to Cx45-overexpressed group and reveals a significant increase in Cx45 mRNA expression and a significant reduction in Cx43 expression in Cx45 overexpressed group.

C) Compares the Cx43 to Cx45 overexpressed groups. It reveals a significant increase of Cx43 mRNA expression in the Cx43 overexpressed group and a significant increase in Cx45 mRNA expression in the Cx45 overexpressed group.

A)

	rAAV.GFP n=8	**rAAV.Cx43 n=7**	**P-Value**
Cx45	0.27±0.086	0.31±0.025	NS
Cx43	0.65±0.23	0.94±0.15	0.02

B)

	rAAV.GFP n=8	rAAV.Cx45 n=7	P-Value
Cx45	0.27±0.086	0.62±0.316	0.007
Cx43	0.65±0.23	0.24±0.22	0.02

C)

	rAAV.Cx43 n=7	rAAV.Cx45 n=7	P-Value
Cx45	0.31±0.025	0.62±0.316	0.02
Cx43	0.94±0.15	0.24±0.22	0.004

All values represented as mean ± SD

3.3.3 Electrophysiology Studies

Fifty two Sprague Dawley rats were studied and all reached maturation. The GFP and Cx43 groups had no significant difference between baseline and final ECG parameters as shown in Table 3.2. The Cx45 group on the other hand, displayed evidence of conduction slowing with prolongation of both the PR and QRS intervals when final and baseline results were compared. When the final PR and QRS intervals of the Cx45 group were compared to those of Cx43 and GFP treated rats there was also a significant prolongation see Table 3.2.

Inducible ventricular tachyarrhythmia Figure 3.8 (a) was not observed in any rat at baseline. Twenty eight days after transduction, 13 rats in the Cx45 treated group had inducible ventricular tachyarrhythmia versus 2 in the Cx43 and none in the GFP treated group Figure 3.7. Furthermore 5 rats in the Cx45 group had high degree atrioventricular nodal block figure 3.6 (b) versus none in the control GFP and Cx43 groups; this did not however reach statistical significance.

Telemetry did not show any spontaneous ventricular tachyarrhythmia in any group.

Table 3.2: ECG Parameters and Arrhythmias

Table below summarises the results for the electrophysiology parameters studied between the groups.

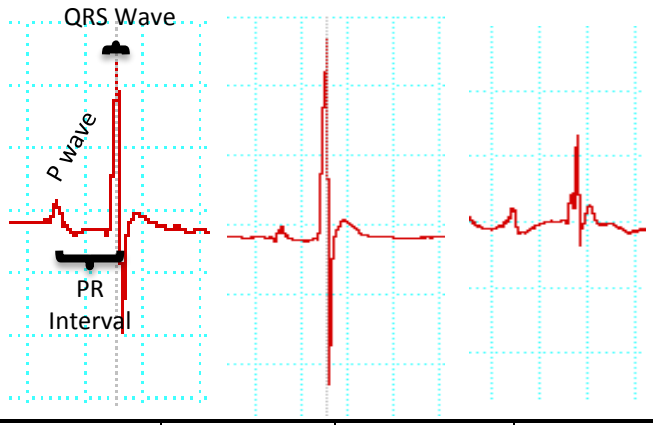

	Treatment groups	GFP n=15	Cx43 n=15	Cx45 n=22	P-Value		
					GFP vs Cx45	GFP vs Cx43	Cx45 vs Cx43
PR Interval (ms)	**Baseline**	44±4.2	50.0±8.1	45.8±6.0	NS	NS	NS
		P=NS	P=NS	P<0.001			
	Post Treatment	47.8±7.3	49.8±6.7	59.0±12.0	0.005	NS	0.038
	Δ	3.68±4.52	0.54±4.9	14±12	0.04	NS	0.001
QRS Duration (ms)	**Baseline**	14.7±1.5	14.0±1.7	14.8±1.9	NS	NS	NS
		P=NS	P=NS	P=0.009			
	Post Treatment	15.4±1.5	14.0±2.4	16.2±1.8	0.014	NS	0.007
	Δ	0.69±1.1	0.04±1.5	1.4±1.8	0.001	NS	0.012
High Block rate		*0*	0	5 (23%)	0.13	NS	0.13

In vivo comparisons of the electrophysiological effects of Cx45 overexpression (rAAV.Cx45), and Cx43 (rAAV.Cx43) overexpression

compared to control rAAV.GFP. EP measurements include: mean PR interval and QRS durations for each group as measured at Day 0 (Baseline) and Day 28 (Post Treatment). Δ = mean difference (post-treatment – baseline). Baseline measurements of both QRS duration and PR interval were similar between the groups. Cx45 overexpression resulted in significant prolongation of PR interval and QRS duration post-treatment compared to baseline Cx45 overexpression and against post-treatment of Cx43 overexpression and post-treatment control. This effect was not observed in the Cx43 post-treatment compared to baseline Cx43 overexpression and post-treatment control.

Figure 3.7 Incidence of Inducible of VT/VF

Figure below shows a bar chart of the percentage of VT/VF noted in each of the groups. There was a significant increase in ventricular tachyarrhythmia noted between the rAAV.Cx45 and rAAV.GFP and rAAV.Cx43 groups. No significant difference between rAAV.GFP and rAAV.Cx43 was observed.

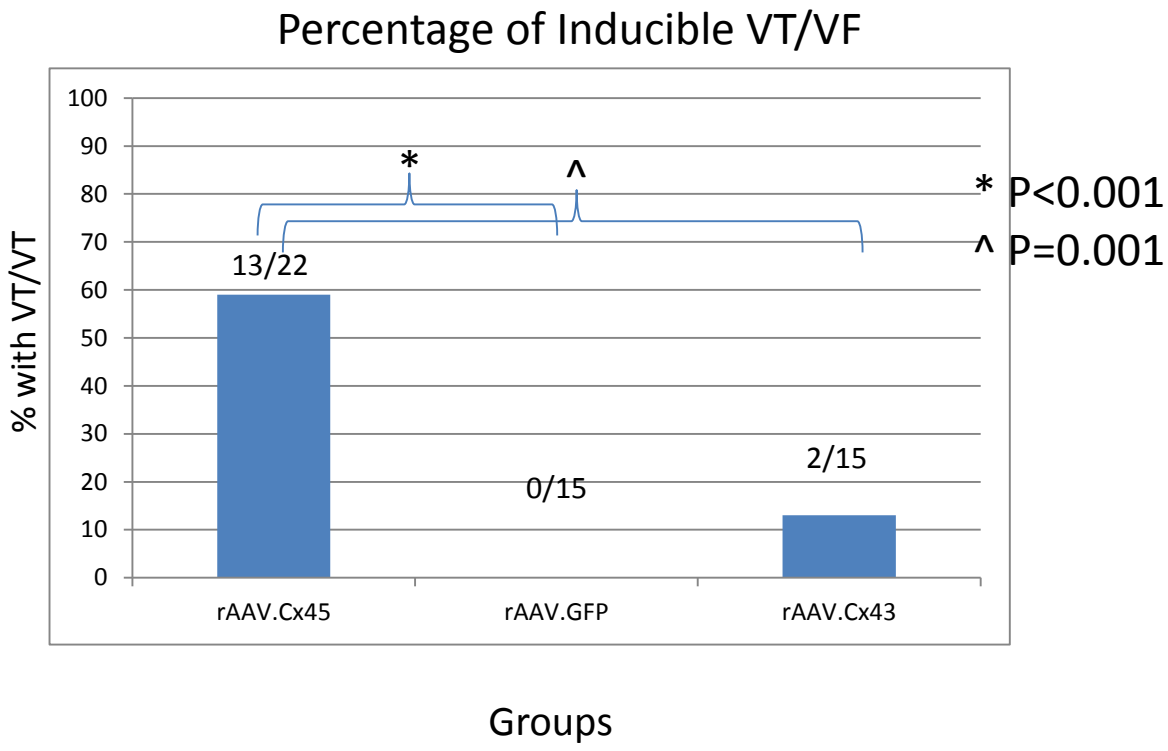

Figure 3.8: Rhythm Strips

A) Evidence of drive train with two extra beats resulting in ventricular tachycardia.

B) Complete heart block seen in a Cx45 overexpressed rat heart; there was dissociation of P wave and QRS complexes.

A)

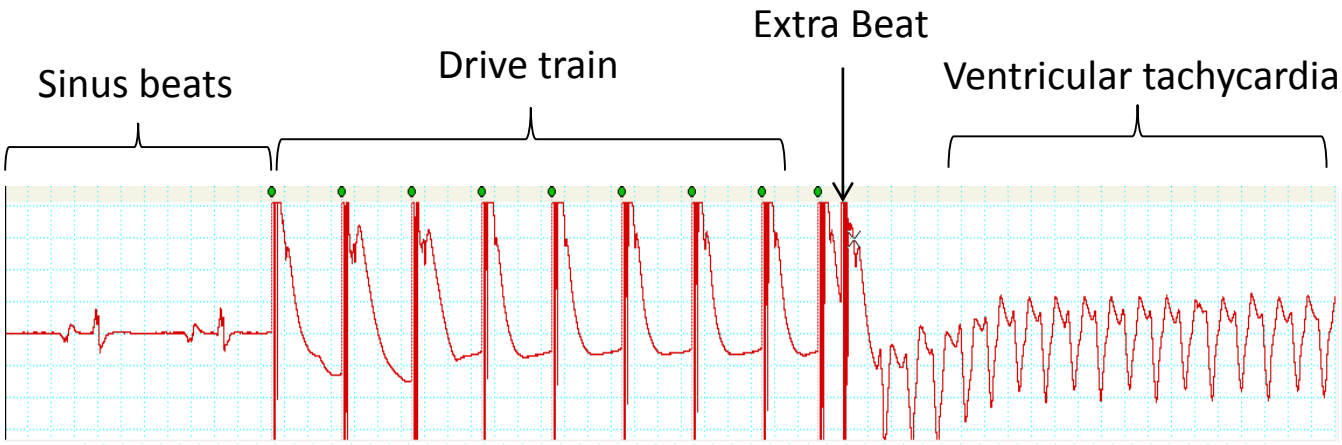

B)

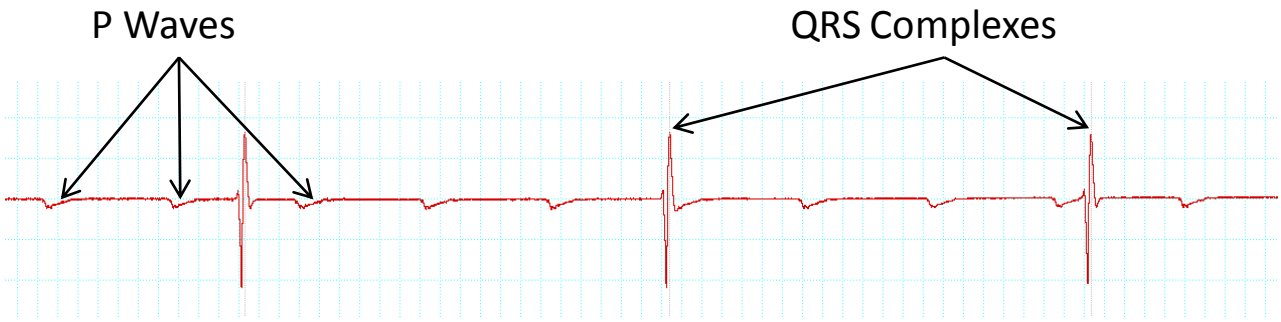

3.3.4 Connexin43/Connexin45 Protein Interaction Studies

To assess for heteromeric gap junction formation as a mechanism for conduction slowing, co-immunostaining was carried out on Cx45 transduced hearts. By confocal microscopy (Figure 3.9) this showed a heterogeneous expression of Cx45 with no alteration in the expected Cx43 expression level and subcellular localisation. Co-localisation of the immuno-reactive signal from the two connexins was observed. To directly assess for protein-protein interaction Duo-link studies and co-immunoprecipitation were performed (Figure 3.10 and 3.11 respectively). These two methods confirmed interaction and further supported Cx45/Cx43 co-localisation.

Figure 3.9 Co-Immunostaining of Connexins in Rat Myocardium

Co-immunostaining for Cx45 (red) and Cx43 (green) in Cx45 overexpressed rat myocardium. Yellow signal identifies areas of possible co-localisation of Cx45 and Cx43. Nuclei labelled blue with DAPI.

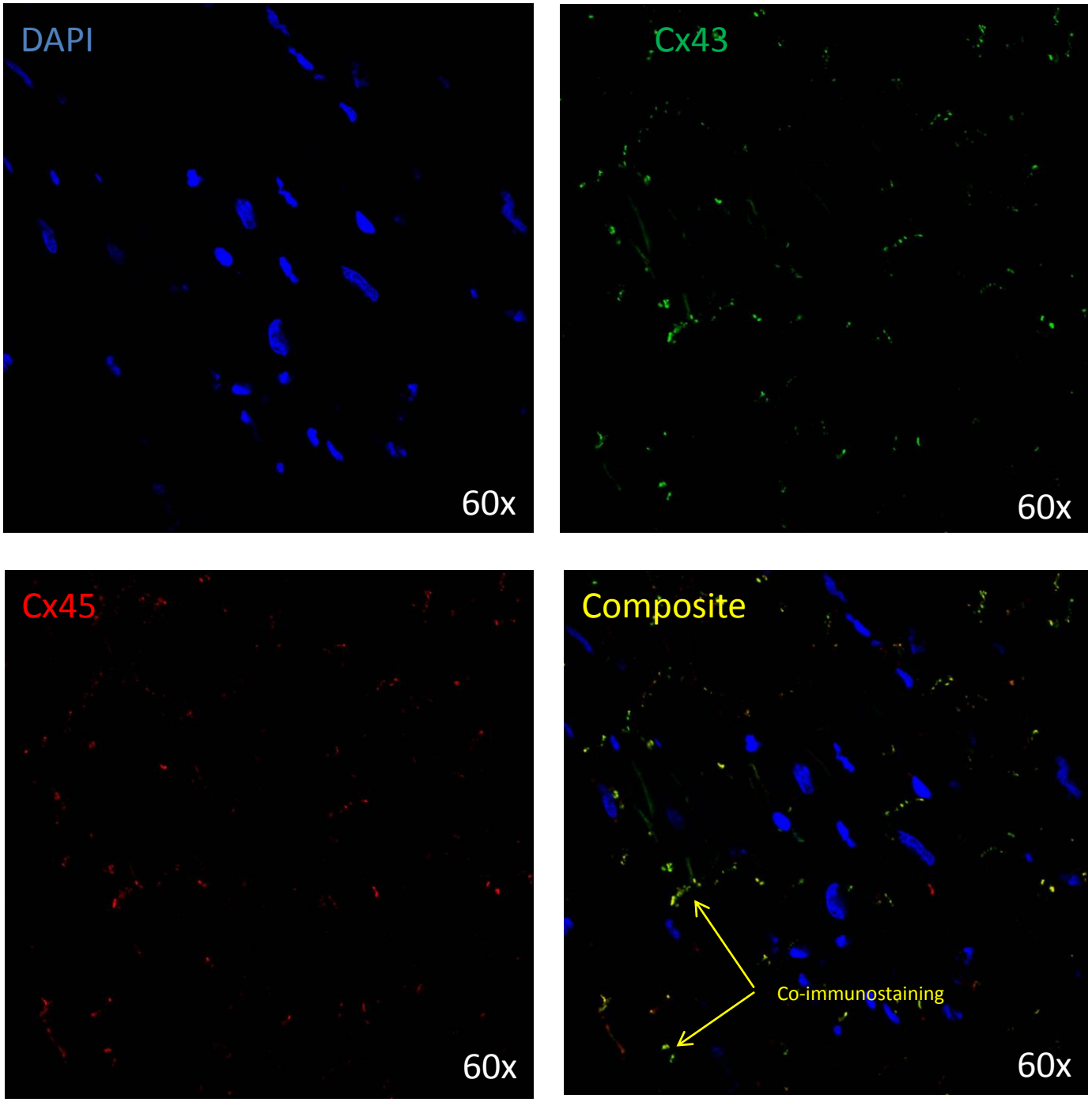

Figure 3.10: Duo-Link

Duo-Link image, the red signal (Duo-Link) identifies areas of co-localisation of Cx43 and Cx45. Nuclei are stained blue.

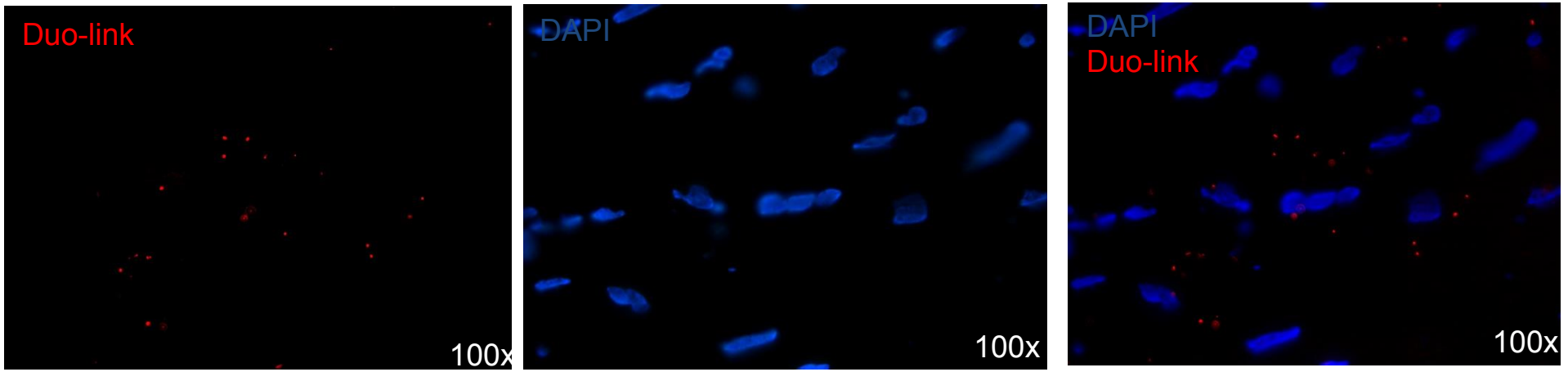

Figure 3.11 Co-immunoprecipitation

The figure below shows co-immunoprecipitation of Cx43 and Cx45 from rat myocardium. Initially Cx45 or Cx43 were immunoprecipitated using monoclonal anti-Cx45 or anti-Cx43 antibodies as in Figure 3.6. The proteins in the immunoprecipitates were resolved by SDS-polyacrylamide gel electrophoresis and subjected to immunoblotting with rabbit polyclonal anti-Cx43 or anti Cx45 antibodies to reveal Cx43 in Cx45 associated proteins and Cx45 in Cx43 antibodies (square boxes). Neither Cx43 nor Cx45 were observed in the negative control.

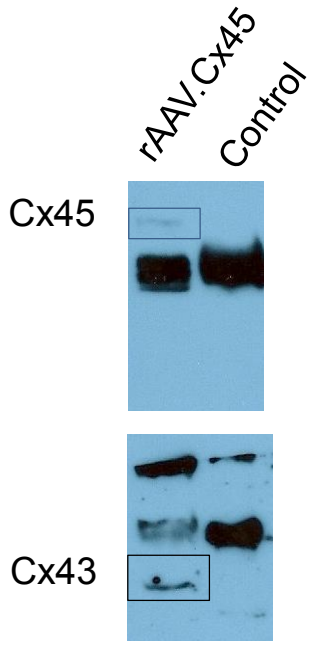

3.3.5 Heart Failure/Fibrosis Studies

To further understand the mechanism behind the increased arrhythmogenesis for Cx45 overexpressed rats, we sought to exclude confounding processes such as heart failure, fibrosis and inflammation. There was no difference in heart to body weight ratios, heart failure gene expression (ANP and βMHC), intramyocardial fibrosis and inflammation between any of the groups (Figures 3.12, 3.13 and Table 3.3 respectively).

Figure 3.12: Haematoxylin and Eosin Stains of Ventricular Tissue.

Representative left ventricular tissue sections stained with H&E from each of the study group. Inflammation score from a total of 60 images (from 5 separate rat hearts) within each group was provided (mean ± SD). No significant difference was observed between means of GFP, Cx43, and Cx45 groups when compared.

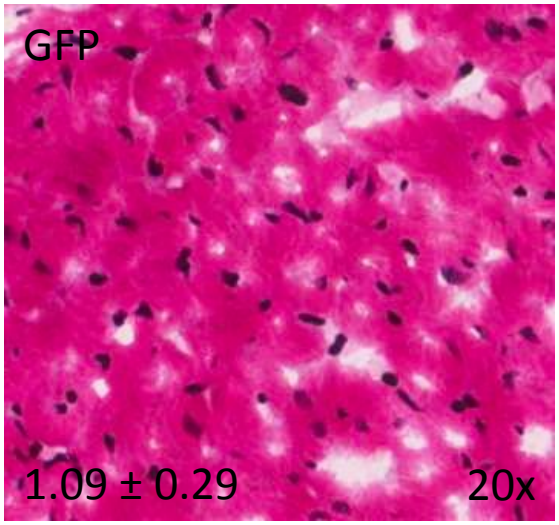

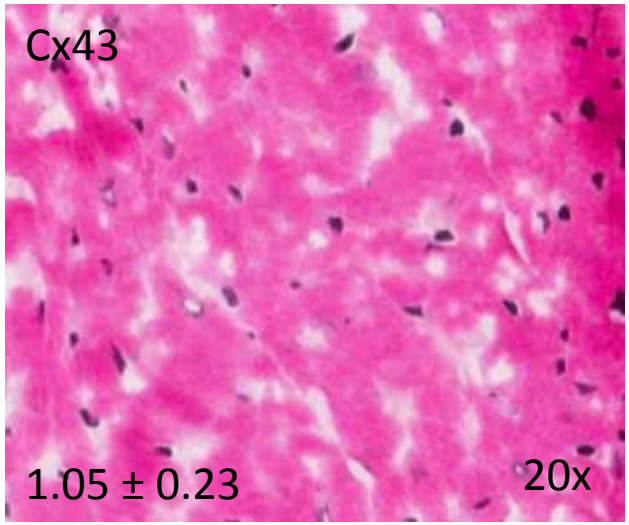

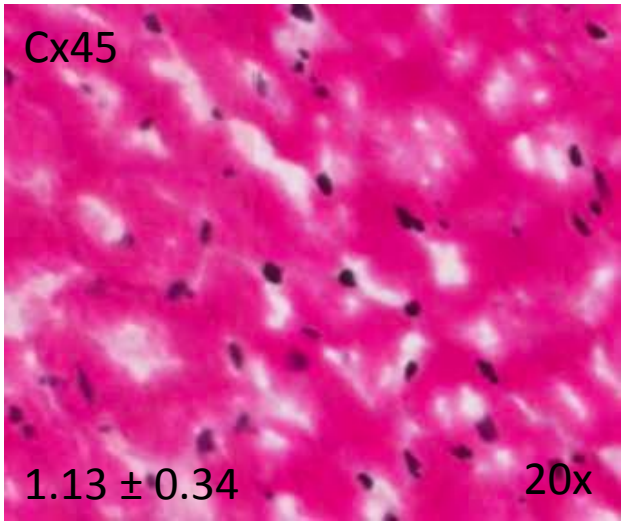

Figure 3.13: Pico-Sirius Red Stains of Ventricular Tissue

Representative left ventricular tissue sections stained with Pico-Sirius Red from each of the study groups. Percentage fibrosis from a total of 60 images (from 5 separate rat hearts) within each group was provided (mean ± SD). No significant difference was observed between means of the GFP, Cx43 and Cx45 groups.

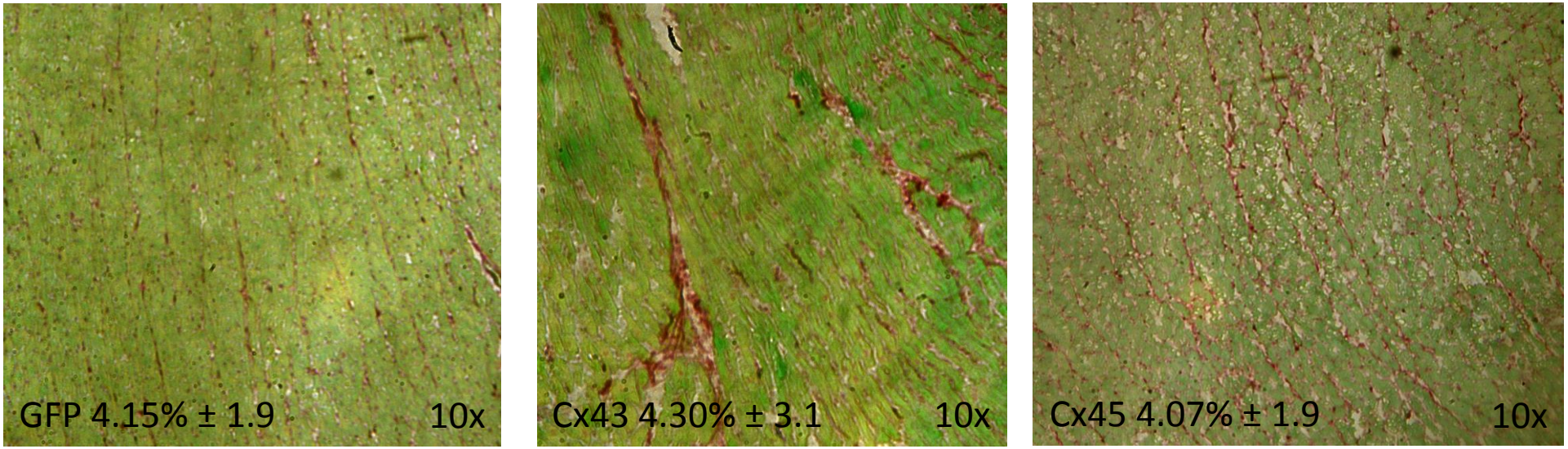

Table 3.3: Heart Failure Parameters

a) Table below shows the mean values of the heart to body ratio in all study groups (mean ± SD). There was no significant difference observed between all groups.

GFP n=15	Cx43 n=15	Cx45 n=22	P-Value
$3.83x10^{-3}±1.9x10^{-4}$	$3.85x10^{-3}±2.3x10^{e-4}$	$3.88x10^{-3}±2.2x10^{-4}$	NS

b) Table below shows the mean values for the heart failure mRNA gene expression in all study groups as mean ± SD. There was no significant difference observed between all groups.

	GFP (n=7)	Cx43 (n=7)	Cx45 (n=7)	P-Value
ANP	0.48±0.63	0.25±0.34	0.36±0.12	NS
βMHC	1.0±0.9	1.5±0.9	0.85±0.8	NS

3.4 Discussion

The main findings of this study were that Cx45 over expression was associated with slowing of myocardial electrical propagation and an increased risk for arrhythmogenesis in the intact heart. Connexin43 overexpression did not have the same effect. This supports previous studies that have suggested that Cx45 may be implicated in the cause of SCD.

Our results support the hypothesis that there was an interaction between Cx45 and Cx43 likely secondary to heteromeric channel formation with the ensuing conduction slowing contributing to arrhythmogenesis. Connexin45 treated hearts were also noted to have a significant reduction in Cx43 as compared to control implying that Cx45 overexpression may affect Cx43 expression. It was likely that Cx45 overexpression alone resulted in arrhythmogenesis. Alternatively, a combination of both increased Cx45 and reduced Cx43 may increase the propensity to arrhythmogenesis. This result was consistent with studies of human heart failure showing an increased Cx45 expression together with reduced Cx43 expression [86, 155]. Heart failure, fibrosis and inflammation were excluded as causes of arrhythmia in this model.

3.4.1 Connexin45

Ventricular tachyarrhythmia is the main cause for SCD. Gap junction remodelling has been investigated as a molecular mechanism for ventricular arrhythmia. Of the known cardiac connexins, knowledge of Cx45 and its functional role in the heart is the most limited. Most investigations have been performed on continuous cell lines such as SkHep1 or HeLa cells [31, 78-80]. In terms of the role of gap junctions composed of Cx45, Valiunas et al. have reported that gap junctions composed of Cx45 have a relatively small unitary conductance (~26pS) when compared to gap junctions composed of Cx40 or Cx43 [83]. This property of Cx45 gap junctions likely underpins the prevalence of this connexin in the AV and sinoatrial nodes. These sites physiologically demand slow but safe electrical conduction.

3.4.2 Connexin43/Connexin45

Studies have suggested that reduced Cx43 expression may result in diminished coupling, conduction slowing and thereby contribute to re-entrant tachyarrhythmia. However data from Cx43 knockout mice showed that there needs to be a greater than 50% reduction in expression to effect significant conduction delay or arrhythmia [88, 156]. It seems, therefore, that the more modest reduction in Cx43 observed in

heart disease is unlikely to be the sole cause of the abnormal rhythm generation. Others such as Peters et al. have suggested altered cellular patters of Cx43 expression allow formation of functional lines of conduction block and therefore enhance re-entry arrhythmia [23].

Given the up-regulation of Cx45, it is conceivable that ventricular gap junction connexins in diseased hearts are made up of oligomers of Cx43 and Cx45. A recent study by Bao et al. had found that Cx45 represents 0.3% of total connexin protein and co-localizes with Cx43 in native ventricular gap junctions [91]. This was mainly noted in the apex and septum of the myocardium. This study, however, reported that overexpressed or down-regulated hearts were not found to have any notable effect in the electrical conduction system. This was in contrast to our study which demonstrated prolongation of AV nodal and QRS width compared to baseline. Of note, an earlier study by the same group showed that Cx45 overexpression resulted in increased susceptibility to ventricular tachyarrhythmia [3]. Differences to our study may relate to differences in the method of overexpression, the amount of overexpression and the animal models employed in the studies.

The functional effects of heteromeric Cx43/Cx45 channel formation on gap junctional intercellular coupling have been assessed in heterologous

expression systems and in primary myocytes [90] [80, 81]. The resulting heteromeric gap junctions yielded disparate functions to their homomeric counterparts raising the possibility that heteromeric channel formation may be one mechanism by which intercellular communication can be altered to effect conduction slowing and predispose to arrhythmia. Notably, Cx45 is overexpressed in human heart failure, a condition also known to predispose to VT/VF and SCD [149]. In our study we hypothesised that the formation of heteromeric Cx43/Cx45 gap junction channels with lower unitary conductance led to the ECG manifestations of prolonged PR interval and widened QRS width. We noted a more marked slowing for the PR interval than the QRS and this is likely due to Cx45 being more pronounced in the AV node than the bundle branches and possible increased expression in the AV node following transduction. Furthermore in our study we had shown co-localisation of Cx45 and Cx43 with immunostaining and direct protein-protein interaction with Duo-Link and co-immunoprecipitation methods. These findings support the hypothesis that heteromeric Cx43/Cx45 channels do exist and are increased in prevalence with Cx45 overexpression leading to slower conduction and inducible ventricular tachyarrhythmia.

3.4.3 Transgenic Overexpression vs. Somatic Gene Transfer

In a transgenic, cardiac-restricted, Cx45 overexpressing mouse model there was an increased incidence of spontaneous and inducible ventricular tachyarrhythmia [90]. Moreover in Cx45 knockout models of mice, they died from heart failure in utero at embryonic day 10. The embryonic hearts were found to be dilated. However even in the absence of Cx45, heart contractions were initiated but there was conduction block through the atrioventricular canal, and the contractions in the outflow tract were not co-ordinated with those in the ventricle. This latter finding implies a functional role for Cx45 in ventricular conduction.

The use of transgenic mice to study connexin biology and arrhythmia is limited by changes in the expression of unintended molecules and the high-level of structural abnormalities encountered [62]. These limitations could explain the genesis of arrhythmia independent of the intended molecular alteration. While it is agreed that use of conditional transgenics may overcome these limitations, the somatic gene transfer approach may be considered superior in this context for the following the reasons. Firstly, acute genetic changes will be induced in the adult heart essentially mimicking those likely to occur in the context of acute and acquired myocardial disease. Secondly, heterogeneity of gene transfer also mimics the heterogeneous pattern of connexin expression in the

diseased heart and is likely to result in higher levels of arrhythmia burden than the low levels seen by Betsuyaku et al [90]. In our studies using somatic gene transfer we achieved a high level of transduction with high levels of conduction slowing and inducible ventricular arrhythmia.

3.4.4 Confounders and Limitations

We have looked in this study at possible confounding factors that predispose to ventricular arrhythmogenesis. Heart failure patients with reduced ejection fraction have increased ventricular arrhythmias [157]. We examined the heart to body weight ratio and heart failure gene activation. The results were the same between the studied and control groups.

A limitation of this study was that we did not look at sodium channel function. Studies had shown that the sodium channel can co-localise with gap junctions at the intercalated disc [158, 159]. The interaction with Cx45 is not known and therefore this could potentially be a contributing factor to conduction slowing and increased arrhythmogenesis.

A further limitation was that the effects of Cx45 overexpression on the post-translational states of Cx43 were not assessed. This in itself may lead to protein to protein interactions that were not assessed and contribute to the slowing of conduction. Moreover the localisation of

Cx43 in the intercalated discs had been shown to be an important factor in arrhythmogenesis and this had not been assessed in this study either.

3.5 Conclusion

Somatic gene transfer of Cx45 with resulting overexpression in the intact rat heart resulted in slowing of conduction (as evidenced by PR and QRS interval prolongation and widening respectively) and an increased susceptibility to ventricular arrhythmia. This was associated with a direct interaction between Cx43 and Cx45 proteins and independent of the presence of heart failure or fibrosis.

CHAPTER 4

SILENCING CONNEXIN45 OVEREXPRESSION AMELIORATES EXCESS VENTRICULAR TACHYARRHYTHMIA: TOWARDS GENE THERAPY OF VENTRICULAR ARRHYTHMIAS

4.1 Introduction and Aims

The previous chapter revealed that overexpression of Cx45 in rat myocardium led to ventricular tachyarrhythmia. Gene transfer technology and molecular cardiology advances make the prospect of using genetic manipulation to favourably modify normal physiological and pathophysiological processes in the heart increasingly plausible.[160]

Short regulatory RNA's such as short hairpin RNA (shRNA) and microRNA are a class of double stranded RNA molecules that are notable for interfering with the expression of specific genes with complementary nucleotide sequences. Their use to specifically silence genes has been

widely appealing as a new method of therapy [161]. Proof of concept studies involving short regulatory RNAs have previously demonstrated therapeutic efficacy in targeting organs such as the eye and nervous system have been undertaken [162-165]. Phase I studies have been performed utilising these short regulatory RNAs to switch off cancer-related genes and stabilize diseases as devastating as cancer with liver metastases [166]. Cardiac applications of this technology have also emerged and led to exciting developments such as viral vector based delivery of shRNAs for the treatment of heart failure [161, 167].

The therapeutic application of shRNAs has advantages over pharmacological agents and antibodies. The main advantage being that shRNA can potentially target all molecules including those not amenable to pharmacotherapy [161]. In addition, they are relatively simple to synthesize compared to small molecules or antibodies. The main disadvantage on the other hand, is that shRNAs can only provide antagonistic effects on their target molecules [161].

In the previous chapter it was demonstrated that Cx45, when overexpressed *in-vivo*, resulted in an increased susceptibility to ventricular tachyarrhythmia. It led to slowing of conduction as evidenced by lengthening of ECG intervals, specifically the PR interval and QRS

duration. This finding provided support for our hypothesis that Cx45 inhibits gap junction function and slows conduction leading to ventricular tachyarrhythmia. In this chapter we explored the corollary of the hypothesis and test the effects of reversing Cx45 overexpression by shRNA mediated silencing of the transgene.

In this study we confirmed that reversal of Cx45 overexpression leads to reversal of arrhythmia susceptibility and explored the effects of Cx43 overexpression simultaneously with Cx45 overexpression. We hypothesized that an increase in the amount of Cx43 relative to Cx45 would also lead to a reduction in ventricular arrhythmia.

4.2 Methods

Three groups of rats were each treated with two vectors as follows (1:1 ratio); (1) rAAV.Cx45 and rAAV.shNS (non-silencing control vector), (2) rAAV.Cx45 and rAAV.sh45 (silencing vector) and (3) rAAV.Cx45 and rAAV.Cx43.

Figure 4.1 Study Protocol Diagram

A total of 3 groups were studied. The rAAV.Cx45/rAAV.shNS acted as the control group. The other 2 groups were rAAV.Cx45/rAAV.sh45 and rAAV.Cx45/rAAV.Cx43. All rats underwent baseline EPS followed by vector injection. EPS was repeated at day 28 followed by removal of ventricular tissue. The ventricles were then probed for Cx45, Cx43 protein and mRNA levels, and inflammation and fibrosis with histological analysis.

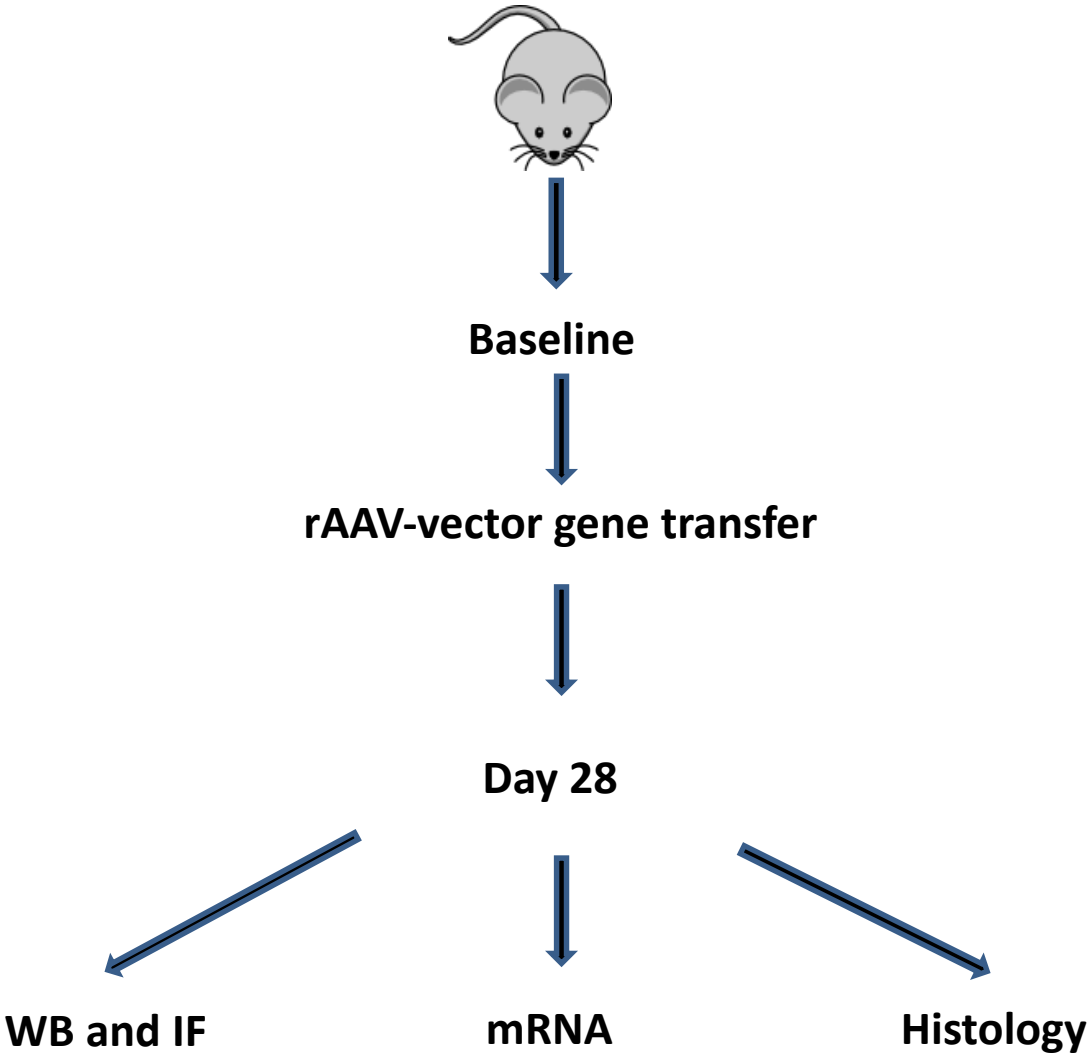

4.2.1 Vector Packaging and Titration

Vector stocks encoding GFP, Cx43, Cx45, non-silencing RNA, silencing RNA targeting Cx45 were produced using the calcium precipitation method as described in Section 2.3. The resulting vectors were designated rAAV.GFP, rAAV.Cx43, rAAV.Cx45, rAAV.shNS and rAAV.sh45, respectively. Vector stock titre was assessed by qPCR as described in Section 2.3.4.

4.2.2 Ventricular Myocardium Transduction

Ventricular myocardium transduction was performed as described in Section 2.10.4. In brief, rats were anesthetized with 2% isoflurane, intubated and baseline electrophysiology studies were carried out. Following this, viral vectors were injected via the tail vein. Repeat EPS was performed at day 28 followed by excision of the ventricles at sacrifice for subsequent histological and molecular analysis of tissues.

4.2.3 Electrophysiological Studies

Electrophysiological studies were performed as described in sections 2.10.3. In brief, recordings were carried out using subcutaneous plunge needle electrodes during simultaneous stimulation via a trans-oesophageal pacing probe. Stimulation was performed with programmed

stimulation and burst pacing. Programmed stimulation involved an 8 beat drive train with a coupling interval of 180milliseconds followed by up to 4 extra beats. Burst pacing involved electrical stimulation using a coupling interval of 90milliseconds for 30seconds followed by 60milliseconds for a further 30seconds.

4.2.4 Morphometric Studies

All rats and their hearts were weighed at the end of the protocol.

4.2.5 Immunoblotting

The ventricles were excised and stored following day 28 of the protocol as described in Section 2.10.7. Protein was extracted and quantified by method of immunoblotting as previously described in the Section 2.6. In brief, samples were subjected to electrophoretic separation in 4-12% BIs-Tris gradient gels, followed by membrane transfer using the iBlot (Invitrogen) gel transfer system. Subsequently, the membranes were washed and incubated with Cx45 or Cx43 primary antibodies followed by secondary antibody incubation and then chemiluminescence system was used to produce immunoblot images.

4.2.6 Immunofluorescence

As described in Section 2.4, the ventricles were excised and stored at day 28 and after the EP studies were performed. Ventricle tissue was then sectioned using the cryostat and subjected to immunostaining. In brief, sections were fixed with 4% (w/v) paraformaldehyde, permeabilised with 0.05% (v/v) Tritom X-100, blocked with Goat serum from (Invitrogen). Slides were incubated with primary antibodies of either Cx45 or Cx43, followed by secondary antibody incubation and mounted with Prolong Gold antifade reagent containing DAPI nuclear stain. Fluorescent images were acquired using the Leica DMIL wide field microscope or Olympus FV 100 confocal laser scanning microscope.

4.2.6 Haematoxylin and Eosin Staining

Following sectioning of ventricular myocardium H&E staining was performed as described in Section 2.5. Images were then acquired as described in Section 2.5.3 and assessed for inflammation. The scoring system was as follows: 1 – absent, 2- occasionally present, 3 - ≤ 50% affected, 4 – 50-90% affected and 5 - ≥90% affected.

4.2.8 Pico-Sirius Red Staining

Following sectioning of ventricle myocardium, Pico-Sirius red staining of the sections was performed as described in Section 2.5.2. Images were then acquired as described in Section 2.5.3 and processed with custom software designed to objectively identify the total pixel area occupied by collagen (red) and the total pixel area occupied by the remaining tissue (green). Collagen density of each myocardial section was calculated as the ratio of collagen relative to the area of the section as demonstrated in Figure 3.2.

4.2.9 Real Time Quantitative PCR

See Sections 2.3.4 and 2.7.3 for full methods. Briefly, sequences for the forward primer, reverse primer and probes were used as described in the methods section. A master mix was made up with 1µl of probe, 0.8µl of each forward and reverse primers, 4.9µl of DNASEfree RNA (Sigmal Aldrich) a master mix 12.5µl (sigma – Aldrich), and 5µl of DNA per PCR reaction. For a negative template control, 5µL of H_20 was used.

Reactions were carried out in triplicates and amplifications were performed with 1 cycle of 95°C for 10 minute, 35 cycles of 95°C for 15 seconds, and 60°C for 2 minutes using a Rotor-Gene 6000 PCR cycler

(Corbett) or Rotor-Gene 3000 PCR cycler (Corbett). Concurrent standard curves were generated. The number of vector DNA molecules in each sample reaction was calculated by comparing threshold cycle values of samples to the standard curve. To determine the final viral vector titre, the number of vector DNA molecules of each sample reaction was corrected for dilution and then averaged.

4.2.10 Statistical Analysis

As described in Section 2.11, quantitative data were expressed as mean ± standard error of the mean. Statistical analyses between control and treatment groups were performed using Fischer's exact test (if samples in a cell were ≤ 5) or using two sample X^2 test (2 x 2 table) on the SPSS (Version 17). Significance was set at $P \leq 0.05$.

4.3 Results

4.3.1 Electrophysiology Studies

The effects of genetic therapies tested on electrophysiological function *in vivo* are summarised in Table 4.1. Overexpression of Cx45 resulted in significant QRS prolongation in the control group rAAV.Cx45/rAAV.shNS ($p=0.046$). In comparison to the control group, co-treatment with a Cx45 silencing vector rAAV.Cx45/rAAV.sh45 significantly reversed this effect to equivalent levels as measured during baseline. Connexin43 overexpression in the Cx45 overexpressed group resulted in no significant reduction in QRS duration as compared to the control group. In contrast, the PR interval was not influenced by any genetic treatments tested.

Short hairpin RNA mediated knockdown of Cx45 in the rAAV.Cx45/rAAV.sh45 group resulted in a significant reduction of inducible VT/VF compared to the non-silencing rAAV.Cx45/rAAV.shNS group. The rAAV.Cx45/rAAV.Cx43 group did not show a significant reduction in susceptibility to VT/VF compared to the rAAV.Cx45/rAAV.shNS group (Table 4.2).

Table 4.1 Electrophysiological Results

EPS parameters are shown for each group.

	rAAV.Cx45 + co-treatment	rAAV.shNS (n=17)	rAAV.sh45 (n=18)	rAAV.Cx43 (n=10)	p – value	
					rAAV.shNS vs rAAV.sh45	rAAV.shNS vs rAAV.Cx43
PR Interval (ms)	Baseline	45.5+/-5.97	46.9+/-4.03	46.9+/-3.19	NS	NS
	Post Treatment	51.4+/-9.17	48.2+/-6.53	47.0+/-5.97	NS	NS
	Δ	4.47+/-4.83	2.69+/-5.49	0.09+/-6.68	NS	NS
QRS Duration (ms)	Baseline	16.2+/-2.17	16.6+/-1.42	15.7+/-2.72	NS	NS
	Post Treatment	17.8 +/- 1.99	16.6+/-2.21	17+/-3.07	0.05	NS
	Δ	1.61+/-1.69ms	0.00+/-2.29	1.32+/-3.04	0.015	NS

In vivo comparison of electrophysiological effects of Cx45 knockdown (rAAV.sh45), and Cx43 overexpression (rAAV.Cx43) following Cx45 overexpression (rAAV.Cx45) in rat hearts. Comparison made against Cx45 overexpressing hearts that have been co-treated with a non-silencing vector (rAAV.shNS). Electrophysiological

measurements include: mean PR interval and QRS durations for each group as measured at Day 0 (Baseline) and Day 28 (Post Treatment). Δ = mean difference (post-treatment – baseline). PR interval was not influenced by treatment and did not change over time. Cx45 overexpression resulted in significant prolongation of QRS duration. This effect was reversed following Cx45 knockdown, but remained unchanged following Cx43 overexpression. All values are mean ± SD.

Figure 4.2 Incidence of Inducible of VT/VF

In vivo comparison of VT/VF propensity in rats following Cx45 knockdown (rAAV.sh45) and Cx43 overexpression (rAAV.Cx43) following Cx45 overexpression (rAAV.Cx45). Ventricular tachyarrhythmia was significantly reduced during Cx45 knockdown but not during Cx43 overexpression as compared to control rAAV.Cx45/rAAV.shNS.

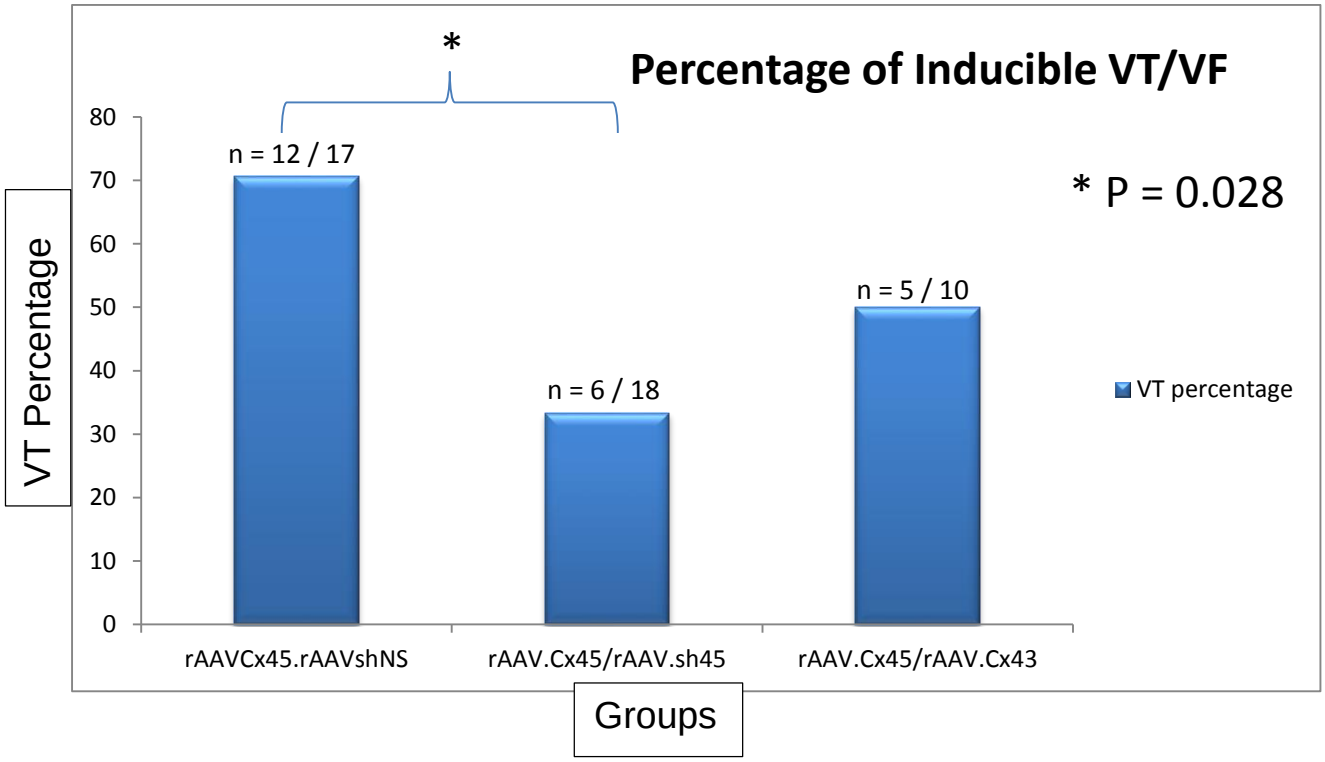

4.3.2 Immunofluorescence

Immunofluorescence revealed less Cx45 immunoreactive signal in rAAV.Cx45/rAAV.sh45 group compared to the non-silencing group (Figure 4.3). There was no appreciable increase in Cx43 expression in the rAAV.Cx45/rAAV.Cx43 group compared to the control given the high level of background Cx43 expression. Furthermore, a high degree of co-localisation between Cx45 and Cx43 was observed in the rAAV.Cx45/rAAV.Cx43 group using confocal microscopy (Figure 4.4).

Figure 4.3 Expression of Cx45 in Rat Myocardium (confocal microscopy)

Connexin45 is represented by green signal. Nuclei were stained blue. Connexin45 is noted in the intercalated discs. As can be noted there was reduced Cx45 signal in rAAV.sh45 treated group compared to the control rAAV.shNS group.

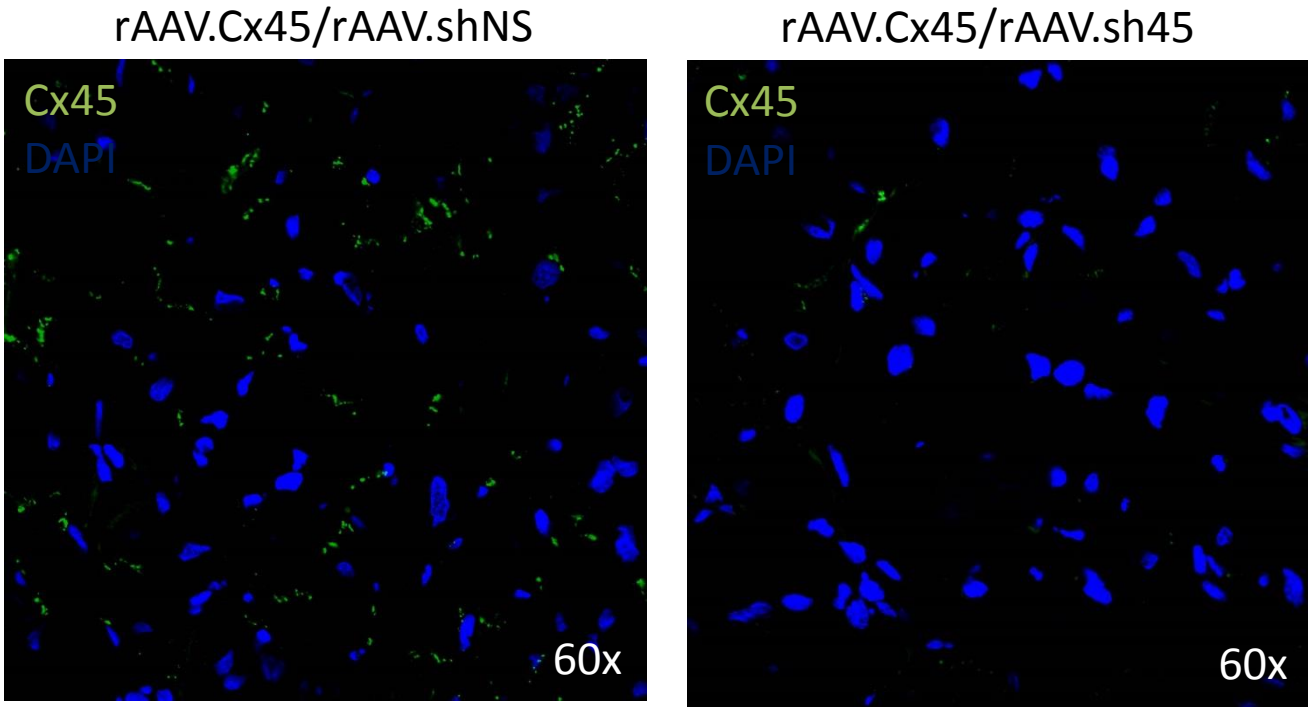

Figure 4.4 Co-Immunostaining of Connexins in Rat Myocardium

Co-immunostaining for Cx45 represented by green signal and Cx43 represented by red signal in Cx45 overexpressed rat myocardium with non-silencing vector. Yellow signal identified areas of possible co-localisation of Cx45 and Cx43. Nuclei were stained blue with DAPI.

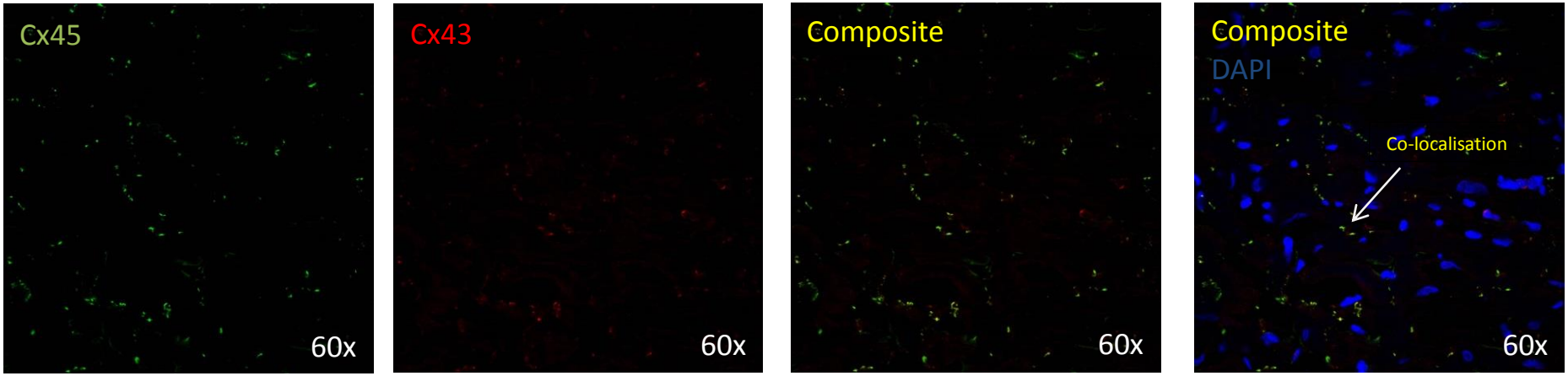

4.3.3 Immunoblotting

Immunoblotting of tissue lysates revealed no appreciable difference in level of Cx43 expression within the ventricles of rats transduced with rAAV.Cx45/rAAV.Cx43 Figure 4.5. This may be due to the significant amount of background Cx43 expression in rat myocardium. However, Cx45 was reduced in the rAAV.Cx45/rAAV.sh45 knockdown group compared to the other two groups as seen in Figure 4.5.

Figure 4.5 Western Blot for Connexin43 and Connexin45 in Transduced Rat Myocardium

Cx45 and Cx43 protein levels are shown by Western blot. The Image on the left was representative and revealed significant Cx45 expression reduction in AAV.Cx45/AAV.shRNA compared to the other groups (n= 3, *P<0.01*). Bottom image “B)” revealed similar Cx43 detected in all myocardium (n=3).

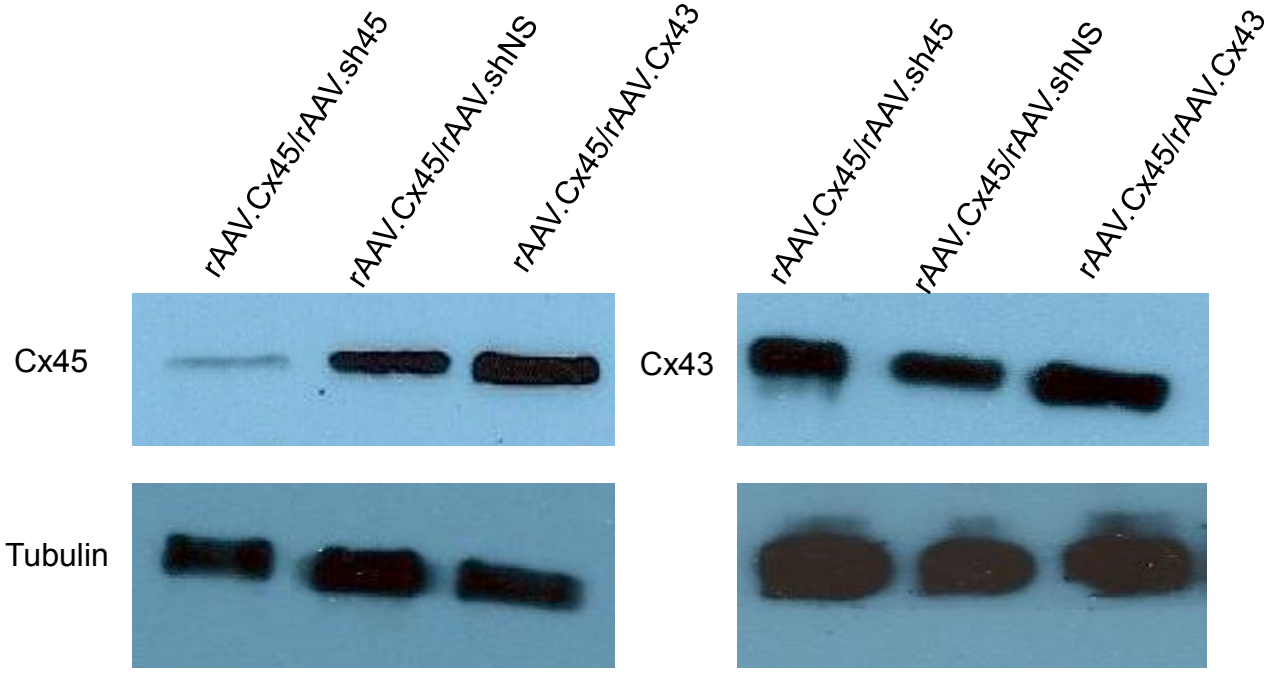

Densitometry	0.13	0.71	1.03	1.05	0.8	1.38

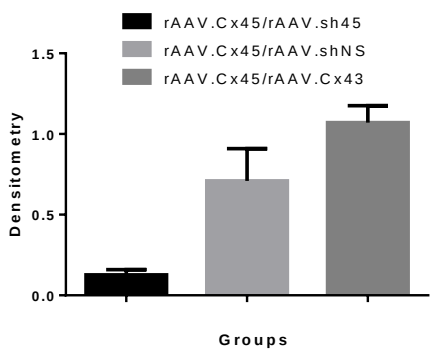

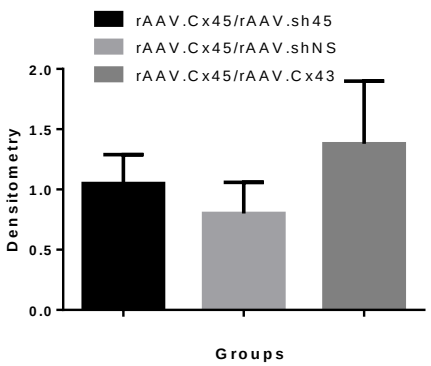

4.3.4 Expression of Connexin43 and 45 mRNA in Transduced Rat Myocardium

There was no significant difference in the expression of Cx43 between the groups. There was a significant 51% reduction in the expression of Cx45 in the rAAV.Cx45/rAAV.sh45 vs. rAAV.Cx45/rAAV.shNS group (Table 4.2).

4.3.5 Fibrosis and Inflammation

Inflammation scores were made of the ventricular tissue stained with H&E. These were found to be similar between the groups (Table 4.3). Furthermore the levels of fibrosis between the groups was also similar (Figure 4.6).

4.3.6 Heart Failure Parameters

The ratio of heart to body weight as a parameter of heart failure was not different between the groups (Figure 4.7).

Table 4.2: Connexin45 and Connexin43 mRNA Expression in Transduced Rat Myocardium

a) Shows Cx45 RNA expression between the rAAV.Cx45/rAAV.shNS (n=8) and rAAV.Cx45/rAAV.sh45 (n=9) groups. There was a significant reduction in Cx45 RNA expression in the rAAV.Cx45/rAAV.sh45 group compared to control.

rAAV.Cx45/rAAV.shNS	rAAV.Cx45/rAAV.sh45	p-value
2.57±1.40	1.25±0.62	0.046

b) Shows the Cx43 RNA expression in the three study groups. Although increased, the Cx43 mRNA level was not significantly higher in the rAAV.Cx45/rAAV.Cx43 (n=6) compared to the other two groups, rAAV.Cx45/rAAV.shNS (n=8) and rAAV.Cx45/rAAV.sh45 (n=9).

rAAV.Cx45/rAAV.shNS	rAAV.Cx45/rAAV.sh45	rAAV.Cx45/rAAV.Cx43	p-value
0.63±0.29	0.54±0.18	0.86±0.26	NS

Table 4.3 Inflammation Score

Table below shows the average inflammation score between the groups.

(n=30 in each group from 5 separate rat hearts, p=NS)

rAAV.Cx45/rAAV.shNS	rAAV.Cx45/rAAV.sh45	rAAV.Cx45/rAAV.Cx43	p-value
1.07±0.26	1.1±0.32	1.06±0.26	NS

Figure 4.6 Percentage Scar

Graph shows a representation of the average scar percentage in each group. n=30 in each group (from 5 separate rat hearts); p = NS

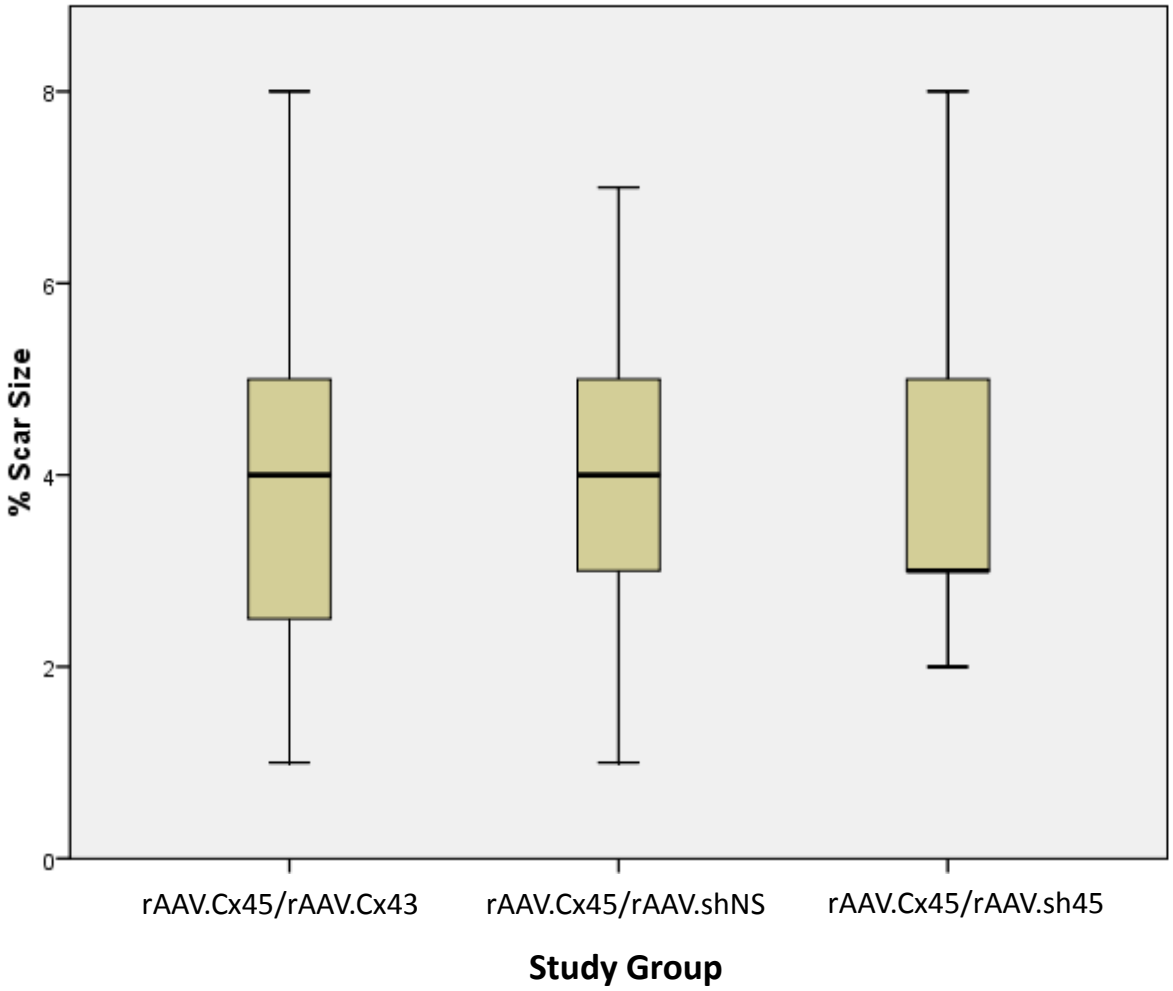

rAAV.Cx45/rAAV.shNS	rAAV.Cx45/rAAV.sh45	rAAV.Cx45/rAAV.Cx43	p-value
4.25±1.33	3.89±1.73	4.07±2.05	NS

Figure 4.7 Heart to Body Weight Ratio

Table below shows the results between the 3 groups with regards to the heart to body weight ratio.

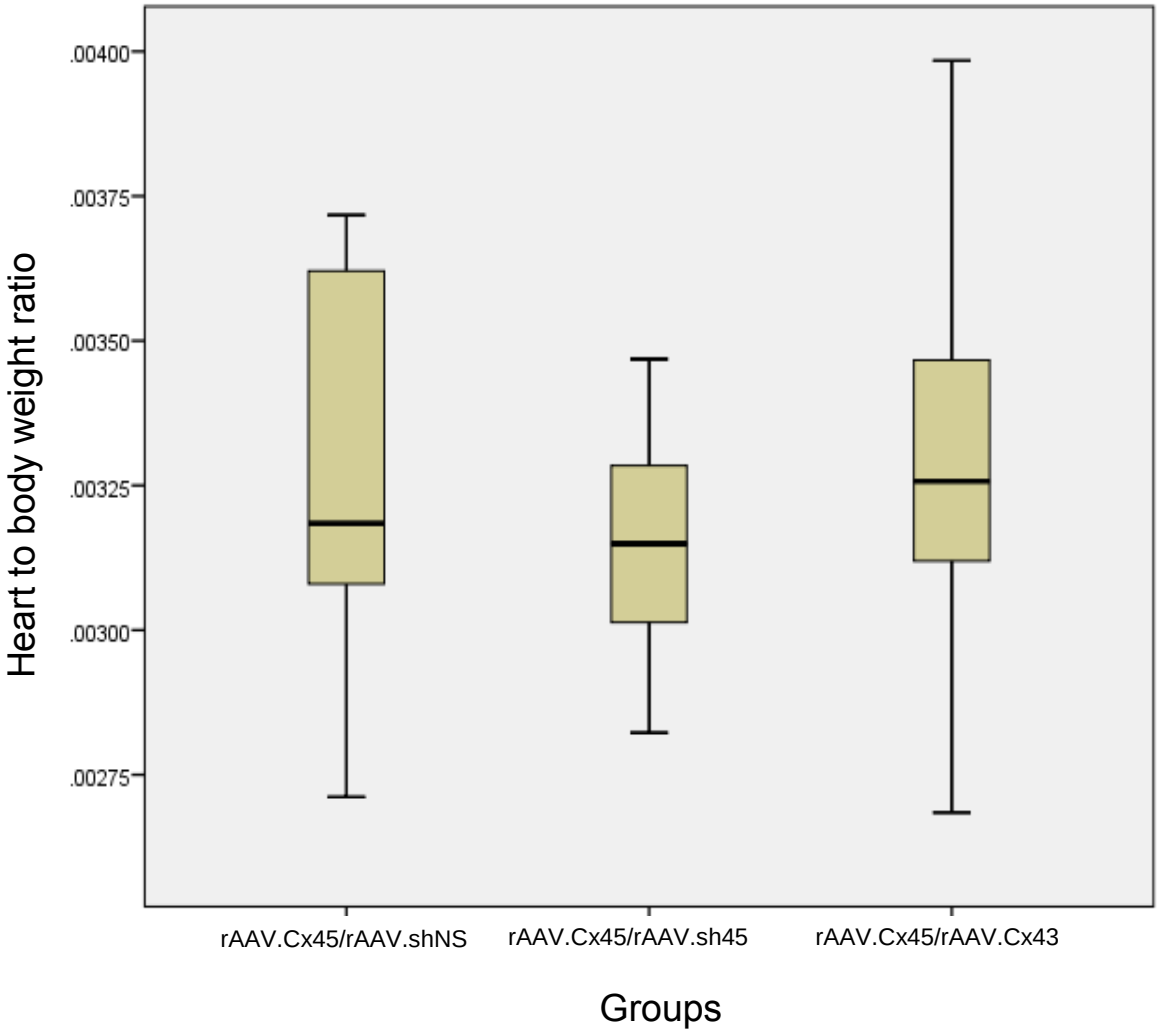

rAAV.Cx45/rAAV.shNS (n=17)	rAAV.Cx45/rAAV.sh45 (n=18)	rAAV.Cx45/rAAV.Cx43 (n=10)	p-value
$3.26x10^{-3}±3.0x10^{-4}$	$3.15x10^{-3}±2.9x10^{-4}$	$3.29x10^{-3}±4.4x10^{-4}$	NS

4.4 Discussion

To the best of my knowledge, this is the first study to confirm that Cx45 knockdown *in vivo* can be achieved by shRNA via a rAAV vector. Delivery of the Cx45 silencing vector to the myocardium not only reduced Cx45 mRNA and protein expression but also decreased ventricular Cx45 dependent conduction slowing, dispersion, and susceptibility to arrhythmias associated with Cx45 overexpression.

The role of Cx45 in cardiac myocytes and its association with heart failure and ventricular tachyarrhythmia is an important area of study. As previously discussed, studies have shown an increase in Cx45 expression in patients with heart failure; an illness with known increased risk of ventricular tachyarrhythmia. In Chapter 3, I was able to confirm this effect *in vivo* by demonstrating that when Cx45 was overexpressed in the normal heart, this led to significant impairment of conduction and increased propensity to ventricular tachyarrhythmias.

Silencing mRNA with short regulatory RNAs such as shRNAs have received increased attention as an exciting and novel method for treating disease by down regulation of specific genes [168, 169]. The use of this

molecular strategy for therapy has already been explored in human trials [168, 170]. With regard to the cardiac application of shRNA, Suckau et al. have designed a shRNA targeting phospholambam (PLB) in cardiomyocytes in both adenoviral and rAAV vectors [167]. This study showed that viral vector mediated shRNA expression and knockdown of PLB was capable of restoring diastolic and systolic function in Sprague Dawley rats with heart failure [167].

In gene therapy studies the viral vector rAAV supported stable transgenic protein expression for more than 1 year [100, 101]. This attests to the capacity for rAAV to confer long-term gene expression and its strength as a clinical vector for applications such as heart failure and as an antiarrhythmic. Long-term gene expression is not possible with adenoviral vector systems in immunocompetent hosts due to the immune response provoked by adenoviral proteins. The Suckau et al. study demonstrated the stability of rAAV-mediated shRNA expression for up to four weeks as evidenced by reduced PLB expression at 4 weeks [167]. Therefore its use in rats with induced heart failure would be ideal and was explored in the next chapter of this thesis.

In our studies Cx45 protein expression was decreased significantly after knockdown with shRNA. Although this reduction was not to the same extent as seen in the steady-state mRNA expression level, this may be due to the non-linear dynamics between mRNA and protein expression and the relatively short half-life of connexin proteins. The achieved level of protein reduction was sufficient to effect a significant reduction in propensity to ventricular tachyarrhythmia. There was also a reversal of the widening of the QRS following knockdown of Cx45. The PR interval on the other hand was not influenced by modulation of Cx45 expression even in conjunction with Cx43 overexpression. This may be due to less efficient transduction of the AV node or demand for higher level Cx45 knockdown before a phenotype becomes evident in this specialised structure.

Connexin43 expression is reduced in heart failure [76, 77]. In Chapter 3 it was shown that Cx45 co-localised with Cx43 when overexpressed in the normal rat heart. This was also confirmed in the current study. This latter finding supports the hypothesis that alteration of the gap junction by heteromeric channel formation results in slowing of conduction and increases propensity to ventricular tachyarrhythmia. In Chapter 3 it was also shown that Cx43 overexpression in the normal rat heart does not alter the myocardial electrophysiology. In the current Chapter we found that

Cx43 overexpression in rats with overexpressed Cx45 (rAAV.Cx43/rAAV.Cx45) did not result in any alteration of the ECG or a reduction in the propensity to arrhythmia, that is, overexpression of Cx43 did not overcome the pro-arrhythmic effects of Cx45 in this model. It is likely that the level of Cx45 overexpression and the inhibitory effects conferred were too great to be overcome by simple overexpression of Cx43 in a one to one stoichiometry. A way to address this would have been to reduce the amount of Cx45 relative to Cx43 in diminishing ratios. Even though an increase Cx43 mRNA and protein was evident this did not achieve statistical significance. One explanation is that Cx45 may have reduced Cx43 expression, as seen in Chapter 3, and co-expression of Cx43 and Cx45 only served to restore expression levels of Cx43. A method to test this would be to transduce the heart with an increased amount of Cx43 vector.

As shown in Chapter 3, the development of heart failure, fibrosis or inflammation were not factors in the effects of Cx45 knockdown on ECG parameters or a reduction in the propensity ventricular tachyarrhythmia in the study system.

Limitations:

A dose dependent effect of vector transduction was not assessed. It is possible that with more knockdown of Cx45 there would be a further reversal of electrical parameters, such as PR interval. Moreover, a dose-dependent effect of Cx43 overexpression may have overcome the inhibitory effects of Cx45 on gap junction function.

4.5 Conclusion

Connexin45 knockdown *in vivo* by shRNA via a rAAV vector reduced Cx45 mRNA and protein expression as well as reversing phenotypic changes. On the other hand, Cx43 overexpression in conjunction with Cx45 overexpression did not reduce the propensity to ventricular tachyarrhythmia.

CHAPTER 5

GENE THERAPY FOR POST MYOCARDIAL INFARCTION VENTRICULAR TACHARRHYTHMIA

5.1 Introduction and Aims

5.1.1 Background

Cardiovascular mortality is the leading cause of death in the industrialized world. Sudden cardiac death occurs most often following acute myocardial infarction [13, 171]. Ventricular tachyarrhythmias are the cause in the majority of cases [172].

We have previously demonstrated that when Cx45 was overexpressed by somatic gene transfer it resulted in conduction slowing as evidenced by widening of both the QRS and PR intervals. This further translated to increased ventricular tachyarrhythmia in the rat model. Protein-protein interaction studies showed an interaction between both Cx45 and Cx43

and likely that heteromeric gap junction formation was a mechanism in the slowing of conduction and the propensity to ventricular tachyarrhythmia.

Furthermore Cx43 mRNA expression was found to be reduced in Cx45 overexpressed rat myocardium but no significant decrease was noted on Cx43 protein expression in the same group. This was explored further in experiments in Chapter 4 where Cx43 was overexpressed in addition to Cx45 in rat myocardium. This resulted in no appreciable reduction in ventricular tachyarrhythmia thereby demonstrating that Cx45 itself must have a role in the propensity to ventricular tachyarrhythmia.

In the following study we tested two approaches to post-MI arrhythmia reduction: one with Cx43 overexpression, and other with Cx45 knockdown.

Method 1: Connexin43 Overexpression

Connexin43 remodelling has been noted following MI. In particular a recurrent finding is a reduction in Cx43 expression in the infarct border–zone [24, 69]. This contributes to alteration in gap junctions and may result in a myocardial re-entrant electrical circuit due to areas of slow conduction

and contributing to ventricular tachyarrhythmia. Greener et al. published data showing Cx43 gene transfer to the healed scar border resulted in overexpression of functional connexins and reduced VT inducibility [64]. Hence, we aimed to also transduce Cx43 in a rodent MI model and note the changes in the cardiac electrophysiology and propensity to ventricular arrhythmia. Differences between Greener's and our study include the different animal models used and the viral vector system employed. We chose rAAV as a vector system as this has the least immunogenicity and would be an ideal vector system to be used in human clinical studies. Moreover we also chose to administer the Cx43 systemically as would be the ideal method in clinical practice not requiring invasive surgery.

Method 2: Connexin45 Knockdown

In-vivo models have been used to elucidate the role of Cx45 in electrical conduction and ventricular arrhythmia. Results however have been difficult to interpret given the inherent limitations with the transgenic models used. These animal models in general may suffer from congenital malformations. Human studies have also shown increased Cx45 in the ischemic and hypertrophic hearts that are associated with increased ventricular arrhythmia [86, 87]. In this Chapter we studied a rat model of MI that mimics acute MI in humans and resulted in an increased

propensity to ventricular tachyarrhythmia. We then assessed the effects for shRNA-mediated knockdown of Cx45 on inducibility of VT in this model.

Short hairpin RNA technology has been gaining wide interest as a new method of therapy given its ability to specifically silence genes [161]. Short hairpin RNAs have gone through phase I trials where it was used to switch off cancer genes and show stabilization of the disease process. An example of this was the “first in human” study by Tabernero et al. These characteristics and early research findings suggested short hairpin RNA would be an appropriate technique for Cx45 knockdown in the current study [166].

In this study we hypothesized that either increasing Cx43 expression or reducing Cx45 in the rat MI model would result in a reduced propensity to ventricular tachyarrhythmia.

5.2 Methods

A total of 4 study groups were assessed (Figure 5.1). The groups were as follows: Cx45 knockdown group (rAAV.sh45) with its control of non-silencing shRNA vector (rAAV.shNS), and Cx43 overexpression group (rAAV.Cx43) with its control of GFP vector (rAAV.GFP).

Figure 5.1: Study Protocol Diagram

A total of 4 groups were studied. The rAAV.GFP acted as the control group for rAAV.Cx43, while rAAV.shNS acted as control for rAAV.sh45. All rats underwent baseline EPS followed by MI formation followed by vector injection. Electrophysiology studies were then repeated at 5 weeks followed by removal of ventricular tissue. The ventricles were then probed for Cx45, Cx43 protein and Cx43 mRNA levels, inflammation and fibrosis with histological analysis.

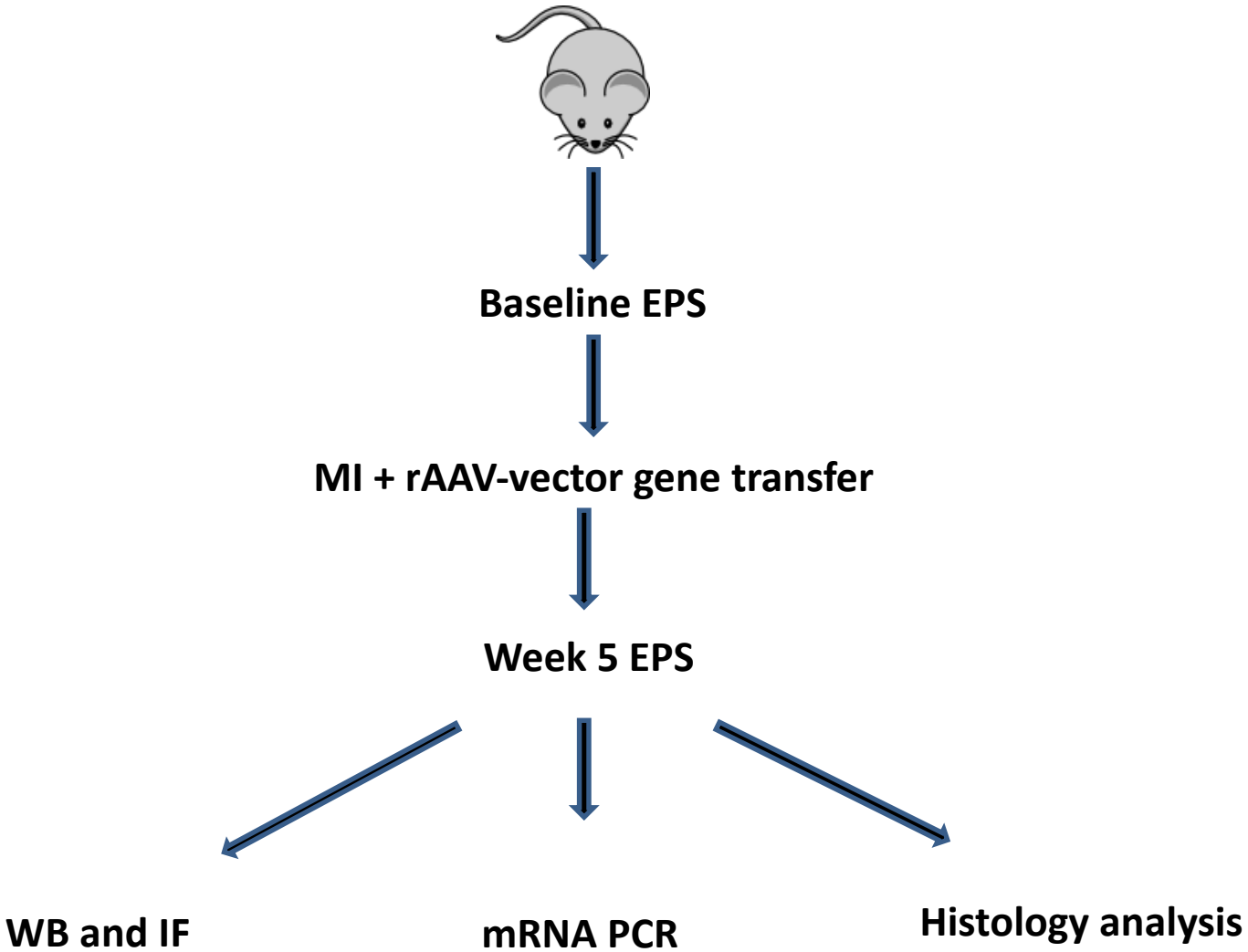

5.2.1 Production of shRNA Vector against Connexin45

Recombinant adeno-associated vector plasmids encoding shRNA to Cx45 and a scrambled non-silencing sequence were constructed by sub-cloning a 200bp Kpn 1 fragment containing the H1 promoter followed by the shRNA from the respective lentiviral vectors PPT. H1.868 and PPT. H1. NS (unpublished reagents produced by Dr Eddy Kizana) into the rAAV.GFP vector. This was done with assistance of Dr Renuka Rao.

Sequencing confirmed that the shRNA expression cassette had been sub cloned into the KpnI site. Plasmids representing the shRNA in forward as well as reverse orientation for both Cx45 and non-silencing sequence were selected to establish knockdown of Cx45 *in vitro*.

To confirm knockdown of Cx45 in vitro, HEK293 cells were co-transfected with rAAV.Cx45 and either rAAV.sh45 or rAAV.shNS plasmids at molar ratios of 1:5 and 1:10. Forty-eight hours after transfection, Cx45 expression at the transcriptional and translational level was determined by real-time qPCR and western blot analyses as previously described in Sections 2.7 and 2.6, respectively.

5.2.2 Vector Packaging and Titration

Vector stocks encoding rAAV.GFP, rAAV.Cx43, rAAV.shNS and rAAV.sh45 were all produced using the calcium phosphate precipitation method as described in Section 2.3. Titre was then assigned to vector stocks by qPCR as described in Section 2.3.4.

5.2.3 Myocardial Infarction and Vector Injection in the Rat

Rat surgery was performed as described in Section 2.10.5. Briefly following anaesthesia, ventilation and baseline EP studies, rats were placed dorsal surface downwards. A total of 10µg of Buprenorphine hydrochloride (Temgesic; Schering-Plough) and 1mg enrofloxacin (Baytril 50; Bayer Healthcare AG) were separately diluted in 1ml of PBS each and administered subcutaneously by injection. The hair of the anterior chest was moistened with 70% (v/v) ethanol (Fronine), shaved with electric clippers (Remington; Spectrum Brands), and removed. Skin disinfection was performed with 10% w/v Povidine-Iodine solution (Betadine; Sanofi-Aventis) prior to skin incision.

Lignocaine 0.1% was initially administered subcutaneously as an antiarrhythmic. Then using a scalpel, a horizontal incision of the skin from

the ventral midline to the left anterior axillary line was made at the level of the 4th intercostal space. Blunt dissection with straight haemostats (Fine Science Tools) of the underlying superficial fascia was performed to mobilise the surrounding skin. The muscles of the left chest wall superficial to the ribs were separated by blunt dissection with straight haemostats (Fine Science Tools). Using curved haemostats (Fine Science Tools), the thoracic cavity was punctured via the 4th intercostal space. The punctured intercostal muscles were blunt dissected with the same curved haemostats and a Castroviejo retractor (Roboz) was inserted to hold open the dissected intercostal space. The pericardial sac was carefully dissected off over the left ventricle with curved forceps (Fine Science Tools). The LAD coronary artery was identified at the level of the left atrial appendage and a 6-0 75cm suture is placed around the artery. The suture ends were passed through a polyethylene tube to form a "snare" like loop with the free ends. The snare loop was then pulled for 10 seconds to assess for cyanosis and then released with return to normal colour thereby demonstrating adequate occlusion of the LAD. The occlusion was then re-applied permanently. Following this the retractor was removed and the rib space closed with a single stitch of 3.0 coated vicryl suture (Ethicon). The skin incision was then closed with a horizontal mattress technique using a 3.0 coated vicryl suture (Ethicon).

A tourniquet was then applied at the proximal end of the rat tail using a rubber band. The tail was warmed in warm water 37^{o} Celsius for 30seconds. A 25gauge needle was used to cannulate the vein at its most distal end, once blood flow was demonstrated, the tourniquet is removed and the viral vector was injected over 30 seconds. The tail vein was flushed with 500µL of saline. The rat was then extubated and left to recover in its cage. Drinking water for rats was supplemented with 0.01% enrofloxacin (Baytril 25; Bayer Healthcare AG).

Five weeks after tail vein injection of viral vector, EP studies were repeated as described in Section 2.10.3. Rats were then euthanized by exposure to CO_2 in a custom made Perspex chamber for 10 minutes and then weighed. The heart was detached from the mediastinum just above the base and rinsed with PBS and subsequently weighed. Studies were carried out at week 5 because in previous studies using post-MI VT model, VT was inducible in about two thirds of animals at this time point [173].

For comparison of Cx45 levels in MI group, a sham group with only a skin incision and no further intervention on the chest was undertaken.

Figure 5.2: Myocardial Infarction Image

The Left Anterior Descending coronary artery was initially located and snared as seen in Image A). Image B) shows side by side images of the same rat with pre and after area of ischemic blanching indicative of successful LAD occlusion.

A)

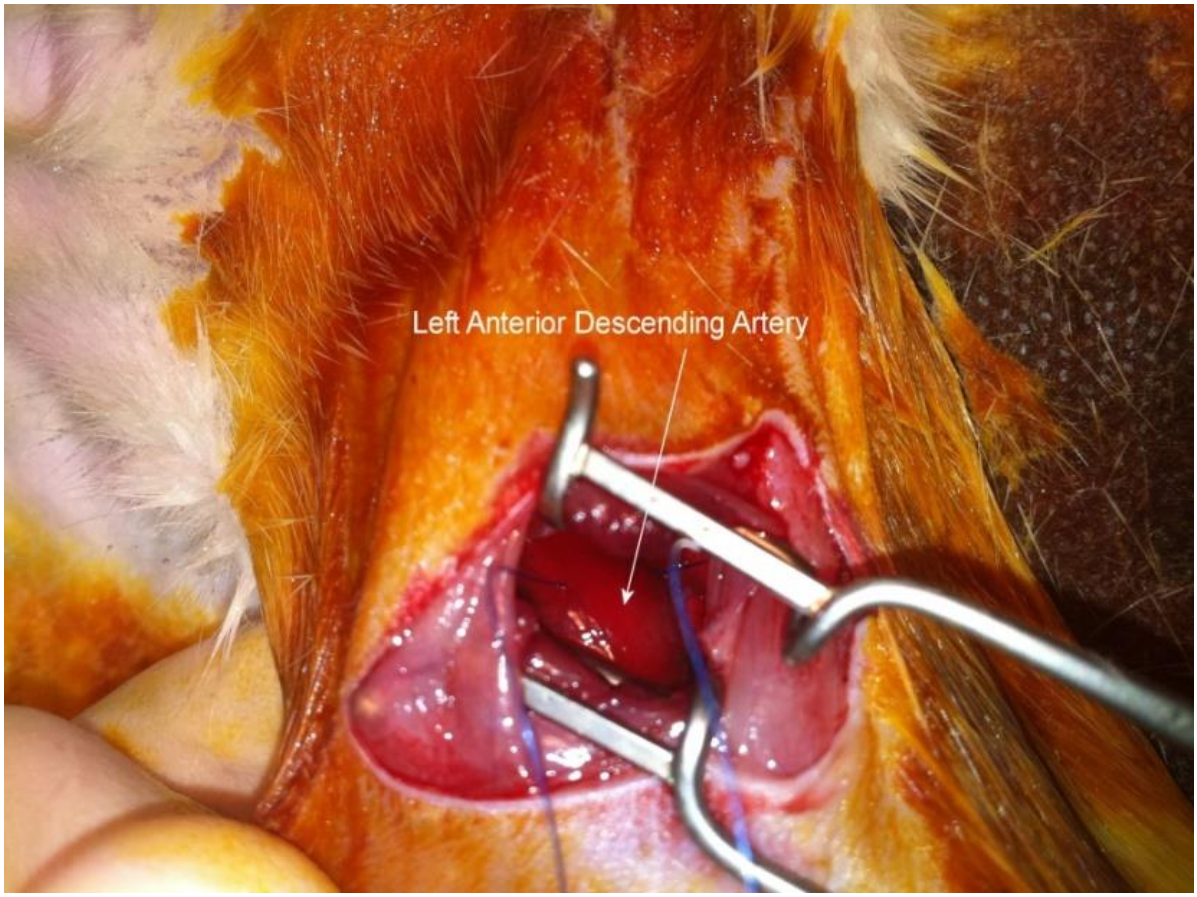

B)

5.2.4 Electrophysiological Studies

Electrophysiological studies were performed as described in Sections 2.10.2 and 2.10.3. In brief, recordings were carried out using subcutaneous needles electrodes and stimulation was performed with a trans-oesophageal pacing probe. Stimulation was with programmed stimulation and extra beats as well as burst pacing. Programmed stimulation was with an 8 beat drive train with a coupling interval of 180millisecond followed by up to 4 extra beats. Burst pacing used a coupling interval of 90millisecond for 30seconds followed by 60milliseconds for a further 30seconds.

5.2.5 Morphometric Studies

All rats and the hearts were weighed at the end of the protocol.

5.2.6 Immunoblotting

The ventricles were excised and stored at the end of the protocol as described in Section 2.10.7. Protein was extracted and quantified as previously described in the Sections 2.6.2. Protein samples then underwent immunoblotting as described in Section 2.6. In brief, samples

were subjected to electrophoretic separation in 4-12% BIs-Tris gradient gels, followed by membrane transfer using the iBlot (Invitrogen) gel transfer system. Following that the membranes were washed and incubated with primary antibodies for Cx45 or Cx43 followed by secondary antibody incubation and then chemiluminescence system was used to produce immunoblot images.

5.2.7 Immunofluorescence

As previously described in Section 2.4, the ventricles were excised and stored the end of the study protocol. Ventricle tissue was then sectioned using the cryostat and subjected to immunostaining. In brief, sections were fixed with 4% (w/v) paraformaldehyde, permeabilised with 0.05% (v/v) Triton X-100, blocked with serum (Invitrogen). Slides were incubated with Cx43 primary antibodies, followed by secondary antibody incubation and cover slipped with Prolong Gold antifade reagent containing DAPI nuclear stain. Fluorescent images were acquired using the Leica DMIL wide field microscope or Olympus FV 100 confocal laser scanning microscope.

5.2.8 Pico-Sirius Red staining

Following excision of ventricular tissue and sectioning Pico-Sirius red staining was performed on the sections as described in Section 2.5.2 (Figure 5.3). Images were then acquired as described in Section 2.5.3 and processed as shown in Figure 3.2 with custom software designed to objectively identify the total pixel area occupied by collagen (red) and the total pixel area occupied by the remaining tissue (green). Collagen density of each myocardial section was calculated as the ratio of collagen relative to the area of the section.

5.2.9 Statistics

Continuous variables were analysed using student T tests or Mann-Whitney U test. Ventricular tachyarrhythmia inducibility was assessed using the fisher exact or X^2 tests. All statistics were conducted at the ≤ 0.05 significance level. Data are presented as mean +/- SD.

Image 5.3: Pico-Sirius in Myocardial Infarction

The image below reveals a Pico-Sirius image of a cross-sectional image of an infarct obtained by the APERIO microscope. The infarcted region is red.

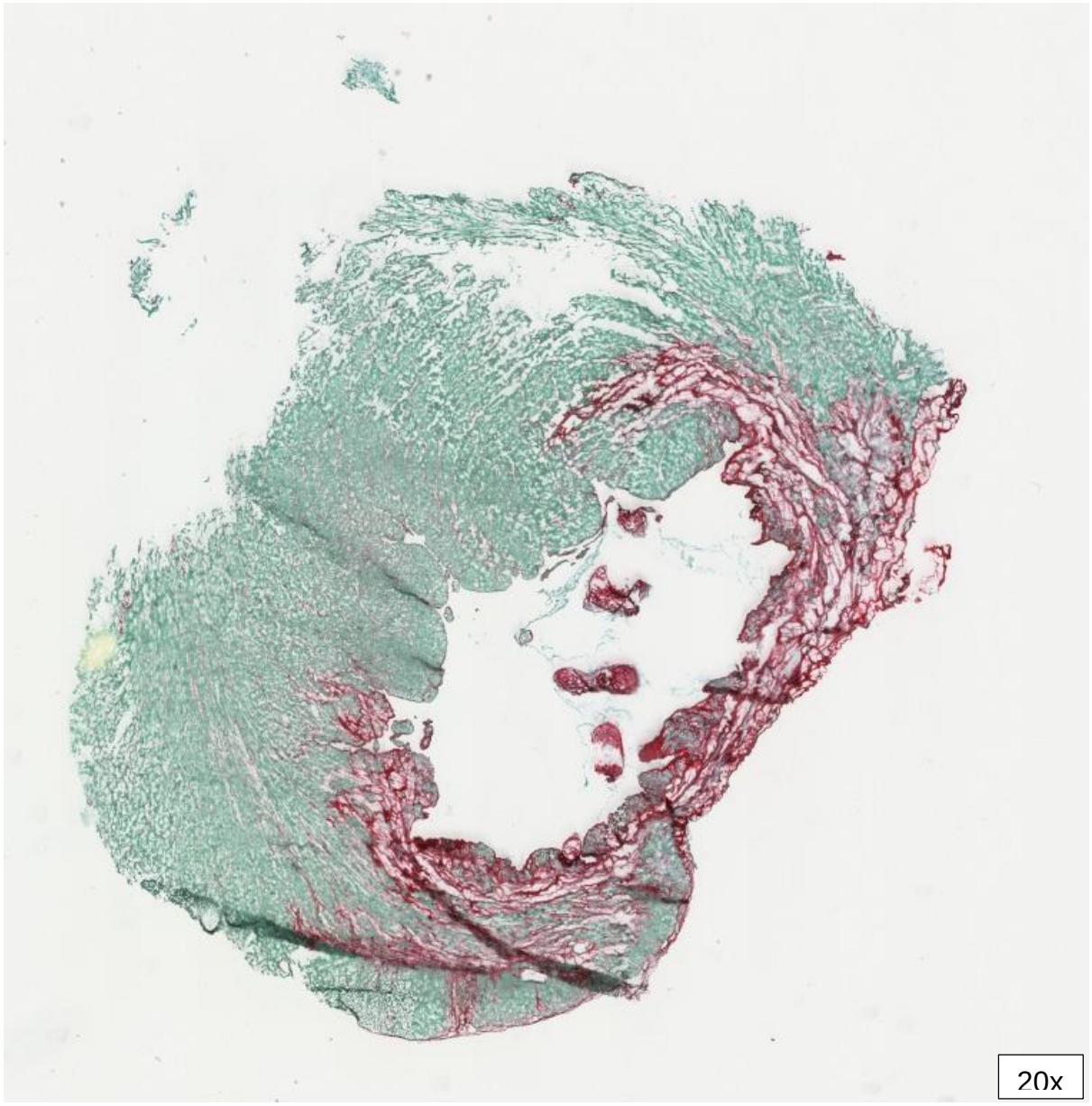

5.3 Results

5.3.1 *In Vitro* Results

In vitro, co-transfection of HEK293 cells with rAAV.sh45 and rAAV.Cx45 resulted in a nine-fold reduction in Cx45 protein expression compared with cells co-transfected with rAAV.shNS and rAAV.Cx45 (Figure 5.4).

5.3.2 Increased Cx45 in Rat Heart following MI

Following MI, ventricular tissue revealed an increase in Cx45 protein expression compared to those rats subjected to sham MI as shown in the western blot in figure 5.5.

Figure 5.4: *In Vitro* shRNA Mediated Knockdown of Connexin45

A) Representative image of a Western blot demonstrating Cx45 protein expression in HEK293 cells is shown. This image revealed reduced signal in rAAV.Cx45/rAAV.sh45 transfected HEK293 cells as compared to control rAAV.Cx45/rAAV.shNS transfected cells.

B) Densitometry results are shown and represented as a bar graph. This was the average of 3 samples (*P<0.05*).

B)

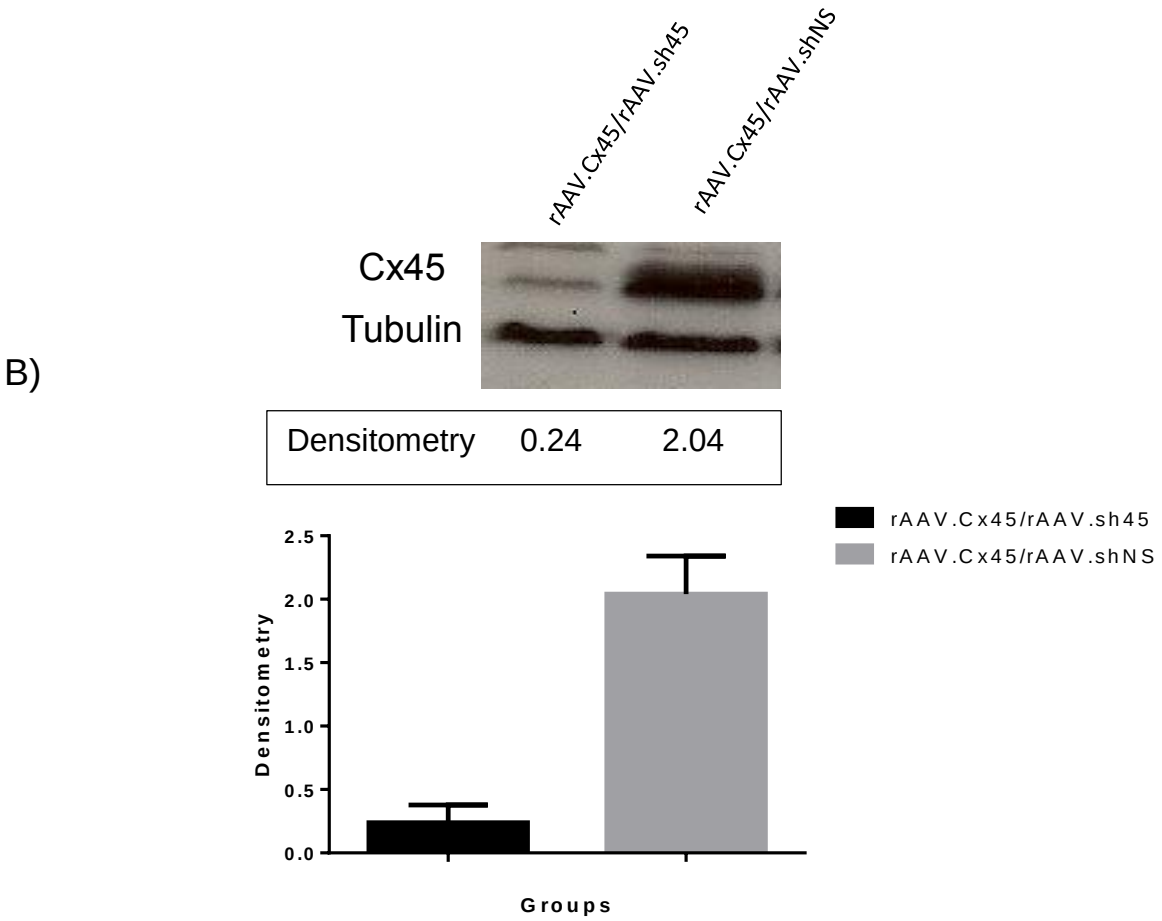

Figure 5.5: Increased Connexin45 expression in Rat Heart following Myocardial Infarction

A) Image below is representative of Cx45 protein expression; there was evidence of Cx45 expression following myocardial infarction in our rat model and no signal in the sham rat model.

B) Densitometry results are shown and represented as a bar graph. This was the average of 3 samples each (*P<0.05).*

B)

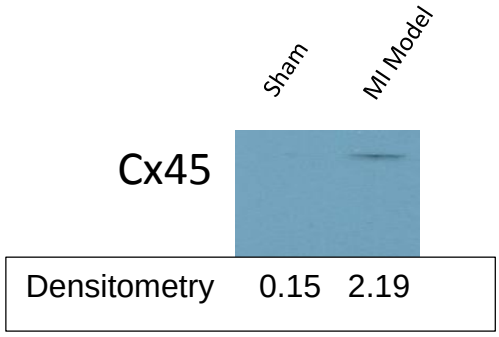

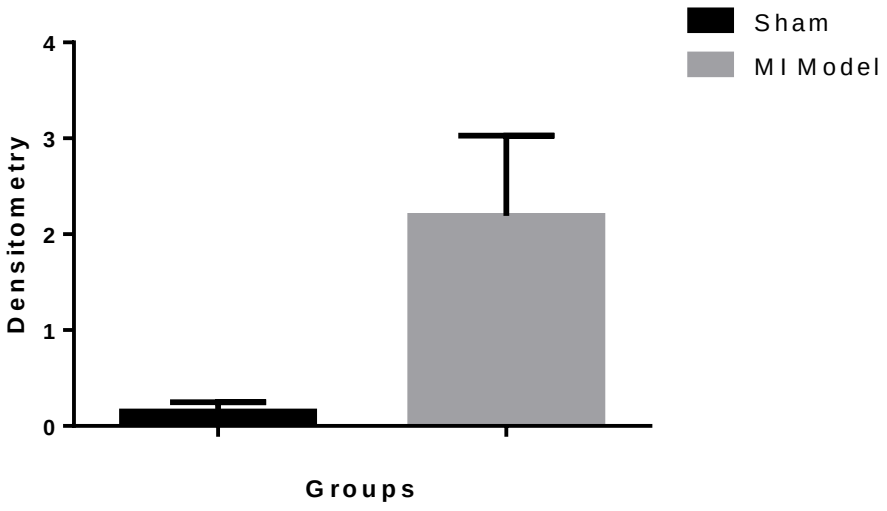

5.3.3 *In Vivo* Transduction of Rat Hearts with rAAV.Cx43 and rAAV.GFP

Thirty one rats started the study and were randomly assigned to either the experimental rAAV.Cx43 (n=16) gene therapy group or the control rAAV.GFP (n=15) group (one rat in the rAAV.GFP group was excluded as it had died during the procedure). All the rAAV.Cx43 rats reached maturation while one rat in the rAAV.GFP had died at 2 weeks post transduction. Post-mortem was carried out. In particular there was no evidence of infective source, therefore the death was presumed to be due to ventricular tachyarrhythmia and was included as part of the inducible VT/VF analysis.

5.3.4 *In Vivo* Transduction of Rat Hearts with rAAV.shCx45 and rAAV.shNS

Thirty nine rats started the study and were randomly assigned to either rAAV.shCx45 (n=22) gene therapy group or rAAV.shNS (n=17) control group. Rats that did not survive the procedure were excluded from the study. Two rats in the rAAV.shNS and two from the rAAVsh45 group were excluded as they had died during infarction. Three rats from the rAAV.shNS did not reach maturation: one died at 72hours, one at two

weeks and the other at three weeks post-transduction. Post-mortems were carried out on all three and as no other cause of death was found, it was presumed to be secondary to ventricular tachyarrhythmia and were included as inducible VT/VF in the analysis. All of the rats in the rAAV.sh45 group reached maturation.

5.3.5 Electrophysiological Effects of *In Vivo* Transduction with rAAVCx43 or rAAV.GFP

Baseline EP studies in both groups did not demonstrate any rats with inducible ventricular tachyarrhythmia.

At 5 weeks following MI there was no significant difference noted in the baseline and final ECG parameters including PR interval and QRS width in the rats treated with rAAV.Cx43 and rAAV.GFP, refer to Table 5.1.

At 5 weeks post MI and vector injection there was a significant reduction in inducible VT in rats treated with rAAV.Cx43 (Figure 5.6). Five rats out of 16 injected with rAAV.Cx43 and 13 rats out of 15 injected with

rAAV.GFP had inducible ventricular arrhythmia as defined in section 2.10.3.

5.3.6 Connexin43 Expression

Connexin43 mRNA expression was noted to be increased nearly two-fold in the rAAV.Cx43 gene therapy group but the difference did not reach statistical significance (2.00±0.73 (n=9) vs 1.18±1.05 (n=6), *P=0.062*) compared to control. This also translated into increased protein expression and immunofluorescence as noted by Western blot analysis and immunofluorescence in figure 5.7 A) and B) respectively. Of note, Cx45 gene expression was similar in the two groups (1.36±1.01 (n=9) vs 1.00±0.53 (n=6), *P =0.46*).

5.3.7 Animal Observation

Rats were monitored on a daily basis with regard to activity level, appetite, respiration, posture and gait. We found no difference between the groups. In addition, we also weighed the animals on Day 0 and at 5 weeks. There was no difference between the groups.

Table 5.1: ECG intervals in Rats with MI and rAAV.Cx43 or rAAV.GFP Transduction

	Treatment Groups	rAAV.Cx43 n=16	rAAV.GFP n=14	P – Value
PR Interval (ms)	Baseline	45.0+/-8.47	44.3+/-4.80	NS
	Post Treatment	46.3+/-5.72	44.2+/-9.94	NS
	Δ	1.3+/-8.0	0.34+/-1.3	NS
QRS Duration (ms)	Baseline	16.8+/-1.87	16.3+/-1.98	NS
	Post Treatment	16.6+/- 1.99	16.2+/-1.90	NS
	Δ	0.1+/-1.3	0.3+/-1.8	NS

In vivo comparison of electrophysiological effects of Cx43 overexpression (rAAV.Cx43) in post-MI rat hearts. Comparison made against GFP (rAAV.GFP) post-MI rat hearts. Electrophysiological measurements include: mean PR interval and QRS durations for each group as measured at Day 0 (Baseline) and Week 5 (Post Treatment). Δ = mean difference (post-treatment – baseline). PR interval and QRS duration was not influenced by treatment and did not change over time.

Figure 5.6: Post MI Inducible VT/VF in rAAV.Cx43 and rAAV.GFP Transduced Rats

Graph below reveals a significant attenuation in VT/VF incidence when post-MI rats were treated with Cx43 (rAAV.Cx43)

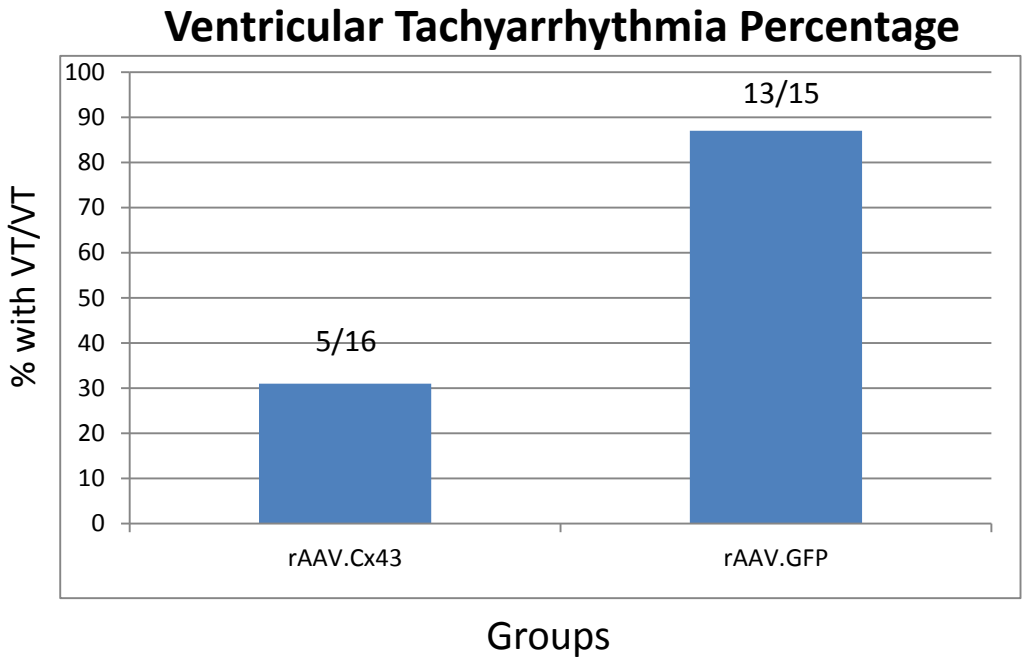

P=0.002

Figure 5.7 Connexin43 and Connexin45 Expression Following MI and Transduction with rAAV.Cx43 and rAAV.GFP

A) The image shown was representative of Cx43 and Cx45 protein expression in rat hearts following MI and transduction with rAAV.Cx43 and rAAV.GFP. Connexin43 expression was increased in the rAAV.Cx43 treated group (2 samples shown) and there was no observed difference in the Cx45 protein expression between the groups.

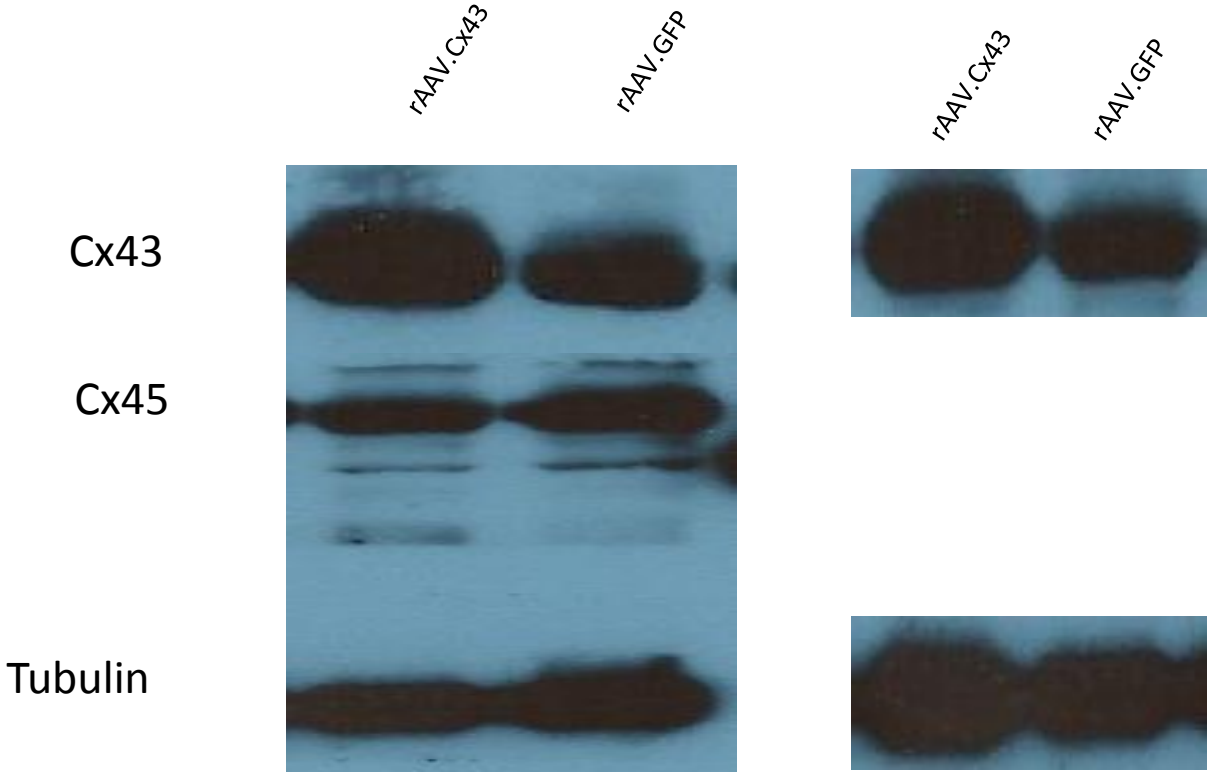

B) Immunostaining and fluorescent microscopy of infarct-scar border in post-MI rat myocardium with anti-Cx43 (red) in both rAAV.Cx43 and rAAV.GFP treated rats. Increased fluorescence of Cx43 was noted in the rAAV.Cx43 group. Nuclei stained blue.

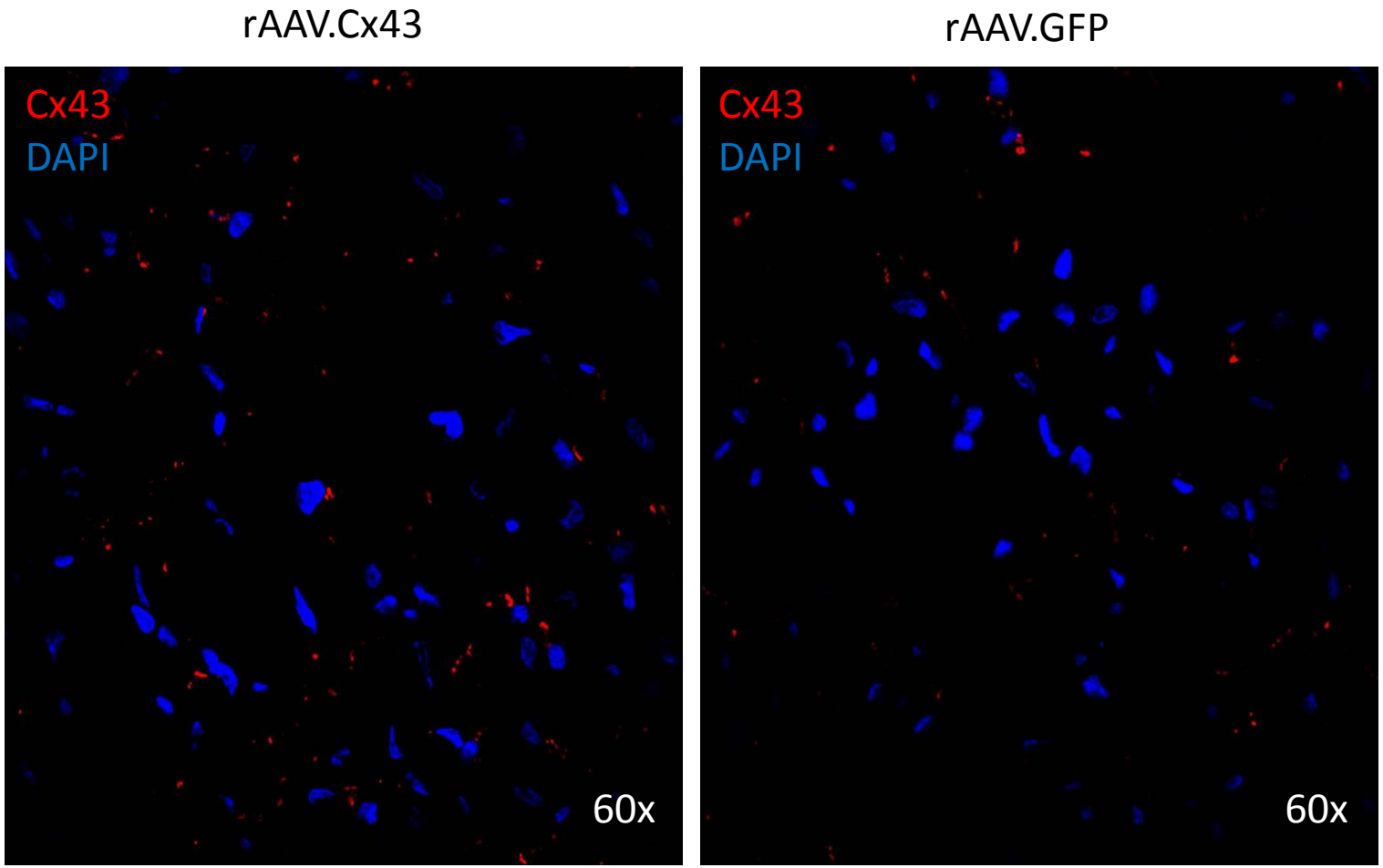

5.3.8 Confounding Factors

Confounding factors that could explain the change in propensity to ventricular tachyarrhythmia were looked for including the presence of myocardial fibrosis and heart failure. To assess for the latter heart to body weight ratio and heart failure gene expression (ANP and βMHC) were determined. We found no significant difference in fibrosis, heart to body weight ratio or heart failure gene expression between the two groups (Table 5.2).

Table 5.2: Myocardial Fibrosis and Heart Failure

	rAAV.Cx43	rAAV.GFP	P-Value
Heart to body weight Ratio	$3.8x10^{e-3}$±$2.2x10^{e-4}$ n=15	$4.0x10^{e-3}$±$4.5x10^{e-4}$ n=16	NS
ANP expression	1.47±1.40 n=10	1.17±1.20 n=8	NS
βMHC expression	3.27±2.08 n=10	2.62±1.53 n=8	NS
Fibrosis % scar	9.5±8.58	9.0±9.2	NS

Table 5.2 demonstrated no significant changes between treated (rAAV.Cx43) and control (rAAV.GFP) post-MI rats in myocardial fibrosis and heart failure parameters.

Fibrosis % scar was calculated from a total of 6 images from 5 separate rat myocardiums.

5.3.9 Results of *In Vivo* Transduction of Rat Hearts with rAAV.sh45 and rAAV.shNS

Baseline EP studies were carried out on all the rats and there was no inducible VT/VF.

Regarding ECG parameters there was no significant difference in the final ECG or change in ECG parameters including PR interval and QRS interval (Table 5.3).

At 5 weeks post MI and vector injection there was a significant reduction in the rate of inducible VT/VF in rats treated with targeted Cx45 knockdown. Eight rats injected with rAAV.sh45 and 12 rats injected with rAAV.shNS had inducible ventricular arrhythmia as defined in section 2.10.3 (Figure 5.8).

There was an increased mortality noted in the rAAV.shNS treated group (n=3) as compared to the rAAV.sh45 treated group (n=0), this however was a small number and did not reach statistical significance

Table 5.3: Electrophysiological Results

	Treatment groups	rAAV.shNS n=22	rAAV.Sh45 n=14	P – Value
PR Interval (ms)	Baseline	45.6+/-6.9	51.8+/-9.16	NS
	Post Treatment	45.8+/-6.54	52.5+/-7.81	NS
	Δ	0.2+/-5.79	0.68+/-8.31	NS
QRS Duration (ms)	Baseline	16.4+/-1.50	17+/-2.45	NS
	Post Treatment	15.9+/- 2.46	16.4+/-1.74	NS
	Δ	-0.5+/-1.63	-0.55+/-2.98	NS

In vivo comparison of electrophysiological effects of Cx45 knockdown (rAAV.sh45) in post-MI rat hearts. Comparison made against non-silencing vector (rAAV.shNS) post-MI rat hearts. Electrophysiological measurements include: mean PR interval and QRS durations for each group as measured at Day 0 (Baseline) and Week 5 (Post Treatment). Δ = mean difference (post-treatment – baseline). PR interval and QRS duration was not influenced by treatment and did not change over time.

Figure 5.8: Post MI Inducible VT/VF in rAAV.shNS and rAAV.sh45 Transduced Rats

Graph below reveals a significant reduction in VT/VF propensity when post-MI rats were treated with Cx45 knockdown (rAAV.sh45) compared to non-silencing vector (rAAV.shNS)

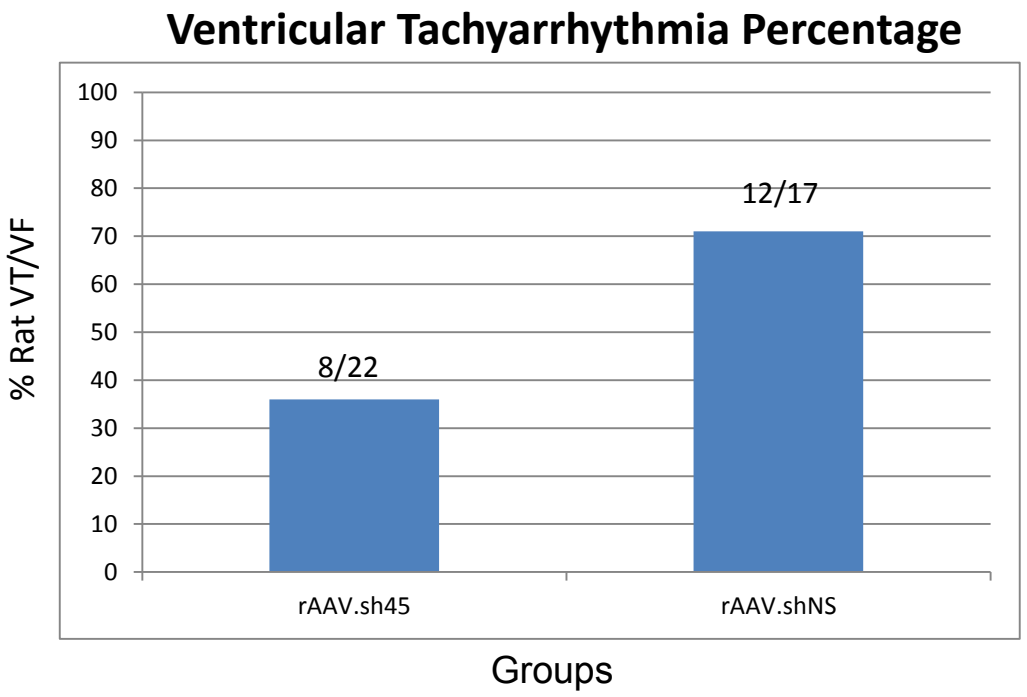

P=0.034

5.3.9 Connexin45 Expression

Connexin45 mRNA expression was halved in those treated with rAAV.shCx45 gene therapy with a trend to significance (1.15+/-1.35 in rAAV.shNS (n=7) vs. 0.456+/-0.549 in rAAV.sh45 (n=9); p=0.06). This, however, translated into a significantly reduced level of Cx45 protein expression on Western blotting (Figure 5.9). Connexin43 expression was similar in the two groups (0.578+/-0.256 in rAAV.shNS (n=7) vs. 0.447+/-0.265 in rAAV.sh45 (n=9); p=NS).

5.3.10 Animal Observation

Rats were monitored on a daily basis for activity level, appetite, respiration, posture and gait. Animals were weighed prior to commencing the procedure and 5 weeks after gene therapy. There were no differences between the groups.

5.3.11 Confounding Factors

Confounding factors that could contribute to an increase in VT/VF were looked into including measures of heart failure such as heart to body weight ratio and heart failure gene expression. The presence of

myocardial fibrosis was also assessed. There was a significant reduction in ANP mRNA expression in the rAAV.sh45 treated group compared to the control group. There was however, no difference in the βMHC gene expression or the morphometric marker of heart failure. There was no difference in the extent of myocardial fibrosis between the two groups (Table 5.4).

Figure 5.9: Western Blot

A) Western blot representative image of Cx45 protein expression in infarcted rats transduced with either rAAV.sh45 or rAAV.shNS. This image reveals reduced signal in rAAV.sh45 transduced infarcts. Average of 3 densitometry results is shown.

B) Western blot representative image of Connexin43 protein expression in infarcted rats transduced with either rAAV.sh45 or rAAV.shNS. This image reveals no difference in signal between both groups. Average of 3 densitometry results is shown.

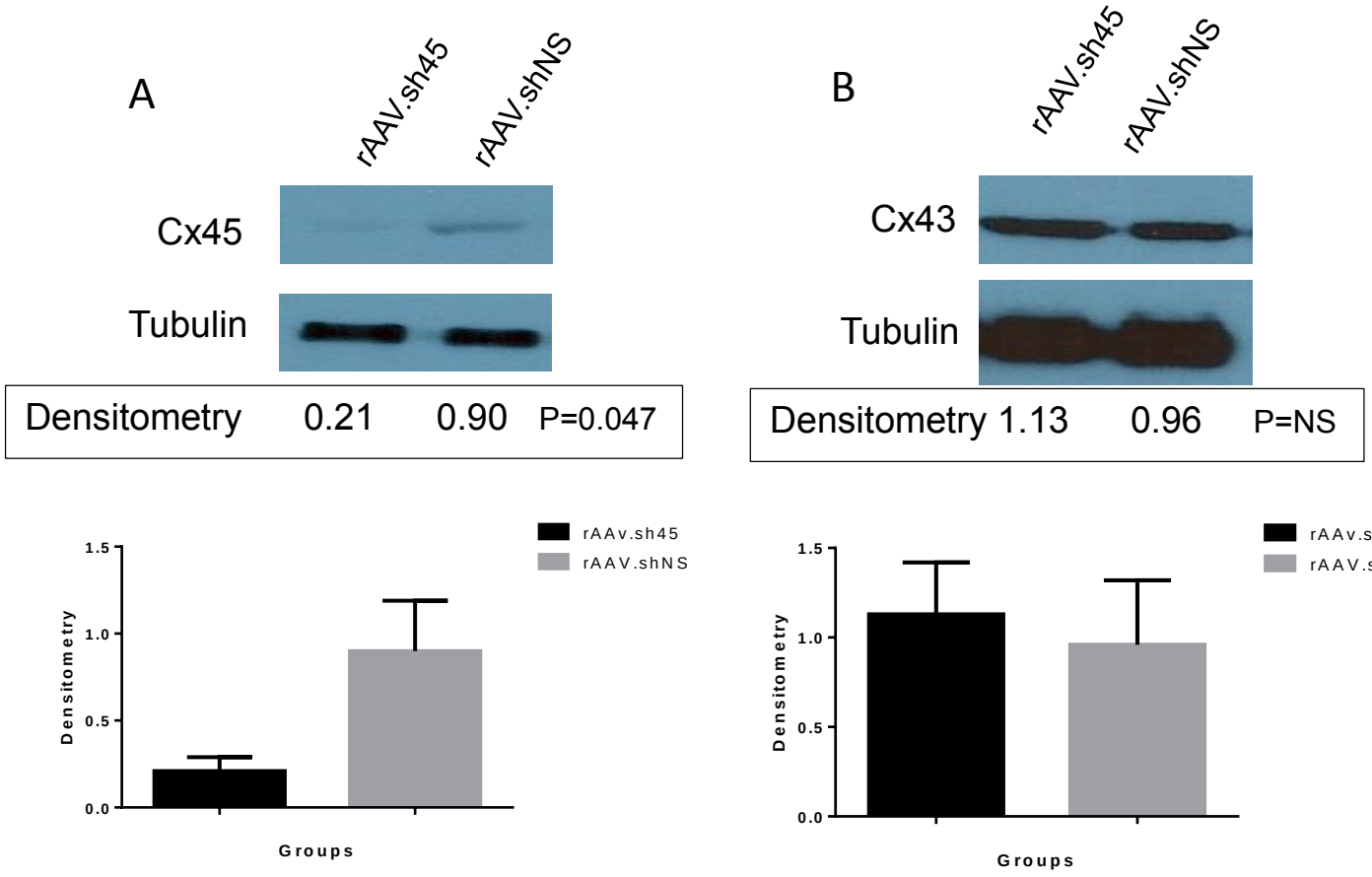

Table 5.4: Confounding Factor Results

	rAAV.shNS	rAAV.Sh45	P – Value
ANP expression	2.76+/-2.00	0.407+/-0.544	0.007
βMHC expression	0.950+/-0.909	0.653+/-0.564	NS
Heart to body weight ratio	$4.07x10^{-3}$+/- $4.26x10^{-4}$	$3.76x10^{-3}$+/- $4.68x10^{-4}$	NS
Fibrosis % scar	13.7+/-13.3	10.6+/-13.1	NS

Table 5.4 demonstrated only a significant reduction in ANP mRNA expression in the Cx45 knockdown (rAAV.sh45) treated group compared to control (rAAV.shNS) group. Other heart failure and fibrosis parameters remain similar between the studied groups.

5.6 Discussion

5.6.1 Connexin43 and Connexin45

Connexin43 is the predominant connexin in the ventricular myocardium and is responsible for electrical propagation through the gap junctions. Cardiac connexins have been shown to interact and form heteromeric channels *in vitro* and studies have shown that co-expression of Cx45 in gap junctions with Cx43 have reduced gap junctional conductance and dye transfer [91, 174-176]. Connexin45 has been shown to be important in early cardiogenesis [84]. It has also been shown to be present in the conduction system indicating a role in the propagation of conduction from the AV node to the ventricular myocardium. In Chapter 3, we were able to confirm that Cx45 overexpression does co-localise with Cx43 resulting in phenotypic changes in keeping with slowing of conductance such as prolongation of PR and QRS intervals.

Human studies of patients with heart failure that have an increased risk of ventricular tachyarrhythmia have also noted an increased Cx45 expression. In other studies it had been shown that there was reduced Cx43 in the myocardium of ischaemic hearts [69]. It is therefore likely that this altered ratio of Cx45/Cx43 expression in the post-MI heart leads to

formation of heteromeric connexin channels. The latter have reduced unitary conductance and will slow electrical conduction. The ensuing slow conduction would confer an increased vulnerability to ventricular tachyarrhythmia via the mechanism of re-entry. We hypothesized that correction of the ratio of Cx45/Cx43 by either Cx45 knockdown or Cx43 overexpression would have the net effect of reduction in propensity of inducible ventricular tachyarrhythmia.

5.6.2 Connexin Gene Therapy and Post-MI Ventricular Tachyarrhythmia

Connexin 43

Our study supports the study by Greener et al. where they assessed the antiarrhythmic effects of injected adenoviral vectors expressing Cx43 in pigs with post-MI VT [64]. They demonstrated reduced VT at two weeks following gene transfer. Their study only used animals with inducible VT for therapy whereas in the current study all animals post-MI were enrolled. Our study revealed a relative increase in Cx43 mRNA and protein expression in the rAAV.Cx43 treated group strongly suggesting transduction with Cx43 vector system.

The absence of significant inflammatory and fibrotic changes and the absence of differences in markers of heart failure between the treated group and the control group indicated that the change in arrhythmia inducibility was not due to structural changes. Thus an adequate level of Cx43 had a protective mechanism against propensity to VT.

Connexin 45

Our study supported the hypothesis that knockdown of Cx45 in rat MI model may decrease the propensity of VT/VF. We observed a significant reduction of arrhythmia in the rAAV.sh45 treated group compared to control. This translated into halving Cx45 mRNA expression in this group and significant reduction in protein expression. We hypothesize that if further knockdown was achieved by increasing the vector dose injected this may have further improved the results. The incidence of VT/VF was reduced with an absolute incidence of ~ 34%.

Connexin43 mRNA and protein expression was noted to be similar between the rAAV.sh45 and rAAV.shNS groups indicating that it was likely that the knockdown of the Cx45 resulted in the reduced propensity to arrhythmia and not Cx43 changes.

Interestingly when heart failure genes were assessed in this group (rAA.sh45) there was significant reduction in the ANP mRNA expression compared to the control group. It is difficult to interpret this finding as the βMHC and the heart to body weight ratio were not significantly altered. Furthermore, the extent of myocardial fibrosis was not different between the two groups. Unfortunately echocardiography and MRI studies were not able to be done during this thesis and may have proved useful as tools to measure LV function.

5.6.3 Adenovirus vs. Recombinant Adeno-associated Virus

The study by Greener et al. used adenovirus as the gene transfer vector. The vector system has many inherent limitations and safety concerns that preclude its application as a gene therapy vector for ventricular arrhythmia. These include lack of capacity to confer long-term transgene expression and high immunogenicity in an immunocompetent host. Recombinant adeno-associated virus on the other hand lacks parental agent pathogenicity, vector related toxicity and has minimal immunogenicity. It also has the capacity for stable long-term transgene expression by virtue of episomal persistence [177]. It is therefore an ideal candidate for human experiments and its use in this study has shown that it is comparable in efficacy to the adenovirus vector used by Greener et

al. Recombinant AAV does have some limitation, the main one being the ability for production of high-titre stocks of consistent purity and bioactivity. This limitation may now be overcome by the new approach of insect cell production described by Kotin et al. [178-180].

5.6.4 Future Research

Transduction efficiency was not assessed in these study groups. This could have been optimised. It is possible that a greater effect on post-MI VT/VF may have been observed by using larger doses of vector or screening rats for pre-existing antibodies and excluding rats with significant titres. Furthermore, the bioactivity of vector stock was not assessed and variability between batches may have affected vector performance and outcomes in our study system. It may prudent to test the vectors *in vitro* for efficient and consistent transduction between the vector batches prior to *in vivo* studies.

A further area that needs to be explored is the extent of MI caused in this rat model. Greener et al. have previously described in their model for MI that the placement of catheter for infarct was imperative, with catheter placement too far reducing incidence of VT and too high the animals do

not survive [135]. With the area of blanching kept as subjectively constant as possible in this group we were able to achieve similar fibrosis levels between the groups making this an unlikely reason for the difference noted in VT/VF between the control groups. However further objective measurements in large animal MI models such as MRI assessment following MI would be helpful for future research.

Ambulatory telemetry would have been useful to determine the extent of spontaneous arrhythmias and to confirm a cardiac cause in animals that had died suddenly. Telemetries were not implanted this group of rats given the concern of further morbidity and mortality on this group of rats but this maybe a worthwhile addition to future experiments in larger animals at the start of MI induction.

Green fluorescence protein has been previously noted to alter conductance in Cx43 gap junctions and it is therefore theoretically possible that it would increase propensity to ventricular tachyarrhythmia [181]. This was not noted in other studies and also our incidence of inducible VT was similar to our non-transduced pilot MI group (~ 70%)

making this unlikely. Further study with other potential reporter genes such as *LacZ* may be useful.

Another consideration was the method used to cause MI. We used completed infarct where in Greener et al. they used infarct reperfusion. This method had been studied in rat model by Ding et al. showing that ischemia reperfusion was an effective method of induction of VT with 70% of rats having inducible VT/VF [173]. Never-the-less in our hands complete ligation of the mid-LAD resulted in similar VT/VF rates as noted by the rAAV.GFP group. Further studies with knockdown of Cx45 using the ischemia-reperfusion technique would be useful in the current clinical era.

Combination rAAV.Cx43 and rAAV.shCx45 or head to head studies comparing Cx43 overexpression with knockdown of Cx45 would be helpful to perform in order to evaluate more options for reducing the propensity of arrhythmia. This would likely require a large number of animals to achieve adequate power to study arrhythmia inducibility and was beyond the scope of this thesis.

Despite the isolated change in ANP gene expression differences in other markers of heart failure were not evident such heart to body weight ratio, cardiac fibrosis or βMHC expression levels when comparing the rAAV.sh45 to the rAAV.shNS infarct groups. We were limited by equipment availability and therefore were unable to assess cardiac function accurately with other modalities such as echocardiography or MRI. It would have been interesting explore this further to assess whether or not Cx45 knock-down was actually improving cardiac function.

5.7 Summary

In summary, Cx43 transduction in the rat post-MI VT model did reduce propensity to ventricular tachyarrhythmia implicating Cx43 overexpression as a protective mechanism in preventing VT/VF. Furthermore knockdown of Cx45 has shown significant reduction of ventricular tachyarrhythmia in this same model, implicating a pathogenic role for this molecule in post-MI VT.

CHAPTER 6

SUMMARY AND GENERAL DISCUSSION

Summary and General Discussion

With an aging population and an attendant increase in the incidence of cardiac disease and SCD there is a need to understand the mechanisms underpinning ventricular arrhythmogenesis. At a molecular level connexins and gap junctions have long been understood to play a role in normal conduction and arrhythmias as outlined in Sections 1.4 and 1.5. Connexin43 has been the most heavily studied connexin in arrhythmogenesis. There is limited and conflicting data on the role of other connexins such as Cx45. In this thesis, the role of Cx45 in cardiac ventricular arrhythmias was studied and found to be relevant. Moreover the gene transfer technology employed in this study lends itself to be developed as a highly novel and innovative treatment approach for life-threatening cardiac arrhythmias.

6.1 Connexin45 and Heart Disease

6.1.1 Summary

Connexins, or gap junction proteins, are a family of structurally related transmembrane proteins that assemble to form vertebrate gap junctions. Connexin43 is the predominant connexin in adult human myocardium, while Cx45 the least prevalent. Connexin40 is mainly located in the atria. The study of Cx45 in this thesis has contributed to the understanding of the role of Cx45 in arrhythmia formation in the “diseased” heart and therefore, may help with the future development of treatments for reducing incidence of sudden cardiac death.

6.1.2 Connexin45 Physiology

Connexin45 has been cloned from mouse, human and rat cDNA. It consists of 396 amino acids in the human and rat genome and 395 in the mouse [81, 175]. Gap junctions composed of Cx45 are selective for cations and are voltage dependent with half maximal activation at +/- 20mV[61, 81]. The molecular weight of Cx45 is between 45kD and 48kD. Importantly homotypic homomeric Cx45 channels have a relatively small unitary conductance of approximately 26pS and therefore would have the potential to slow conduction when present

in gap junctions [83]. For heterotypic Cx43–Cx45 channels, the unitary conductance has been reported at approximately 50-60pS, corresponding to the Ohmic sum of the predicted conductances for each of the homomeric native connexons [182]. Connexin45 is noted to be moderately permeable to fluorescent dyes such as LY, DCF but not 6CF [79]. With regards to post-translational modifications, there have been reports of 15 possible phosphorylation sites for PKC in human Cx45, and 17 in rodents[31].

6.1.3 Connexin45 and Normal Myocardium

Connexin45 has an indispensable role for the development and function of the embryonic heart. In foetal heart tissue, it has been found to be the first connexin to be expressed and therefore essential in myocardial maturation [84, 85]. It is the only cardiac connexin essential for cardiogenesis and embryonic survival. During myocardium development, Cx45 expression is reduced. In the adult myocardium, it is the predominant connexin in the atrial conduction system consisting of the sinus node and AV node [183]. In addition to the nodes, Cx45 is expressed in the His bundle, the bundle branches and at lower levels in proximal Purkinje fibres. Connexin45 has also been noted to be present in very low levels in the working myocardium of the ventricle as well as the atria [183]. In Chapter 3 of this thesis,

Cx45 was overexpressed in the normal heart. As predicted by the known physiology of Cx45 gap junctions and the role of this molecule in the SA and AV nodes, markers of slowed conduction were observed on the surface ECG, namely prolonged PR intervals and QRS width. Furthermore, there was an increased incidence of high degree AV block.

6.1.4 Connexin45 in Diseased Myocardium

Connexin45 expression increases under pathological conditions. This has been reported in the context of human heart failure, a condition known to predispose to ventricular tachyarrhythmia [149]. Down-regulation of Cx45 did not produce any notable deficits in electrical conduction in adult mice hearts as studied by Bao et al. [91]. Connexin45 has been found essential for the viability of the embryo but when mice were generated in which deletion of Cx45 was specifically induced in cardiomyocytes of adult mice, these mice remained viable [183]. Betsuyaku et al. on the other hand had shown that when genetically modified Cx45 over-expressing mice were produced, these were susceptible to ventricular tachyarrhythmia *in vivo* [3]. This model has its limitations given that germ-line gene modifications were made which would have the potential to result in altered expression of unintended/other molecules. When compared to the germ-line approach,

somatic gene transfer is more relevant for modelling the clinical pathophysiology of acute MI and subsequent alterations in gene expression pattern. Results presented in Chapter 3 of this thesis have shown that with somatic gene transfer there was an increased incidence of ventricular tachyarrhythmia. Heart failure was not a confounding factor as observed by no change in heart failure genes or weight gain. However a reduction in Cx43 expression was identified which could be an important confounding factor and may have led to the propensity for arrhythmia. Never-the-less when both Cx43 and Cx45 were transduced in the normal myocardium there remained a high incidence of arrhythmia in this group. This showed that Cx45's role in promoting arrhythmogenesis is important, regardless of Cx43 expression in the myocardium.

6.1.5 Connexin45 Knockdown Results in Reduction of Ventricular Tachyarrhythmia

As shown in human studies Cx45 is up-regulated in human heart failure. When overexpressed by somatic or transgenic methods Cx45 results in an increased propensity to ventricular tachyarrhythmia. It is therefore conceivable that knocking down Cx45 in those models would reverse the slowing of conduction and thereby result in reduction of ventricular tachyarrhythmia. In Chapter 5, the rAAV.sh45 vector successfully reduced

Cx45 expression in Cx45 transduced HEK293 cells *in vitro*. This also occurred *in vivo* where Cx45 transduced rat myocardium showed reduction in Cx45 expression when treated with rAAV.sh45 vector compared to the control group (Chapter 4). Furthermore phenotypic changes such as the QRS duration and VT inducibility were reversed when rAAV.sh45 was introduced into Cx45 overexpressed rats. On the other hand, when Cx43 was transduced into Cx45 overexpressed rats (to overcome the down regulation noted in Chapter 3 following overexpression with Cx45) there were no phenotypic changes noted. This further implicates Cx45 as mechanistic factor involved in ventricular arrhythmia.

It was hypothesised that knockdown of Cx45 could be used to reduce the predisposition to arrhythmia after MI. A model was chosen in which similar overexpression of Cx45 was expected. In section 5.3.2, I demonstrated that indeed Cx45 is increased in the Post-MI rat model. As expected transduction of rAAV.sh45 decreased this Cx45 expression compared to the control MI model. This translated to a reduction of in incidence of VT/VF. This finding adds weight to the hypothesis that excess Cx45 is a factor in the pathogenesis of ventricular arrhythmia after myocardial infarction.

6.1.6 Limitations

The mechanism by which conduction slowing causes ventricular tachyarrhythmia in the setting of acute gene transfer in the rat myocardium requires further clarification. Our understanding of how Cx45 transduction gives rise to a re-entrant circuit is limited. It is likely the formation of heteromeric channels Cx43/Cx45 form resulting in conduction slowing thereby reducing the circuit length and thus re-entry may occur in smaller tissue volumes. Other factors in the myocardium likely to play a role in conduction slowing and not studied in this thesis are changes in expression of ion channels subserving excitation and action potential propagation such as the sodium and calcium channels. Abnormal Cx43 localisation and post-translation modification have been found to be important factors in arrhythmia in the acute MI and post MI models. These events were not studied in this thesis. Another limitation of this thesis is that the rat myocardium and human myocardium are clearly different in respect to size, ion channel expression and even ECG characteristics. Therefore what maybe significant in the rat heart may not necessarily be so for human myocardium. Lastly, transduction was not cell specific and therefore non-myocytes transduced with Cx45 may also play a role in modulating impulse propagation and alter the propensity for ventricular tachyarrhythmia.

Limited Treatment Potential to Reduce Ventricular Tachyarrhythmia in Post-MI Model.

The question arises as to why did knockdown of Cx45 or overexpression of Cx43 not reduced VT/VF in all animals. Several potential explanations can be deduced including inadequate gene transfer, altered Cx45, Cx43, or rAAV.sh45 processing after gene transfer, incorrect targeting of the gene transfer, or increased mass or complexity of the border-zone region in the failed rats. Another potential explanation is that for knockdown to occur successfully there needs to be sufficient number of viable myocardial cells within the scar region that are capable of successful gene transfer and expression. This thereby would reduce conduction slowing and the propensity to ventricular tachyarrhythmia. Another important consideration is that Cx45 knockdown alone is insufficient to reduce VT/VF, and that there are likely other process such as ion channel changes, Cx43 modulation as well as possible fibrotic changes and other processes not fully assessed that contribute to the propensity to ventricular tachyarrhythmia. Finally the presence of neutralising antibodies in a few of those animals may have rendered our viral vector ineffective in transmitting the transgene to the required target.

6.2 Connexin43 and Ventricular Tachyarrhythmia

6.2.1 Connexin43 Physiology

Connexin43 is the most prevalent connexin in the myocardium. The molecular weight of Cx43 is between 41 to 46 kDa depending on its phosphorylated state [63]. Connexin43 gap junctions are permeable to organic ions and molecules of less than 1K Da [63]. Homomeric-homotypic Cx43 channels have a high conductance of 100-120ps, much greater than homomeric-homotypic Cx45 channels at 26pS. Connexin43 has been extensively studied and shown to be permeable to many different dyes including LY, DCF, carboxyfluorescein, and N- biotinamide hydrochloride[184].

6.2.2 Connexin 43 Expression in Diseased Hearts

Peters et al. have studied patients with both hypertrophied myocardium as well as ischemic hearts and noted a reduced content of Cx43 in gap junctions [69]. This was noted in particular at the border zone of infarcted and normal myocardium [24, 69]. This implied there was some alteration in the gap junction that would result in areas of slowing of conduction that support myocardial re-entry and ventricular tachyarrhythmia. Other

studies had also supported the above findings showing that Cx43 was also reduced in patients with other types of cardiomyopathies [77, 87]. To study the hypothesis that reduced Cx43 results in ventricular arrhythmia, conditional Cx43 knockout mice were studied. These experiments revealed significant conduction delay and arrhythmia but only when Cx43 expression was reduced to 70-90% of baseline levels [88, 89].

6.2.3 Connexin43 Overexpression and Ventricular Tachyarrhythmia

Greener et al. [64] published a study using somatic gene transfer of Cx43 to the healed myocardial scar border. In this study, pigs were subjected to MI and the infarct allowed to heal. Adenoviral vector mediated Cx43 gene transfer resulted in Cx43 expression, reduced conduction slowing and reduced VT inducibility with programmed stimulation. There are many important differences between the study by Greener and the current thesis. In the former pigs that had been previously known to have inducible VT were employed and there was targeted gene transfer to the expected infarct border zone. This would be difficult in humans as it would imply invasive thoracic surgery to get to the infarct zone and utilize directed gene transfer. A simpler and more generalizable method would

be to use systemic gene transfer as used in the current study or gene transfer via the commonly used, intracoronary route.

The study by Greener et al. treated pigs with recurrent VT, which in clinical experience would be a more efficient use of scarce resources. However the use of rAAV vector system would be more applicable to clinical practice, given the stability of expression and reduced immunogenicity of the virus in humans compared to adenovirus vector system. Nevertheless the current study supports Greener's findings that Cx43 overexpression can reduce inducible ventricular tachyarrhythmia. This was independent of worsening heart function as expected following MI.

6.2.4 Benefits of Using Connexin43

Connexin43 is the most prevalent connexin in the myocardium and its biology is well understood. It is generally thought that the heart is over-engineered with Cx43 given that heterozygous knockout mice show no abnormal cardiac phenotype. It is, therefore possible to speculate that with further expression of Cx43 that this would be unlikely to result in any unwanted gap junction modulation that could result in adverse alterations

of conduction. The latter may not hold true for other connexins such as Cx45 or Cx40.

6.2.5 Limitations

Connexin43 overexpression may have a role in the future regarding therapy for VT and thereby SCD reduction in the post-MI patient population. More studies are needed to define the most efficacious approach for overexpression of Cx43 for gene therapy of post-MI VT. Variables that need to be addressed in these studies include: dose of vector to be injected, delivery method, and expression cassette design including choice of promoter, for example. Moreover, the mechanism of effect is not fully understood. Large animal models and high resolution, multipoint mapping of electrical activation could be used to assess the effects of gene therapy on conduction at the MI border-zone. In addition, MRI of the scar border could be used to assess if there is a reduction is scar tissue that could underpin the improved conduction.

An additional consideration with Cx43 gene therapy for post MI VT is the time of vector injection. In the current study all rats were injected at time of MI. Studies in transgenic mice in whom Cx43 was engineered to remain

open during MI have shown that this would generally increase infarct size [185]. This was not observed in the current study and likely due to the 3-4 day delay in gene expression following vector administration and that somatic Cx43 overexpression resulted in functionally normal gap junctions which are likely to close appropriately. Similarly, Greener et al. had used somatic gene transfer following infarction and this reduced VT. Further studies need to be carried out determine the optimal time for vector delivery.

6.3 Gene Therapy using Regulatory Short RNAs to Modulate Connexin Gene Expression

6.3.1 Regulatory Short RNAs

Short or small RNAs are 20-40 nucleotide long noncoding RNA molecules present in most eukaryotic organisms that regulate gene expression in a sequence-specific manner either transcriptionally or post-transcriptionally [169]. These small RNAs are derived from double-stranded RNAs (dsRNAs) and can induce gene silencing through specific base-pairing with the target molecules. There are two well defined classes of small RNAs: microRNAs and short hairpin RNA (shRNA) [169]. Gary Ruvkam

and Victor Ambros, the pioneers in microRNA research, found that a small temporal non-coding RNA could regulate translation by base pairing to the 3” untranslated region of a coding messenger RNA [186, 187]. Since then there has been a vast amount of research into microRNA. MicroRNA led to the birth of short hairpin RNA. Unlike microRNA, shRNA is designed to target a single transcript rather than hundreds of transcripts and is therefore more useful in single gene disorders. The benefits are vast, specifically in their ability to knockdown unwanted or disease causing genes. Short hairpin RNAs are perfectly complementary to their mRNA targets. Their target sites may disperse throughout the entire transcript giving it a wide use in illnesses. The shRNA differ to the microRNA and cause RNA degradation while microRNA causes translational suppression. They can also facilitate RNA degradation depending on extent of complementarity to the target sequence. Their use has already been investigated widely in cancer-genetics. Numerous clinical trials using microRNA have begun [170]. In addition to modulators for the treatment of variety of diseases, microRNAs can be used as potential biomarkers in clinical diagnostics.

6.3.2 Short-hairpin RNA use in Cardiac Gene Therapy

Short Hairpin RNA therapeutics has already been widely utilized in pre-clinical models of cardiac gene therapy [167, 168, 188]. Huang et al. described its use in ischemic heart disease [168]. They studied the knockdown of prolyl hydroxylase-2 (PHD2) protein in adult mice hearts. Infarcts were created with LAD ligation and vector directly injected into the myocardium. Compared to controls they demonstrated significant improvement in angiogenesis and contractility. Bioluminescence imaging detected plasmid-mediated transgene expression for 4 to 5 weeks. Echocardiography showed improved fractional shortening compared to the control group at week 4. Histological analysis showed increased presence of small capillaries and venules in the infarcted zones by CD31 staining. Suckau et al. studied shRNA in a heart failure rat model [167]. In this study they injected vector intravenously. The rAAV vector-expressed shRNA silenced phospholamban (rAAV9-shPLB) in the heart. They reported cardiac PLB protein was reduced to 25% of baseline. Recombinant AAV9-shPLB therapy was noted to restore diastolic and systolic functional parameters to normal ranges. Cardiac dilatation was also reversed and a reduction of cardiac hypertrophy and fibrosis was noted. Importantly they showed that rAAV9 had a high affinity for myocardium and low affinity for liver and other organs. No evidence was

found of shRNA deregulation or hepatotoxicity by rAAV-mediated shRNA therapy [167]. Hence the use of rAAV9 shRNA to deliver targeted gene knockdown in cardiac therapy would be efficacious and safe given the findings in the above model when translated to clinical practice.

6.4 Limitations of Gene therapy

The nature of the vector-host interaction can be potentially limiting in gene therapy, particularly in humans. The vector particles are replication-deficient but their use has not been fully investigated in humans and therefore they may give rise to side effects that we are currently unaware of. In addition given these are foreign particles the human immune system is likely to mount an immune response. Although the latter will depend on the type of vector employed. In the current study we chose to use rAAV because it has minimal immunogenicity. No inflammatory response was seen in rat hearts transduced with this vector in this study. There is, however, the problem of neutralising antibodies to rAAV capsid proteins. Some animals have pre-existing neutralising antibodies to a number of rAAV capsid serotypes [189]. Neutralising antibodies can be formed due to natural infections or as a result of vector exposure. The presence for neutralising antibodies would preclude vector injection of the same

serotype. If additional vector is required this could be delivered via a rAAV with a different capsid and therefore bypass any neutralising antibodies.

For a small number of rats in the current study gene therapy appeared to have no effect. Several explanations exist. Firstly the vector may not have been injected into the venous system and therefore it did not reach the heart. Secondly the batch of viral particles used was ineffective and therefore no active particles were used. Thirdly, it is possible that the rodent was immune to our viral vector due the presence of antibodies. These and other limitations of gene therapy would need to be addressed before any human trials can be commenced.

A further issue in gene therapy is that of transduction of unintended targets. The use of specific vectors and promoters helps to limit this but targeting is never perfect. In the current study, rAAV was used because of its tropism for heart muscle. Other tissues such as liver and lung will also be transduced but to a much lesser extent. The effect of unintended transduction was not assessed in the current study but will need to be considered when translating this technology to humans.

With regard to the use of small regulatory RNA molecules for gene therapy, one of the most important translational hurdles is the stability of shRNA once delivered *in vivo*. Endogenous microRNA is highly stable when secreted into the circulation as they resist nucleases by being enclosed into micro-vesicles or exosomes. One way to improve stability of regulatory RNAs is to express them from vectors. As seen in the current study rAAV2/9 was capable of expression at 5 weeks following vector injection. The effects of the shRNA targeting Cx45 were also evident at this time point with continued reduction on the Cx45 steady state levels. Other than viral vector based expression there are other methods to improve stability of regulatory RNA molecule. These include chemical modifications to the nucleic acids such as, phosphorothioate, 2′-O-methyl RNA, 2′-Fluoro-RNA and 2′O-methoxy-ethyl RNA, all of which provide greater nuclease resistance. Another modification that also confers nuclease resistance results in molecules known as locked nucleic acid. Locked nucleic acids are widely used in synthesis for microRNA inhibiting drugs, sometimes referred to as antagomirs. This modification utilizes a bridge between the 2′O group and 4′ carbon atom also referred to as 2′O-4′C-methylene linked ribonucleotides [190, 191].

6.5 Future directions

Further evaluation within a large animal model is required given the limitations with a small animal model. Somatic gene transfer should be performed globally as well as in the scar area alone to understand both focal and diffuse overexpression as well as knockdown of genes in the prevention of VT. A larger myocardium would allow for 3 dimensional electro-anatomical mapping of VT circuits and subsequent correlation with tissue and in turn allow a better understanding of the origin of VT and effects of gene therapy. A larger heart will also more closely mimic the human myocardium. More-over an optimal dose for Cx43 transduction is required, and further studies carrying out difference vector amounts would facilitate the understanding of the optimum dose.

6.6 Connexins and Ventricular Arrhythmias – Final Comments

The clinically relevant studies described within this thesis provide the first direct evidence for a role of Cx45 in the pathogenesis of post-MI VT. In addition to confirming previous findings with respect to the ability of Cx45 to modify myocardial electrical stability, they also represent the first ever in-vivo non-transgenic genotype-phenotype correlation between Cx45

and VT. This thesis also provides incremental evidence for the role Cx43 gene therapy in reduction of post-MI ventricular tachyarrhythmia.

The studies performed in this thesis are an important first step in using somatic gene transfer techniques to treat post-MI VT in humans. The next step would be to recreate these studies in a large animal model of post-MI ventricular tachyarrhythmia that recapitulates the same human condition. This would enable preclinical safety and efficacy studies to be undertaken prior to seeking regulatory approval for the translation of this technology to human application.

CHAPTER 7

BIBLIOGRAPHY

1. Zheng, Z.J., et al., *Sudden cardiac death in the United States, 1989 to 1998.* Circulation, 2001. **104**(18): p. 2158-63.
2. Yamada, K.A., et al., *Up-regulation of connexin45 in heart failure.* J Cardiovasc Electrophysiol, 2003. **14**(11): p. 1205-12.
3. Betsuyaku, T., et al., *Overexpression of cardiac connexin45 increases susceptibility to ventricular tachyarrhythmias in vivo.* Am J Physiol Heart Circ Physiol, 2006. **290**(1): p. H163-71.
4. De Groot, J.R. and R. Coronel, *Acute ischemia-induced gap junctional uncoupling and arrhythmogenesis.* Cardiovasc Res, 2004. **62**(2): p. 323-34.
5. Myerburg, R.J., K.M. Kessler, and A. Castellanos, *Sudden cardiac death: epidemiology, transient risk, and intervention assessment.* Ann Intern Med, 1993. **119**(12): p. 1187-97.
6. Myerburg, R.J., et al., *Frequency of sudden cardiac death and profiles of risk.* Am J Cardiol, 1997. **80**(5B): p. 10F-19F.
7. Zipes, D.P. and H.J. Wellens, *Sudden cardiac death.* Circulation, 1998. **98**(21): p. 2334-51.
8. Zipes, D.P., et al., *ACC/AHA/ESC 2006 guidelines for management of patients with ventricular arrhythmias and the prevention of sudden cardiac death: A report of the American College of Cardiology/American Heart Association Task Force and the European Society of Cardiology Committee for Practice Guidelines (Writing Committee to Develop Guidelines for Management of Patients With Ventricular Arrhythmias and the Prevention of Sudden Cardiac Death) Developed in collaboration with the European Heart Rhythm Association and the Heart Rhythm Society.* Europace, 2006. **8**(9): p. 746-837.
9. Zaman, S., et al., *Outcomes of Early Risk Stratification and Targeted Implantable Cardioverter-Defibrillator Implantation After ST-Elevation Myocardial Infarction Treated With Primary Percutaneous Coronary Intervention.* Circulation, 2009. **120**(3): p. 194-200.
10. Wit, A.L. and M.J. Janse, *Experimental models of ventricular tachycardia and fibrillation caused by ischemia and infarction.* Circulation, 1992. **85**(1 Suppl): p. I32-42.
11. Luu, M., et al., *Diverse mechanisms of unexpected cardiac arrest in advanced heart failure.* Circulation, 1989. **80**(6): p. 1675-80.
12. Myerburg, R.J., K.M. Kessler, and A. Castellanos, *Sudden cardiac death. Structure, function, and time-dependence of risk.* Circulation, 1992. **85**(1 Suppl): p. I2-10.
13. Sheharyar Ali, M., and Eduardo S. Antezano, MD, *Sudden Cardiac Death.* Southern Medical Journal, 2006. **Volume 99 May 2006**(Number 5): p. 9.
14. Podrid, P.J., T. Fuchs, and R. Candinas, *Role of the sympathetic nervous system in the genesis of ventricular arrhythmia.* Circulation, 1990. **82**(2 Suppl): p. I103-13.
15. Huikuri, H.V., A. Castellanos, and R.J. Myerburg, *Sudden death due to cardiac arrhythmias.* N Engl J Med, 2001. **345**(20): p. 1473-82.
16. Spooner, P.M. and D.P. Zipes, *Sudden death predictors: an inflammatory association.* Circulation, 2002. **105**(22): p. 2574-6.
17. Thompson, B.S., *Sudden cardiac death and heart failure.* AACN Adv Crit Care, 2009. **20**(4): p. 356-65.
18. Thomas, K.E. and M.E. Josephson, *The role of electrophysiology study in risk stratification of sudden cardiac death.* Prog Cardiovasc Dis, 2008. **51**(2): p. 97-105.

19. Latif, N., et al., *Characterization of molecules mediating cell-cell communication in human cardiac valve interstitial cells.* Cell Biochem Biophys, 2006. **45**(3): p. 255-64.
20. Khoo, C.W. and G.Y. Lip, *Insights from the dabigatran versus warfarin in patients with atrial fibrillation (RE-LY) trial.* Expert Opin Pharmacother, 2010. **11**(4): p. 685-7.
21. Saez, J.C., et al., *Plasma membrane channels formed by connexins: their regulation and functions.* Physiol Rev, 2003. **83**(4): p. 1359-400.
22. Coppen, S.R., et al., *Connexin45 expression is preferentially associated with the ventricular conduction system in mouse and rat heart.* Circ Res, 1998. **82**(2): p. 232-43.
23. Peters, N.S., et al., *Disturbed connexin43 gap junction distribution correlates with the location of reentrant circuits in the epicardial border zone of healing canine infarcts that cause ventricular tachycardia.* Circulation, 1997. **95**(4): p. 988-96.
24. Smith, J.H., et al., *Altered patterns of gap junction distribution in ischemic heart disease. An immunohistochemical study of human myocardium using laser scanning confocal microscopy.* Am J Pathol, 1991. **139**(4): p. 801-21.
25. van Veen, A.A., H.V. van Rijen, and T. Opthof, *Cardiac gap junction channels: modulation of expression and channel properties.* Cardiovasc Res, 2001. **51**(2): p. 217-29.
26. Miura, T., T. Miki, and T. Yano, *Role of the gap junction in ischemic preconditioning in the heart.* Am J Physiol Heart Circ Physiol, 2010. **298**(4): p. H1115-25.
27. Desplantez, T., et al., *Cardiac connexins Cx43 and Cx45: formation of diverse gap junction channels with diverse electrical properties.* Pflugers Arch, 2004. **448**(4): p. 363-75.
28. Sheikh, F., R.S. Ross, and J. Chen, *Cell-cell connection to cardiac disease.* Trends Cardiovasc Med, 2009. **19**(6): p. 182-90.
29. Gottlieb, I., et al., *Diagnostic accuracy of arterial phase 64-slice multidetector CT angiography for left atrial appendage thrombus in patients undergoing atrial fibrillation ablation.* J Cardiovasc Electrophysiol, 2008. **19**(3): p. 247-51.
30. Valiunas, V., E.C. Beyer, and P.R. Brink, *Cardiac gap junction channels show quantitative differences in selectivity.* Circulation research, 2002. **91**(2): p. 104-11.
31. van Veen, A.A., H.V. van Rijen, and T. Opthof, *Cardiac gap junction channels: modulation of expression and channel properties.* Cardiovascular research, 2001. **51**(2): p. 217-29.
32. Dhein, S., et al., *Improving cardiac gap junction communication as a new antiarrhythmic mechanism: the action of antiarrhythmic peptides.* Naunyn-Schmiedeberg's Archives of Pharmacology, 2009. **381**(3): p. 221-234.
33. Salameh, A. and S. Dhein, *Pharmacology of gap junctions. New pharmacological targets for treatment of arrhythmia, seizure and cancer?* Biochim Biophys Acta, 2005. **1719**(1-2): p. 36-58.
34. Cascio, W., et al., *Ischemia-induced arrhythmia: the role of connexins, gap junctions, and attendant changes in impulse propagation.* Journal of Electrocardiology, 2005. **38**(4): p. 55-59.
35. Delmar, M., et al., *Effects of increasing intercellular resistance on transverse and longitudinal propagation in sheep epicardial muscle.* Circ Res, 1987. **60**(5): p. 780-5.
36. Dhein, S., *Pharmacology of gap junctions in the cardiovascular system.* Cardiovasc Res, 2004. **62**(2): p. 287-98.
37. Jongsma, H.J. and R. Wilders, *Gap junctions in cardiovascular disease.* Circ Res, 2000. **86**(12): p. 1193-7.
38. de Groot, J.R., et al., *Intrinsic heterogeneity in repolarization is increased in isolated failing rabbit cardiomyocytes during simulated ischemia.* Cardiovasc Res, 2003. **59**(3): p. 705-14.
39. Morley, G.E., et al., *Characterization of conduction in the ventricles of normal and heterozygous Cx43 knockout mice using optical mapping.* J Cardiovasc Electrophysiol, 1999. **10**(10): p. 1361-75.
40. Lerner, D.L., et al., *Accelerated onset and increased incidence of ventricular arrhythmias induced by ischemia in Cx43-deficient mice.* Circulation, 2000. **101**(5): p. 547-52.

41. Thomas, S.P., et al., *Impulse propagation in synthetic strands of neonatal cardiac myocytes with genetically reduced levels of connexin43.* Circ Res, 2003. **92**(11): p. 1209-16.
42. Dhein, S., et al., *Improving cardiac gap junction communication as a new antiarrhythmic mechanism: the action of antiarrhythmic peptides.* Naunyn Schmiedebergs Arch Pharmacol, 2010. **381**(3): p. 221-34.
43. Muller, A., et al., *Increase in gap junction conductance by an antiarrhythmic peptide.* Eur J Pharmacol, 1997. **327**(1): p. 65-72.
44. Muller, A., et al., *Actions of the antiarrhythmic peptide AAP10 on intercellular coupling.* Naunyn Schmiedebergs Arch Pharmacol, 1997. **356**(1): p. 76-82.
45. Dhein, S., et al., *Protein kinase Calpha mediates the effect of antiarrhythmic peptide on gap junction conductance.* Cell Commun Adhes, 2001. **8**(4-6): p. 257-64.
46. Hagen, A., A. Dietze, and S. Dhein, *Human cardiac gap-junction coupling: effects of antiarrhythmic peptide AAP10.* Cardiovasc Res, 2009. **83**(2): p. 405-15.
47. Miura, T., T. Miki, and T. Yano, *Role of the gap junction in ischemic preconditioning in the heart.* American journal of physiology. Heart and circulatory physiology, 2010. **298**(4): p. H1115-25.
48. Dhein, S., *Cardiac ischemia and uncoupling: gap junctions in ischemia and infarction.* Advances in cardiology, 2006. **42**: p. 198-212.
49. Severs, N.J., et al., *Gap junction alterations in human cardiac disease.* Cardiovasc Res, 2004. **62**(2): p. 368-77.
50. Luke, R.A. and J.E. Saffitz, *Remodeling of ventricular conduction pathways in healed canine infarct border zones.* J Clin Invest, 1991. **87**(5): p. 1594-602.
51. van der Velden, H.M., et al., *Altered pattern of connexin40 distribution in persistent atrial fibrillation in the goat.* J Cardiovasc Electrophysiol, 1998. **9**(6): p. 596-607.
52. Yan, H., et al., *[Expression of connexin in atrium of patients with atrial fibrillation and its signal transduction pathway].* Zhonghua Yi Xue Za Zhi, 2004. **84**(3): p. 209-13.
53. Li, D.Q., Y.B. Feng, and H.Q. Zhang, *[The relationship between gap junctional remodeling and atrial fibrillation in patients with rheumatic heart disease].* Zhonghua Yi Xue Za Zhi, 2004. **84**(5): p. 384-6.
54. Maeda, S. and T. Tsukihara, *Structure of the gap junction channel and its implications for its biological functions.* Cell Mol Life Sci, 2011. **68**(7): p. 1115-29.
55. Sohl, G., *Gap junctions and the connexin protein family.* Cardiovascular Research, 2004. **62**(2): p. 228-232.
56. Kaba, R.A., et al., *Comparison of connexin 43, 40 and 45 expression patterns in the developing human and mouse hearts.* Cell Commun Adhes, 2001. **8**(4-6): p. 339-43.
57. Kanter, H.L., J.E. Saffitz, and E.C. Beyer, *Molecular cloning of two human cardiac gap junction proteins, connexin40 and connexin45.* Journal of molecular and cellular cardiology, 1994. **26**(7): p. 861-8.
58. Lin, X., et al., *Dynamic model for ventricular junctional conductance during the cardiac action potential.* American journal of physiology. Heart and circulatory physiology, 2005. **288**(3): p. H1113-23.
59. Alcolea, S., et al., *Downregulation of connexin 45 gene products during mouse heart development.* Circulation research, 1999. **84**(12): p. 1365-79.
60. Davis, L.M., et al., *Distinct gap junction protein phenotypes in cardiac tissues with disparate conduction properties.* J Am Coll Cardiol, 1994. **24**(4): p. 1124-32.
61. Chaldoupi, S.M., et al., *The role of connexin40 in atrial fibrillation.* Cardiovascular research, 2009. **84**(1): p. 15-23.
62. Lo, C.W., *Role of gap junctions in cardiac conduction and development: insights from the connexin knockout mice.* Circulation research, 2000. **87**(5): p. 346-8.
63. Schulz, R. and G. Heusch, *Connexin 43 and ischemic preconditioning.* Cardiovasc Res, 2004. **62**(2): p. 335-44.

64. Greener, I.D., et al., *Connexin43 gene transfer reduces ventricular tachycardia susceptibility after myocardial infarction.* J Am Coll Cardiol, 2012. **60**(12): p. 1103-10.
65. Baba, S., et al., *Remodeling in cells from different regions of the reentrant circuit during ventricular tachycardia.* Circulation, 2005. **112**(16): p. 2386-96.
66. Cabo, C., et al., *Heterogeneous gap junction remodeling in reentrant circuits in the epicardial border zone of the healing canine infarct.* Cardiovasc Res, 2006. **72**(2): p. 241-9.
67. Jain, S.K., R.B. Schuessler, and J.E. Saffitz, *Mechanisms of delayed electrical uncoupling induced by ischemic preconditioning.* Circ Res, 2003. **92**(10): p. 1138-44.
68. Ursell, P.C., et al., *Structural and electrophysiological changes in the epicardial border zone of canine myocardial infarcts during infarct healing.* Circ Res, 1985. **56**(3): p. 436-51.
69. Peters, N.S., et al., *Reduced content of connexin43 gap junctions in ventricular myocardium from hypertrophied and ischemic human hearts.* Circulation, 1993. **88**(3): p. 864-75.
70. Guerrero, P.A., et al., *Slow ventricular conduction in mice heterozygous for a connexin43 null mutation.* J Clin Invest, 1997. **99**(8): p. 1991-8.
71. Eloff, B.C., et al., *High resolution optical mapping reveals conduction slowing in connexin43 deficient mice.* Cardiovasc Res, 2001. **51**(4): p. 681-90.
72. Morley, G.E., D. Vaidya, and J. Jalife, *Characterization of conduction in the ventricles of normal and heterozygous Cx43 knockout mice using optical mapping.* J Cardiovasc Electrophysiol, 2000. **11**(3): p. 375-7.
73. Danik, S.B., et al., *Modulation of cardiac gap junction expression and arrhythmic susceptibility.* Circ Res, 2004. **95**(10): p. 1035-41.
74. Ai, X., W. Zhao, and S.M. Pogwizd, *Connexin43 knockdown or overexpression modulates cell coupling in control and failing rabbit left ventricular myocytes.* Cardiovasc Res, 2010. **85**(4): p. 751-62.
75. Roell, W., et al., *Engraftment of connexin 43-expressing cells prevents post-infarct arrhythmia.* Nature, 2007. **450**(7171): p. 819-24.
76. Kostin, S., et al., *Gap junction remodeling and altered connexin43 expression in the failing human heart.* Mol Cell Biochem, 2003. **242**(1-2): p. 135-44.
77. Dupont, E., et al., *Altered connexin expression in human congestive heart failure.* J Mol Cell Cardiol, 2001. **33**(2): p. 359-71.
78. Kurtz, L., et al., *Replacement of connexin 40 by connexin 45 causes ectopic localization of renin-producing cells in the kidney but maintains in vivo control of renin gene expression.* American journal of physiology. Renal physiology, 2009. **297**(2): p. F403-9.
79. Desplantez, T., et al., *Cardiac connexins Cx43 and Cx45: formation of diverse gap junction channels with diverse electrical properties.* Pflugers Archiv : European journal of physiology, 2004. **448**(4): p. 363-75.
80. Martinez, A.D., et al., *Connexin43 and connexin45 form heteromeric gap junction channels in which individual components determine permeability and regulation.* Circulation research, 2002. **90**(10): p. 1100-7.
81. Koval, M., et al., *Transfected connexin45 alters gap junction permeability in cells expressing endogenous connexin43.* The Journal of cell biology, 1995. **130**(4): p. 987-95.
82. Hermans, M.M., et al., *pH sensitivity of the cardiac gap junction proteins, connexin 45 and 43.* Pflugers Archiv : European journal of physiology, 1995. **431**(1): p. 138-40.
83. Valiunas, V., *Biophysical properties of connexin-45 gap junction hemichannels studied in vertebrate cells.* The Journal of general physiology, 2002. **119**(2): p. 147-64.
84. Kruger, O., et al., *Defective vascular development in connexin 45-deficient mice.* Development, 2000. **127**(19): p. 4179-93.
85. Kumai, M., et al., *Loss of connexin45 causes a cushion defect in early cardiogenesis.* Development, 2000. **127**(16): p. 3501-12.
86. Yamada, K.A., et al., *Up-regulation of connexin45 in heart failure.* J Cardiovasc Electrophysiol, 2003. **14**(11): p. 1205-12.

87. Akar, F.G., et al., *Mechanisms underlying conduction slowing and arrhythmogenesis in nonischemic dilated cardiomyopathy.* Circ Res, 2004. **95**(7): p. 717-25.
88. Eckardt, D., et al., *Functional role of connexin43 gap junction channels in adult mouse heart assessed by inducible gene deletion.* J Mol Cell Cardiol, 2004. **36**(1): p. 101-10.
89. van Rijen, H.V., et al., *Slow conduction and enhanced anisotropy increase the propensity for ventricular tachyarrhythmias in adult mice with induced deletion of connexin43.* Circulation, 2004. **109**(8): p. 1048-55.
90. Betsuyaku, T., et al., *Overexpression of cardiac connexin45 increases susceptibility to ventricular tachyarrhythmias in vivo.* American journal of physiology. Heart and circulatory physiology, 2006. **290**(1): p. H163-71.
91. Bao, M., et al., *Residual Cx45 and its relationship to Cx43 in murine ventricular myocardium.* Channels (Austin), 2011. **5**(6): p. 489-99.
92. Kay, M.A., J.C. Glorioso, and L. Naldini, *Viral vectors for gene therapy: the art of turning infectious agents into vehicles of therapeutics.* Nat Med, 2001. **7**(1): p. 33-40.
93. Nishikawa, M. and L. Huang, *Nonviral vectors in the new millennium: delivery barriers in gene transfer.* Hum Gene Ther, 2001. **12**(8): p. 861-70.
94. Isner, J.M., et al., *Assessment of risks associated with cardiovascular gene therapy in human subjects.* Circ Res, 2001. **89**(5): p. 389-400.
95. Kizana, E., *Therapeutic prospects of cardiac gene transfer.* Heart Lung Circ, 2007. **16**(3): p. 180-4.
96. Guzman, R.J., et al., *Efficient gene transfer into myocardium by direct injection of adenovirus vectors.* Circ Res, 1993. **73**(6): p. 1202-7.
97. Barr, E., et al., *Efficient catheter-mediated gene transfer into the heart using replication-defective adenovirus.* Gene Ther, 1994. **1**(1): p. 51-8.
98. Trono, D., *Lentiviral vectors: turning a deadly foe into a therapeutic agent.* Gene Ther, 2000. **7**(1): p. 20-3.
99. Carter, P.J. and R.J. Samulski, *Adeno-associated viral vectors as gene delivery vehicles.* International journal of molecular medicine, 2000. **6**(1): p. 17-27.
100. Nakai, H., et al., *Isolation of recombinant adeno-associated virus vector-cellular DNA junctions from mouse liver.* J Virol, 1999. **73**(7): p. 5438-47.
101. Hoshijima, M., et al., *Chronic suppression of heart-failure progression by a pseudophosphorylated mutant of phospholamban via in vivo cardiac rAAV gene delivery.* Nat Med, 2002. **8**(8): p. 864-71.
102. Palomeque, J., et al., *Efficiency of eight different AAV serotypes in transducing rat myocardium in vivo.* Gene therapy, 2007. **14**(13): p. 989-97.
103. Bell, C.L., et al., *The AAV9 receptor and its modification to improve in vivo lung gene transfer in mice.* J Clin Invest, 2011. **121**(6): p. 2427-35.
104. Asokan, A. and R.J. Samulski, *An emerging adeno-associated viral vector pipeline for cardiac gene therapy.* Hum Gene Ther, 2013. **24**(11): p. 906-13.
105. Fang, H., et al., *Comparison of adeno-associated virus serotypes and delivery methods for cardiac gene transfer.* Hum Gene Ther Methods, 2012. **23**(4): p. 234-41.
106. Qi, Y., et al., *Selective tropism of the recombinant adeno-associated virus 9 serotype for rat cardiac tissue.* J Gene Med, 2010. **12**(1): p. 22-34.
107. Bish, L.T., et al., *Percutaneous transendocardial delivery of self-complementary adeno-associated virus 6 achieves global cardiac gene transfer in canines.* Mol Ther, 2008. **16**(12): p. 1953-9.
108. Gao, G., et al., *Transendocardial delivery of AAV6 results in highly efficient and global cardiac gene transfer in rhesus macaques.* Hum Gene Ther, 2011. **22**(8): p. 979-84.
109. Fish, K.M., et al., *AAV9.I-1c delivered via direct coronary infusion in a porcine model of heart failure improves contractility and mitigates adverse remodeling.* Circ Heart Fail, 2013. **6**(2): p. 310-7.

110. Pleger, S.T., et al., *Cardiac AAV9-S100A1 gene therapy rescues post-ischemic heart failure in a preclinical large animal model.* Sci Transl Med, 2011. **3**(92): p. 92ra64.
111. Louis Jeune, V., et al., *Pre-existing anti-adeno-associated virus antibodies as a challenge in AAV gene therapy.* Hum Gene Ther Methods, 2013. **24**(2): p. 59-67.
112. Donahue, J.K., et al., *Focal modification of electrical conduction in the heart by viral gene transfer.* Nat Med, 2000. **6**(12): p. 1395-8.
113. Koransky, M.L., R.C. Robbins, and H.M. Blau, *VEGF gene delivery for treatment of ischemic cardiovascular disease.* Trends Cardiovasc Med, 2002. **12**(3): p. 108-14.
114. Edelberg, J.M., et al., *Molecular enhancement of porcine cardiac chronotropy.* Heart, 2001. **86**(5): p. 559-62.
115. Gwon, H.C., et al., *The feasibility and safety of fluoroscopy-guided percutaneous intramyocardial gene injection in porcine heart.* Int J Cardiol, 2001. **79**(1): p. 77-88.
116. Sanborn, T.A., et al., *Percutaneous endocardial transfer and expression of genes to the myocardium utilizing fluoroscopic guidance.* Catheter Cardiovasc Interv, 2001. **52**(2): p. 260-6.
117. Losordo, D.W., et al., *Phase 1/2 placebo-controlled, double-blind, dose-escalating trial of myocardial vascular endothelial growth factor 2 gene transfer by catheter delivery in patients with chronic myocardial ischemia.* Circulation, 2002. **105**(17): p. 2012-8.
118. Raake, P., et al., *Myocardial gene transfer by selective pressure-regulated retroinfusion of coronary veins: comparison with surgical and percutaneous intramyocardial gene delivery.* J Am Coll Cardiol, 2004. **44**(5): p. 1124-9.
119. Boekstegers, P., et al., *Myocardial gene transfer by selective pressure-regulated retroinfusion of coronary veins.* Gene Ther, 2000. **7**(3): p. 232-40.
120. Kupatt, C., et al., *Retroinfusion of NFkappaB decoy oligonucleotide extends cardioprotection achieved by CD18 inhibition in a preclinical study of myocardial ischemia and retroinfusion in pigs.* Gene Ther, 2002. **9**(8): p. 518-26.
121. Schwarz, E.R., et al., *Evaluation of the effects of intramyocardial injection of DNA expressing vascular endothelial growth factor (VEGF) in a myocardial infarction model in the rat--angiogenesis and angioma formation.* J Am Coll Cardiol, 2000. **35**(5): p. 1323-30.
122. Vera Janavel, G.L., et al., *Effect of vascular endothelial growth factor gene transfer on infarct size, left ventricular function and myocardial perfusion in sheep after 2 months of coronary artery occlusion.* J Gene Med, 2012. **14**(4): p. 279-87.
123. Bull, D.A., et al., *Effect of Terplex/VEGF-165 gene therapy on left ventricular function and structure following myocardial infarction. VEGF gene therapy for myocardial infarction.* J Control Release, 2003. **93**(2): p. 175-81.
124. Mack, C.A., et al., *Biologic bypass with the use of adenovirus-mediated gene transfer of the complementary deoxyribonucleic acid for vascular endothelial growth factor 121 improves myocardial perfusion and function in the ischemic porcine heart.* J Thorac Cardiovasc Surg, 1998. **115**(1): p. 168-76; discussion 176-7.
125. Landau, C., A.K. Jacobs, and C.C. Haudenschild, *Intrapericardial basic fibroblast growth factor induces myocardial angiogenesis in a rabbit model of chronic ischemia.* Am Heart J, 1995. **129**(5): p. 924-31.
126. Lazarous, D.F., et al., *Adenoviral-mediated gene transfer induces sustained pericardial VEGF expression in dogs: effect on myocardial angiogenesis.* Cardiovasc Res, 1999. **44**(2): p. 294-302.
127. Kornowski, R., et al., *Delivery strategies to achieve therapeutic myocardial angiogenesis.* Circulation, 2000. **101**(4): p. 454-8.
128. Katz, M.G., et al., *Gene delivery technologies for cardiac applications.* Gene Ther, 2012. **19**(6): p. 659-69.
129. Neyroud, N., et al., *Gene delivery to cardiac muscle.* Methods Enzymol, 2002. **346**: p. 323-34.

130. Hajjar, R.J., et al., *Modulation of ventricular function through gene transfer in vivo.* Proc Natl Acad Sci U S A, 1998. **95**(9): p. 5251-6.
131. Maurice, J.P., et al., *Enhancement of cardiac function after adenoviral-mediated in vivo intracoronary beta2-adrenergic receptor gene delivery.* J Clin Invest, 1999. **104**(1): p. 21-9.
132. Champion, H.C., et al., *Robust adenoviral and adeno-associated viral gene transfer to the in vivo murine heart: application to study of phospholamban physiology.* Circulation, 2003. **108**(22): p. 2790-7.
133. Lazarous, D.F., et al., *Pharmacodynamics of basic fibroblast growth factor: route of administration determines myocardial and systemic distribution.* Cardiovasc Res, 1997. **36**(1): p. 78-85.
134. Bostick, B., et al., *Adeno-associated virus serotype-9 microdystrophin gene therapy ameliorates electrocardiographic abnormalities in mdx mice.* Hum Gene Ther, 2008. **19**(8): p. 851-6.
135. Sasano, T., et al., *Ventricular tachycardia from the healed myocardial infarction scar: validation of an animal model and utility of gene therapy.* Heart Rhythm, 2009. **6**(8 Suppl): p. S91-7.
136. Sambrook, J. and M.J. Gething, *Protein structure. Chaperones, paperones.* Nature, 1989. **342**(6247): p. 224-5.
137. Huang, X., et al., *AAV2 production with optimized N/P ratio and PEI-mediated transfection results in low toxicity and high titer for in vitro and in vivo applications.* J Virol Methods, 2013.
138. McClure, C., et al., *Production and titering of recombinant adeno-associated viral vectors.* J Vis Exp, 2011(57): p. e3348.
139. Gray, S.J., et al., *Production of recombinant adeno-associated viral vectors and use in in vitro and in vivo administration.* Curr Protoc Neurosci, 2011. **Chapter 4**: p. Unit 4 17.
140. Sastry, L., et al., *Titering lentiviral vectors: comparison of DNA, RNA and marker expression methods.* Gene Ther, 2002. **9**(17): p. 1155-62.
141. LG Luna, Manual of Histologic Staining Methods of the Armed Forces Institute of Pathology, third edition, McGraw Hill
142. Igarashi, T., et al., *Connexin gene transfer preserves conduction velocity and prevents atrial fibrillation.* Circulation, 2012. **125**(2): p. 216-25.
143. Bradford, M.M., *A rapid and sensitive method for the quantitation of microgram quantities of protein utilizing the principle of protein-dye binding.* Anal Biochem, 1976. **72**: p. 248-54.
144. Soderberg, O., et al., *Direct observation of individual endogenous protein complexes in situ by proximity ligation.* Nat Methods, 2006. **3**(12): p. 995-1000.
145. Brockway, B.P., P.A. Mills, and S.H. Azar, *A new method for continuous chronic measurement and recording of blood pressure, heart rate and activity in the rat via radio-telemetry.* Clin Exp Hypertens A, 1991. **13**(5): p. 885-95.
146. Alcolea, S., et al., *Downregulation of connexin 45 gene products during mouse heart development.* Circ Res, 1999. **84**(12): p. 1365-79.
147. Peters, N.S., *Myocardial gap junction organization in ischemia and infarction.* Microsc Res Tech, 1995. **31**(5): p. 375-86.
148. Peters, N.S., et al., *Cardiac arrhythmogenesis and the gap junction.* J Mol Cell Cardiol, 1995. **27**(1): p. 37-44.
149. Yamada, K.A., et al., *Up-regulation of connexin45 in heart failure.* Journal of cardiovascular electrophysiology, 2003. **14**(11): p. 1205-12.
150. Xiao, X., J. Li, and R.J. Samulski, *Production of high-titer recombinant adeno-associated virus vectors in the absence of helper adenovirus.* J Virol, 1998. **72**(3): p. 2224-32.
151. Grieger, J.C., V.W. Choi, and R.J. Samulski, *Production and characterization of adeno-associated viral vectors.* Nat Protoc, 2006. **1**(3): p. 1412-28.

152. Xu, R., et al., *Stability of infectious recombinant adeno-associated viral vector in gene delivery.* Med Sci Monit, 2005. **11**(9): p. BR305-8.
153. Huang, X., et al., *AAV2 production with optimized N/P ratio and PEI-mediated transfection results in low toxicity and high titer for in vitro and in vivo applications.* J Virol Methods, 2013. **193**(2): p. 270-7.
154. Iravanian, S., et al., *Functional reentry in cultured monolayers of neonatal rat cardiac cells.* Am J Physiol Heart Circ Physiol, 2003. **285**(1): p. H449-56.
155. Kaprielian, R.R., et al., *Downregulation of immunodetectable connexin43 and decreased gap junction size in the pathogenesis of chronic hibernation in the human left ventricle.* Circulation, 1998. **97**(7): p. 651-60.
156. van Rijen, H.V., et al., *Slow conduction and enhanced anisotropy increase the propensity for ventricular tachyarrhythmias in adult mice with induced deletion of connexin43.* Circulation, 2004. **109**(8): p. 1048-55.
157. Moss, A.J., et al., *Prophylactic implantation of a defibrillator in patients with myocardial infarction and reduced ejection fraction.* N Engl J Med, 2002. **346**(12): p. 877-83.
158. Cohen, S.A., *Immunocytochemical localization of rH1 sodium channel in adult rat heart atria and ventricle. Presence in terminal intercalated disks.* Circulation, 1996. **94**(12): p. 3083-6.
159. Mays, D.J., et al., *Localization of the Kv1.5 K+ channel protein in explanted cardiac tissue.* Journal of Clinical Investigation, 1995. **96**(1): p. 282-92.
160. Kizana, E. and I.E. Alexander, *Cardiac gene therapy: therapeutic potential and current progress.* Curr Gene Ther, 2003. **3**(5): p. 418-51.
161. Bumcrot, D., et al., *RNAi therapeutics: a potential new class of pharmaceutical drugs.* Nat Chem Biol, 2006. **2**(12): p. 711-9.
162. Shen, J., et al., *Suppression of ocular neovascularization with siRNA targeting VEGF receptor 1.* Gene Ther, 2006. **13**(3): p. 225-34.
163. Nakamura, H., et al., *RNA interference targeting transforming growth factor-beta type II receptor suppresses ocular inflammation and fibrosis.* Mol Vis, 2004. **10**: p. 703-11.
164. Thakker, D.R., et al., *Neurochemical and behavioral consequences of widespread gene knockdown in the adult mouse brain by using nonviral RNA interference.* Proc Natl Acad Sci U S A, 2004. **101**(49): p. 17270-5.
165. Thakker, D.R., et al., *siRNA-mediated knockdown of the serotonin transporter in the adult mouse brain.* Mol Psychiatry, 2005. **10**(8): p. 782-9, 714.
166. Tabernero, J., et al., *First-in-humans trial of an RNA interference therapeutic targeting VEGF and KSP in cancer patients with liver involvement.* Cancer Discov, 2013. **3**(4): p. 406-17.
167. Suckau, L., et al., *Long-term cardiac-targeted RNA interference for the treatment of heart failure restores cardiac function and reduces pathological hypertrophy.* Circulation, 2009. **119**(9): p. 1241-52.
168. Huang, M., et al., *Short hairpin RNA interference therapy for ischemic heart disease.* Circulation, 2008. **118**(14 Suppl): p. S226-33.
169. Kim, V.N., *Small RNAs: classification, biogenesis, and function.* Mol Cells, 2005. **19**(1): p. 1-15.
170. Hayes, J., P.P. Peruzzi, and S. Lawler, *MicroRNAs in cancer: biomarkers, functions and therapy.* Trends Mol Med, 2014. **20**(8): p. 460-9.
171. Stecker, E.C., et al., *Public health burden of sudden cardiac death in the United States.* Circ Arrhythm Electrophysiol, 2014. **7**(2): p. 212-7.
172. Bigger, J.T., Jr., et al., *Ventricular arrhythmias in ischemic heart disease: mechanism, prevalence, significance, and management.* Prog Cardiovasc Dis, 1977. **19**(4): p. 255-300.
173. Ding, C., et al., *High-resolution optical mapping of ventricular tachycardia in rats with chronic myocardial infarction.* Pacing Clin Electrophysiol, 2010. **33**(6): p. 687-95.
174. Lal, R. and M.F. Arnsdorf, *Voltage-dependent gating and single-channel conductance of adult mammalian atrial gap junctions.* Circ Res, 1992. **71**(3): p. 737-43.

175. Koval, M., et al., *Transfected connexin45 alters gap junction permeability in cells expressing endogenous connexin43.* J Cell Biol, 1995. **130**(4): p. 987-95.
176. Steiner, E. and L. Ebihara, *Functional characterization of canine connexin45.* J Membr Biol, 1996. **150**(2): p. 153-61.
177. Chu, D., et al., *Direct comparison of efficiency and stability of gene transfer into the mammalian heart using adeno-associated virus versus adenovirus vectors.* J Thorac Cardiovasc Surg, 2003. **126**(3): p. 671-9.
178. Urabe, M., C. Ding, and R.M. Kotin, *Insect cells as a factory to produce adeno-associated virus type 2 vectors.* Hum Gene Ther, 2002. **13**(16): p. 1935-43.
179. Airenne, K.J., et al., *Baculovirus: an insect-derived vector for diverse gene transfer applications.* Mol Ther, 2013. **21**(4): p. 739-49.
180. Smith, R.H., J.R. Levy, and R.M. Kotin, *A simplified baculovirus-AAV expression vector system coupled with one-step affinity purification yields high-titer rAAV stocks from insect cells.* Mol Ther, 2009. **17**(11): p. 1888-96.
181. Carnarius, C., et al., *Green fluorescent protein changes the conductance of connexin 43 (Cx43) hemichannels reconstituted in planar lipid bilayers.* J Biol Chem, 2012. **287**(4): p. 2877-86.
182. Moreno, A.P., *Biophysical properties of homomeric and heteromultimeric channels formed by cardiac connexins.* Cardiovasc Res, 2004. **62**(2): p. 276-86.
183. Frank, M., et al., *Connexin45 provides optimal atrioventricular nodal conduction in the adult mouse heart.* Circ Res, 2012. **111**(12): p. 1528-38.
184. Martinez, A.D., et al., *Connexin43 and connexin45 form heteromeric gap junction channels in which individual components determine permeability and regulation.* Circ Res, 2002. **90**(10): p. 1100-7.
185. Maass, K., et al., *Cx43 CT domain influences infarct size and susceptibility to ventricular tachyarrhythmias in acute myocardial infarction.* Cardiovasc Res, 2009. **84**(3): p. 361-7.
186. Wightman, B., I. Ha, and G. Ruvkun, *Posttranscriptional regulation of the heterochronic gene lin-14 by lin-4 mediates temporal pattern formation in C. elegans.* Cell, 1993. **75**(5): p. 855-62.
187. Lee, R.C., R.L. Feinbaum, and V. Ambros, *The C. elegans heterochronic gene lin-4 encodes small RNAs with antisense complementarity to lin-14.* Cell, 1993. **75**(5): p. 843-54.
188. Hong, J., et al., *Cardiac RNAi therapy using RAGE siRNA/deoxycholic acid-modified polyethylenimine complexes for myocardial infarction.* Biomaterials, 2014. **35**(26): p. 7562-73.
189. Rapti, K., et al., *Neutralizing antibodies against AAV serotypes 1, 2, 6, and 9 in sera of commonly used animal models.* Mol Ther, 2012. **20**(1): p. 73-83.
190. Burnett, J.C. and J.J. Rossi, *RNA-based therapeutics: current progress and future prospects.* Chem Biol, 2012. **19**(1): p. 60-71.
191. Shukla, S., C.S. Sumaria, and P.I. Pradeepkumar, *Exploring chemical modifications for siRNA therapeutics: a structural and functional outlook.* ChemMedChem, 2010. **5**(3): p. 328-49.